NASA CONTRACTOR REPORT

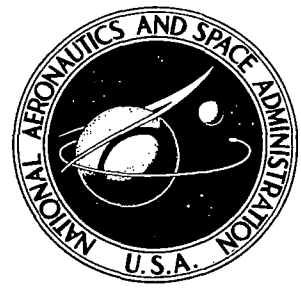

NASA CR-1092

LUNAR ORBITER IV

Extended-Mission Spacecraft Operations and Subsystem Performance

Prepared by
THE BOEING COMPANY
Seattle, Wash.
for Langley Research Center

NATIONAL AERONAUTICS AND SPACE ADMINISTRATION • WASHINGTON, D. C. • JUNE 1968

LUNAR ORBITER IV

Extended-Mission Spacecraft Operations

and Subsystem Performance

Issued by Originator as Boeing Document D2-100754-4 (Vol. IV)

Prepared under Contract No. NAS 1-3800 by
THE BOEING COMPANY
Seattle, Wash.

for Langley Research Center

NATIONAL AERONAUTICS AND SPACE ADMINISTRATION

For sale by the Clearinghouse for Federal Scientific and Technical Information
Springfield, Virginia 22151 – CFSTI price $3.00

Contents

Page

1.0 SUMMARY 1

2.0 INTRODUCTION 3
2.1 Spacecraft Description 3
2.2 Mission Objectives 3
2.3 Operational Organization 5

3.0 FLIGHT OPERATIONS 7
3.1 Spacecraft Control 8
3.1.1 Command Activity 9
3.1.2 Spacecraft Telemetry 10
3.2 Flight Path Control 10
3.2.1 Tracking Data Editing 10
3.2.2 Orbit Determination 10
3.2.3 Guidance Maneuvers 19

4.0 FLIGHT DATA 29
4.1 Environmental Data 29
4.1.1 Radiation 29
4.1.2 Micrometeoroids 29
4.2 Special Experiments 29
4.2.1 Lunar Surface Conductivity Experiment 29
4.2.2 Manned Space Flight Network/Apollo Goss Navigational Qualification Support 29
4.2.3 Voice Relay Experiment 31
4.2.4 Ionosphere Effects Experiment 32

5.0 SPACECRAFT SUBSYSTEM PERFORMANCE 33
5.1 Summary 33
5.2 Subsystem Performance 33
5.2.1 Attitude Control Subsystem 33
5.2.2 Communications Subsystem 50
5.2.3 Power Subsystem 54
5.2.4 Photo Subsystem 58
5.2.5 Structures and Mechanisms Subsystem 59
5.2.6 Velocity and Reaction Control Subsystem 63
5.3 Special Flight Tests 73
5.3.1 Three-Axis Gyro Drift Test 73
5.3.2 Canopus Tracker Bright-Object Shutter and Map Voltage Test 75
5.3.3 Special Star Tracker Test 81
5.3.4 TWTA On/Off Cycling Test 84
5.3.5 Battery Discharge Test 84
5.3.6 High-Gain-Antenna 360-Degree Rotation Test 84
5.3.7 TWTA Operation at Reduced Voltage Test 84
5.3.8 Camera Thermal Door Test 90
5.3.9 Paint Degradation Test 91

APPENDIX 95

Figures

Page

2-1 Lunar Orbiter Spacecraft 4
2-2 Lunar Orbiter Subsystems 5

3-1 Orbit Inclination 23
3-2 Orbit Perilune 23
3-3 Argument of Perilune 24
3-4 Perilune Altitude 24
3-5 Apolune Decrease Maneuver 26
3-6 Perilune Decrease Maneuver 27
3-7 Predicted Perilune Altitude Following Perilune Decrease Maneuver 28
3-8 Site IIP-2 Coverage Following Perilune Decrease Maneuver 28

4-1 Radiation Dosage Measurement, Looper and Cassette 30

5-1 Attitude Control Subsystem 34
5-2 Gyro Wheel Current 39
5-3 Yaw Gyro Wheel Current 40
5-4 IRU and EMD Temperature vs Time 41
5-5 IRU Drift 42
5-6 Spacecraft Attitude History 44
5-7 Canopus Tracker Performance 46
5-8 Coarse Sun Sensor Calibration 46
5-9 Pitch Jet Firing 48
5-10 Pitch Jet Anomaly 48
5-11 N_2 Isolation Squib Firing 49
5-12 Communication Subsystem 51
5-13 Transponder Temperature 51
5-14 Equipment Mount Deck Temperature 51
5-15 Transponder Power 52
5-16 TWTA Operation 53
5-17 Power Subsystem 54
5-18 Battery Discharge Characteristics 55
5-19 Battery Discharge Characteristics 56
5-20 Power Response to Antenna Rotation 57
5-21 Photo Subsystem 58
5-22 EMD Temperature Comparison 61
5-23 Spacecraft Pitch Angle History 61
5-24 EMD Temperature History (TWTA) 62
5-25 EMD Temperature History (Transponder) 62
5-26 EMD Temperature History (IRU) 63
5-27 Velocity and Reaction Control Subsystem 63
5-28 Spacecraft Tankage Pressure History 64
5-29 Extended-Mission Profile – Temperature 64
5-30 Nitrogen Supply Utilization 65
5-31 Limit Cycle Operation 66
5-32 Velocity Change – Perilune Decrease Maneuver 67
5-33 Tank Pressures – Perilune Decrease Maneuver 68
5-34 TVC Actuator Position – Perilune Decrease Maneuver 68

Figures (Continued)

Page

5-35 Attitude Control – Perilune Decrease Maneuver 69
5-36 Velocity Change – Apolune Decrease Maneuver 70
5-37 Tank Pressures – Apolune Decrease Maneuver 71
5-38 TVC Actuator Position – Apolune Decrease Maneuver 71
5-39 Attitude Control – Apolune Decrease Maneuver 72
5-40 Gyro Drift Test 74
5-41 Gyro Drift Comparison 74
5-42 Orbit Geometry 76
5-43 Sun Sensor Position 77
5-44 Bright-Object-Sensor Operation (−Yaw) 77
5-45 Bright-Object-Sensor Operation (+Yaw) 78
5-46 Star Map (+17 Degrees Yaw) 78
5-47 Star Map (−20 Degrees Pitch) 79
5-48 Star Map (+40 Degrees Pitch) 79
5-49 Star Map (−20 Degrees Pitch) 80
5-50 Star Map (−17 Degrees Yaw) 80
5-51 High-Gain-Antenna Rotation Test 85
5-52 High-Gain-Antenna Rotation Test 86
5-53 High-Gain-Antenna Rotation Test 87
5-54 High-Gain-Antenna Rotation Test 88
5-55 Bus Voltage Performance 89
5-56 TWTA Power 90
5-57 Paint Coupon Performance 92
5-58 Paint Coupon Performance 93

Tables

		Page
3-1	Orbit Parameter Summary	7
3-2	Programmer Map Summary	9
3-3	Telemetry Data Summary	11
3-4	Tracking Data Summary	14
3-5	Station Timing Synchronization	18
3-6	Master File Tracking Data Tapes	18
3-7	Lunar Harmonic Coefficients (LRC 11/11)	19
3-8	Orbit Determination Summary	20
3-9	Orbit Determination Data Summary	21
3-10	Maneuver Design	25
3-11	Predicted vs Actual Comparison Postmaneuver Orbital Elements	27
4-1	Radiation Data	29
4-2	Lunar Surface Conductivity Data Periods	31
4-3	MSFN/AGNQ Tracking Summary	31
5-1	Extended-Mission Maneuvers	35
5-2	Wheel Currents	41
5-3	Maneuver Summary	43
5-4	Drift Rates	43
5-5	Star Tracker History	45
5-6	Sun Sensor Limit	46
5-7	Commanded Actuator Position	46
5-8	Position Error Deadband Limits	47
5-9	Attitude Control Subsystem Condition	50
5-10	Solar Panel Degradation	54
5-11	Power Subsystem Data	57
5-12	Photo Subsystem Temperatures and Pressures	60
5-13	Major Events Using Nitrogen Gas	66
5-14	Velocity Control Maneuvers	73
5-15	Test Sequence	75
5-16	Star Tracker Test Sequence	81
5-17	Star Tracker Test Results	83
5-18	Paint Coupon Performance	94

Abbreviations

AGNQ	Apollo Goss Navigation Qualification
ASU	acquire Sun
BOS	bright-object sensor
CAO	Canopus sensor
CAO*	Canopus sensor off
CDZ	close dead zone
CLC	closed loop-celestial
COGL	command generation and programmer simulation program
DACON	data controller
DATL	data alarm summary
DSN	Deep Space Network
DSS	Deep Space Station
EMD	equipment mount deck
FAT	flight acceptance test
FPAC	flight path analysis and control
GMT	Greenwich Mean Time
GOSS	ground operation support system
IH	inertial hold
IRU	inertial reference unit
JPL	Jet Propulsion Laboratory
MDE	mission-dependent equipment
MSFN	Manned Space Flight Network
NASA	National Aeronautics and Space Administration
NDZ	narrow dead zone
ODPL	orbit determination program
ODPX	orbit data generation program
OMS	optical-mechanical scanner
PIM	pitch minus
PIP	pitch plus
ROM	roll minus
ROP	roll plus
RTC	real-time command
SFOF	space flight operations facility
SLOE	senior Lunar Orbiter engineer
SPAC	spacecraft performance analysis and command
SPC	stored-program command
TTY	telemetry
TVC	thrust vector control
TWT	traveling-wave tube
TWTA	traveling-wave-tube amplifier
VCO	variable change oscillator
YAP	yaw plus
YAM	yaw minus
ΔV	velocity change

1.0 Summary

Active tracking of the Lunar Orbiter IV spacecraft was accomplished successfully from the start of the extended mission on Day 152 (June 1, 1967) through Day 198 (July 17). On the next scheduled tracking period on Day 202 (July 21), contact with the spacecraft could not be made. After repeated unsuccessful attempts to make contact with the spacecraft over a period of 26 days, the Lunar Orbiter IV extended mission was officially terminated on Day 228 (August 16). The reason contact with the spacecraft was unobtainable is not known.

During extended-mission active tracking, the primary objectives of selenodetic data acquisition and lunar environment monitoring were accomplished. All secondary objectives—which included nine special exercises, Manned Space Flight Network/Apollo GOSS navigational qualification (MSFN/AGNQ), three experiments, and completion of photographic film rewind and readout—were initiated prior to the loss of the spacecraft.

The Mission V selenodetic data acquisition phase of this extended mission was initiated following the orbit transfers on Day 156 (June 5), which lowered the perilune altitude from 2,578 to 74 kilometers, and on Day 159 (June 8), which lowered the apolune altitude from 6,084 to 3,952 kilometers. During the next 18 days, 134 hours of tracking data were collected and processed, and used by the Lunar Orbiter project office to develop the 7/28B lunar harmonics model for Mission V.

Of significance in lunar environmental data was a 1.5-rad increase in excess of normal background level recorded by the looper scintillation counter between Day 157 (June 6) and Day 158 (June 7). There were no micrometeoroid hits sustained during the extended mission.

The special exercises that were designed to probe the limits of the spacecraft's capabilities and to illuminate potential operational problems for subsequent missions yielded the results summarized in the paragraphs below.

Tests indicate that the photographic mission planned for Lunar Orbiter V is feasible for attitude control system operation. The orbit transfers performed on Days 156 (June 5) and 159 (June 8) produced an orbit similar to that designed for Mission V. Under these conditions the star Canopus could be tracked from 80 degrees before to 35 degrees after the South Pole. The spacecraft did not exhibit any high sources of glint to the Canopus tracker. The Canopus tracker bright-object sensor closed at a 76.8-degree cone angle from the Sun and opened at 77.3 degrees. Inertial reference unit gyro drift was minimal and showed little if any degradation since launch.

Lunar Orbiter IV was the first Lunar Orbiter to be subjected to long periods of battery overcharge not interrupted by discharge periods. On Day 155 (June 4), a battery discharge test was run after a 31-day period of constant overcharge; it showed that no detrimental effects on battery characteristics had occurred.

Absorptivity and emissivity data on several experimental paint samples were gathered and used in studies of paint degradation due to the solar environment.

The data acquired during the lunar surface conductivity, ionosphere, and voice relay experiments were forwarded via the NASA experiment coordinator to the requestor for evaluation and reporting.

During this extended mission, the MSFN/AGNQ effort consisted of five tracking periods in which the Apollo sites acquired 52.4 hours of two-way tracking, 25.9 hours of three-way tracking, and 7.4 hours of ranging data.

The last successful contact with the spacecraft was on Day 198 (July 17). Analysis of the spacecraft telemetry data and the projected perilune data failed to provide any information that would suggest an impending catastrophic subsystem failure or a lunar impact at the time contact was lost. SPAC emergency fault isolation procedures were used in an attempt to regain contact with

the spacecraft. Although these procedures were unsuccessful, the operation was designed with the assumption that the spacecraft was responding to all commands but had a failed transmitter.

The natural impact of Lunar Orbiter IV, predicted from all available data and the LRC 2/28B lunar model, was expected to occur about Day 304 (October 31) at approximately 22 to 30 degrees W longitude.

The Lunar Orbiter IV extended mission was officially terminated by mission directive on Day 228 (August 16).

2.0 Introduction

This volume describes spacecraft control and flight path analysis and control operations conducted during this extended mission and discusses spacecraft performance during these operations. Complete data packages have been prepared for each experiment and special exercise under separate cover and forwarded to the requestor via the NASA experiment coordinator. The highlights of each special exercise and experiment are summarized herein.

Transition from the photographic mission to the extended-mission phase was completed on Day 152 (June 1). All spacecraft systems were operational—with the exception of the photo subsystem and the camera thermal door, which had displayed anomalous behavior during the photo mission. The spacecraft was in an orbit inclined 85 degrees to the lunar equator with an apolune altitude of 6,233 kilometers, a perilune altitude of 2,587 kilometers, and a period of 721 minutes. The spacecraft was operating in wide deadzone (2.0 degrees) and pitched off the sunline at plus 40 degrees for thermal relief. The communications subsystem was operating in Mode 1 with the TWTA on.

2.1 SPACECRAFT DESCRIPTION

The 853-pound Lunar Orbiter spacecraft is 6.83 feet high, spans 17.1 feet from the tip of the rotatable high-gain dish antenna to the tip of the low-gain antenna, and measures 12.4 feet across the solar panels. Figure 2-1 shows the spacecraft in the flight configuration with all elements fully deployed (the mylar thermal barrier is not shown). Major components are attached to the largest of three deck structures, which are interconnected by a tubular truss network. Thermal control is maintained by controlling emission of internal energy and absorption of solar energy through the use of a special paint covering the bottom side of the deck structure. The entire spacecraft periphery above the large equipment-mounting deck is covered with a highly reflective aluminum-coated mylar shroud, providing an adiabatic thermal barrier. In addition to its structural functions, the tank deck is designed to withstand radiant energy from the velocity control engine to minimize heat losses. Three-axis stabilization is provided by using the Sun and Canopus as primary angular references, and by a three-axis inertial system when the vehicle is required to operate off celestial references, during maneuvers, or when the Sun and/or Canopus are occulted by the Moon. The spacecraft subsystems are shown in block diagram form in Figure 2-2.

2.2 MISSION OBJECTIVES

The primary objective of this extended mission was to secure information that may be used to increase scientific knowledge of the size and shape of the Moon, the properties of its gravitational field, and the lunar environment. Secondary objectives were to develop standard operating procedures, conduct special experiments and exercises, and explore the use of Lunar Orbiter subsystems for other applications. During this extended mission the following exercises and experiments were included.

- *Canopus tracker bright-object sensor and map voltage test* to determine bright-object-sensor operation and sensitivity of the star tracker;
- *Three-axis gyro drift measurement* to determine gyro drift;
- *Special star tracker test* to test the star tracker under proposed Mission V conditions;
- *Battery discharge test* to determine battery performance;
- *High-gain-antenna 360-degree rotation test* to observe TWTA operation during antenna rotation;
- *Camera thermal door test* to analyze thermal door operation;
- *Lunar surface conductivity experiment* to test conductivity of the Moon's surface;
- *MSFN/Apollo Goss navigation qualification support* to qualify Apollo tracking stations;
- *Voice relay experiment* to test feasibility of relaying voice by a lunar orbiting spacecraft;

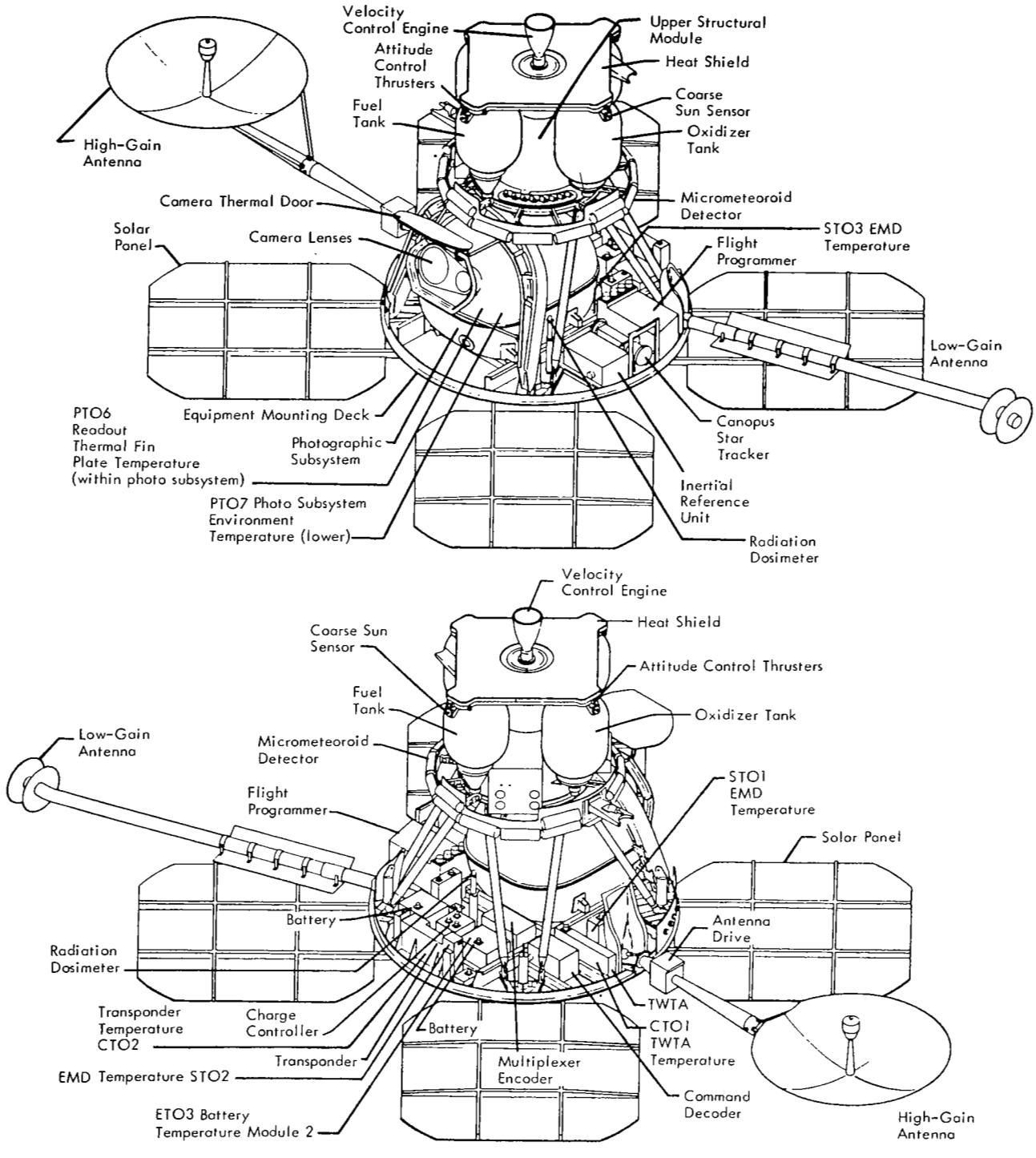

Note: Shown with Thermal Barrier Removed

Figure 2-1: Lunar Orbiter Spacecraft

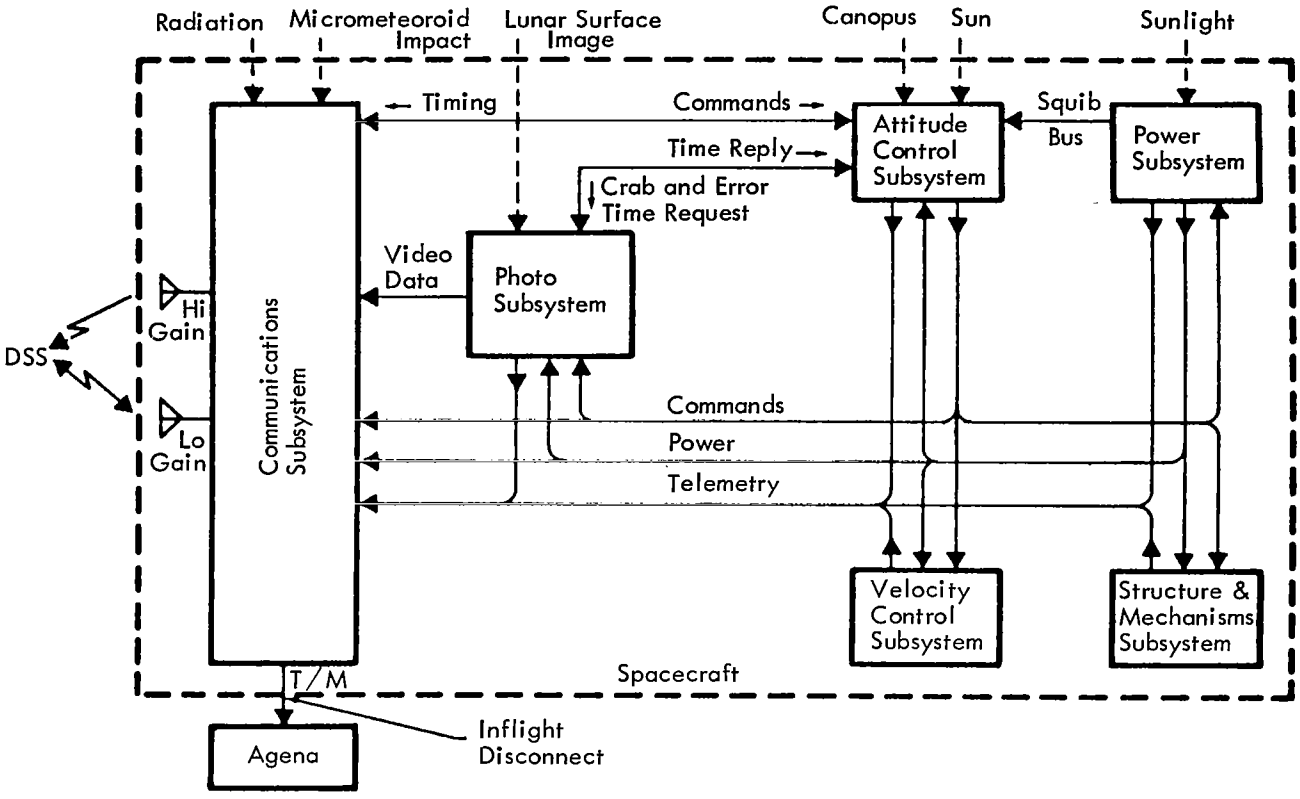

Figure 2-2: Lunar Orbiter Subsystems

- *TWTA operation at reduced voltage test* to determine operation of TWTA under Mission V conditions.
- *Ionosphere experiment* to determine the effects of the Earth's ionosphere on doppler and ranging data;
- *Paint coupon/ thermal test* to test paint degradation under space environments.

Other objectives included rewinding the photographic film from Frame 100 to Frame 23 to place the leader splice on the camera supply spool plus read out selected frames during the rewind. In addition, the SFOF communications processor was to be evaluated for Mission V operations.

2.3 OPERATIONAL ORGANIZATION

The extended mission of Lunar Orbiter IV was conducted using a centralized method of control from the Space Flight Operations Facility at Pasadena, California, that was similar to that adopted for the photographic missions. Primary differences between extended and photographic mission activities are described in the following paragraphs.

Manning at the SFOF and at the DSS's was at a significantly reduced level during the extended mission than during the photographic mission. Manning at the DSS's was reduced by limiting the MDE personnel to the SLOE, assistant SLOE, and MDE systems engineer. During the photographic mission, the additional services of a video engineer, supporting film processing personnel, and telemetry operators were required. Manning at the SFOF was reduced in several areas. The NASA mission advisors were no longer required; however, a small NASA scientific team located at the Langley Research Center was available for selenodetic studies and consultation. The mission director also was no longer required at the SFOF, but available at Langley for key decisions. It was possible to reduce the size of the operational teams because of shorter track-

ing periods and a decrease in the level of operational activity. For those periods of increased activity such as preparation for and during a velocity maneuver, personnel from Seattle were sent to the SFOF to augment the extended-mission team. During long (but infrequent) tracking periods such as MSFN tracks, which lasted up to 32 hours, the extended-mission team was also augmented by personnel from Seattle.

A list of the manning provided by the contractor at the SFOF for extended-mission tracks is shown below. In addition to these personnel, the space flight operations director and a reduced (from the photographic mission) complement of JPL personnel such as track chief and communications personnel were required to support the tracking periods.

- Assistant space flight operations director

- SPAC
  1. Command programmer analyst
  2. Attitude control analyst
  3. Power/thermal analyst
  4. Communications system analyst
  5. SPAC software analyst
  6. Photo subsystem analyst
  7. Command coordinator

- DACON
  Data controller

- FPAC
  1. Flight chief
  2. Orbit determination analyst
  3. Guidance analyst

3.0 Flight Operations

An extended-mission flight operations plan was developed within the constraints of (1) DSN commitment for tracking coverage during the extended mission, and (2) nitrogen gas available for attitude control. This plan is described in the following paragraphs.

The primary purpose of the initial part of this extended mission was to obtain tracking data to develop lunar harmonics for a Mission V type orbit. To accomplish this, two orbit transfers were performed shortly after the extended mission started. One result of these orbit transfers was to rotate the line of apsides such that the natural perilune altitude decay caused the spacecraft to impact the lunar surface during the month of October, 1967. Orbit parameters before and after the transfers are shown in Table 3-1. Orbit parameters for the final orbits of Mission V are also shown; comparing the adjusted Mission IV orbits with the final Mission V orbits shows the same inclination and relatively good agreement in perilune altitude. Although a limitation in the amount of pro-

Table 3-1: Orbit Parameter Summary

Event	Day		Perilune (km)	Apolune (km)	Inclination (deg)	Period (min)
	GMT	Calendar				
Start extended mission	152	June 1	2578	6084	85	721
Lower perilune altitude ΔV=186.7 sec=117.9	156	June 5	2590	6233	85	721
			75			500
Lower apolune altitude ΔV=70.5 sec=42.8	159	June 8	76	6090	84	500
				3949		344
Last O.D. before contact lost	191	July 10	64	3966	85	344
Contact lost	202	July 21	–	–	–	–
Mission terminated	228	August 16				
Mission V final orbits	–	–	100	1500	85	191

pellants available prevented an exact Mission V orbit, there was enough similarity to enable the generation of Lunar Gravity Models 7/28A and 7/28B, which were used successfully during Mission V. To obtain sufficient tracking data during this period, Lunar Orbiter IV was tracked for selenodesy purposes in preference to the other extended-mission spacecraft.

Thermal control of the spacecraft was maintained by using the appropriate off-Sun angle, within power constraints. Keeping the battery temperature within satisfactory operating limits was of prime consideration in determining off-Sun angle.

The spacecraft had 3.5 pounds of nitrogen at the end of the photo mission, which was not enough to complete a nominal 11-month extended mission. Lunar Orbiter II could complete the 11-month extended mission if maneuvering were limited, and Lunar Orbiter III had promise of getting almost 11 months of extended mission if maneuvering were limited. To conserve the gas on board Lunar Orbiters II and III, it was decided to use Lunar Orbiter IV to support all activities requiring an attitude reference. The wide-attitude control deadzone, 2.0 degrees, was used whenever possible to conserve the limited supply of nitrogen gas.

The SFOF communications processor was used to process spacecraft telemetry data and to send commands and predicts to the DSN. Commands were transmitted to the spacecraft using an offset frequency to prevent inadvertent commands from being received by any of the other extended-mission spacecraft. (A technique discussed further in Section 3.1.) To ensure that inadvertent commands had not been received by the spacecraft after commanding of other extended-mission spacecraft (Lunar Orbiters II and III), a "quick-look" by sampling several telemetry frames to check the programmer's status was always made at the completion of commanding the other spacecraft.

It was planned to wind the photographic film onto the camera supply spool and place the splice under several wraps of leader to remove the tension.

Operations directives that detailed support requirements and the sequence of events to be followed were prepared for each tracking pass. The directives were a plan for the tracking period and served as the tool by which the mission plan was implemented.

3.1 SPACECRAFT CONTROL

Spacecraft control required multiple-spacecraft operation techniques to enable noninterference with two other extended-mission Lunar Orbiters using approximately the same best lock frequency. Multiple-spacecraft operation was accomplished by acquiring and tracking Lunar Orbiter IV using offset frequency predicts similar to those employed during the prime mission. This technique biased the tracking synthesizer frequency by a plus or minus 330 Hz from the spacecraft best lock frequency (Xa). By selecting the appropriate direction (based on Xa for the other extended-mission spacecraft and occultation times) from which to approach the Xa to obtain uplink lock and then tuning to the offset frequency, no inadvertent commands were received by any of the extended-mission spacecraft.

After spacecraft acquisition, real-time telemetry readout was obtained at the SFOF via high-speed data line and 60-wpm teletype. The telemetry data was processed in real time by an IBM 7044 computer or in conjunction with an IBM 7094 computer, then displayed on 100-wpm teletype machines, X-Y plotters, and bulk printers for analysis.

Commands used to change the spacecraft programmer memory were normally generated by COGL, sent to the DSS, and transmitted to the spacecraft. Such programmer commands were used to perform housekeeping functions and to conduct experiments and special exercises. The programmer maps were supplemented by RTC updates as required, which did not necessitate use of the COGL program.

Lunar Orbiters II, III, and IV spacecraft were operated by stored-program maps that automatically updated the Sun reference periodically. Although Lunar Orbiter IV was designated as

the primary spacecraft for a majority of the tracking passes, the other spacecraft were tracked for a brief period during each pass to verify flight programmer operation and to monitor other-subsystem status. Likewise, when Lunar Orbiter IV was the secondary spacecraft, its status was also checked by quick-look monitoring.

3.1.1 Command Activity

The housekeeping programmer core map consisted of acquiring the Sun reference every 72 hours and pitching plus 40 degrees for thermal relief. The values were selected using gyro drift characteristics and power/thermal requirements as constraints. As shown in Table 3-2, this map was used only until Day 152 due to lower than calculated gyro drift rates, frequent tracking periods, and other spacecraft activity which necessitated "jumping out of" the cruise map.

A total of 422 RTC's and a total of 234 SPC's were executed during the extended mission through Day 198, the last successful track period of Lunar Orbiter IV. A total of 216 additional

Table 3-2:
Programmer Map Summary

Map Number	Time Transmitted to Spacecraft day – hr – mn	Time Span Effectivity day-hr-mn/day-hr-mn	Purpose
43*	152-11-53	151-01-00/152-00-59	Flight Plan (Acquire Sun, pitch plus 40 degrees, wait 72 hours, repeat)
44	155-11-35	152-00-59/155-11-50	1) Battery deep discharge test 2) Nitrogen isolation valve squib firing sequence
45	155-19-05	155-11-50/155-22-01	Preparations for perilune changing velocity maneuver
45 Update	156-19-00	155-22-01/158-00-00	
46**	159-00-00	158-00-00/158-23-59	Canopus update between velocity maneuvers
46 Update	159-20-30	158-23-59/160-00-00	Parameter update for apolune changing velocity maneuver
47	163-12-15	160-00-00/163-16-42	Canopus tracker bright-object sensor and map voltage test
48	164-01-00	N/A	Photo subsystem test sequences
49	167-21-50	N/A	Camera thermal door test
Antenna rotation sequence	186-21-40	N/A	Rotate high-gain antenna 1 degree left every 3.5 seconds

* Transmitted but not used – superseded by map 44
** Transmitted but not used – superseded by map 46 update

RTC's were attempted to reestablish contact with the spacecraft. Although normal housekeeping functions as well as special sequences were normally accomplished by SPC's, RTC's were needed to augment stored-program sequences so as to initiate and terminate video readouts, cycle the Canopus tracker as required by glint conditions, and perform other various required functions.

3.1.2 Spacecraft Telemetry

A total of 288.6 hours of telemetry data was processed for 24 Lunar Orbiter IV tracking passes. Table 3-3 contains a summary of telemetry data by station and includes a listing of the significant activities accomplished during each pass. The Surveyor assist listed in Table 3-3 consisted of identifying the transmissions to be that from the Lunar Orbiter spacecraft during the unsuccessful attempt to "wake up" the Surveyor. This was done by changing the transmission frequency from the spacecraft.

Problems encountered were typical of those experienced during the prime missions such as minor communications outages and computer internal restarts. Standard workaround methods such as processing TTY data and using raw hexidecimal data were employed to minimize data problems. The communications processor caused the raw TTY data to lag behind real time, which caused frequent deletion of data in order to return to real time.

A data and alarm summary containing a majority of the telemetry channels for each frame was processed for all tracking passes to provide a permanent record of the telemetry data.

3.2 FLIGHT PATH CONTROL

Flight path control of the spacecraft during the extended mission is the responsibility of the FPAC portion of the flight team. The functions carried out by this team are identical to those during the primary mission (i.e., tracking data editing, orbit determination, and guidance maneuver calculations). The processes used to perform these functions are the same as in the prime mission, except that data quantity is less due to decreased tracking time.

3.2.1 Tracking Data Editing

Tracking data editing is the process of monitoring, analyzing, and judging the quality of the doppler and range radar tracking data transmitted to the SFOF from the DSN. The data is provided from three DSN stations – Madrid, Spain (Station 62); Woomera, Australia (Station 41); and Goldstone, California (Station 12) – in three types: continuous-count doppler, ranging units, and antenna pointing angles. The pointing angles were not used due to the small arc traversed by the spacecraft in lunar orbit. Table 3-4 is a summary of the tracking data obtained during the extended mission. Computer programs TDPX and ODGX were used to edit and process the tracking data. Tables 3-4 and 3-5 provide information used for this editing and processing. Table 3-6 contains a list of master file (tracking data) tapes generated by TDPX; both tapes sent to Langley Research Center and those kept in the Jet Propulsion Laboratory tape library are listed.

3.2.2 Orbit Determination

Orbit determination is the process of computing the spacecraft trajectory that coincides best with the tracking data. The computer program used during the extended mission, identical to that used during the primary mission, is identified as ODPL and calculates orbit determinations from the tracking data prepared by the editing programs.ODPL uses a fourth-order spherical harmonic expansion of the lunar potential field. NASA provided the coefficients for the lunar model on November 11, 1966 (see Table 3-7). The following general procedures were to be used in the orbit determination procedures.

- Use at least two orbits of doppler data. Both two-way (CC3) and three-way (C3) doppler is to be used with data weights of 0.1 cycle per second.
- Use doppler data from at least two different stations.
- Use range units calculated only for visual assistance of the determination.
- Do not use perilune data in the determination. This can be accomplished by omitting all data from 20 minutes before to 20 minutes after perilune. After ODPL

Table 3-3: Telemetry Data Summary

Day	GMT	Deep Space Station	Activities
152	13:46-14:26	12	Surveyor Assist
153	19:12-24:00	41	a. Film rewind b. Selenodesy
155	10:39-15:30	62	a. Battery discharge test
155	11:06-23:05	12	b. Film rewind c. Canopus reference update d. Three-axis gyro drift test e. Selenodesy f. Ionosphere experiment
156	12:31-23:48	12	a. Film rewind
156/157	20:29-06:15	41	b. Selenodesy c. Canopus reference update d. Orbit adjust (perilune) e. Isolation squib fired
158/159	14:31-01:27	12	a. Film rewind
158/159	21:58-01:00	41	b. Canopus reference update c. Selenodesy
159/160	17:50-02:26	12	a. Canopus reference update
159/160	23:22-08:00	41	b. Film rewind c. Orbit adjust (apolune) d. Selenodesy
161	14:55-21:25	62	a. Selenodesy
161/162	16:05-04:11	12	b. Film rewind c. MSFN/AGNQ Antenna update

Table 3-3 (Continued)

Day	GMT	Deep Space Station	Activities
163	10:00-19:00	62	a. MSFN/AGNQ
163/164	17:58-04:00	12	b. Canopus tracker bright-object sensor and map voltage test
164	02:29-07:00	41	c. Selenodesy
164	17:00-23:30	62	a. Voice relay experiment
164/165	18:43-06:48	12	b. Film rewind
			c. Selenodesy
166/167	20:19-07:00	12	a. Canopus reference update
			b. Selenodesy
167	18:01-24:00	62	a. Selenodesy
167/168	23:44-07:00	12	b. Camera thermal door test
168	15:00-24:00	62	a. Camera thermal door test
168/169	22:28-09:24	12	b. Ionosphere experiment
			c. Selenodesy
170/171	23:31-02:15	62	a. MSFN/AGNQ
171	02:11-10:31	12	b. Selenodesy
171	11:43-19:15	41	
172/173	20:20-03:50	62	a. Selenodesy
			b. Comm processor evaluation
173	14:01-21:31	41	a. Camera thermal door test
173/174	20:55-04:52	62	b. Selenodesy
			c. Comm processor evaluation
176	08:02-08:30	12	a. Quick look
			b. Comm processor evaluation

Table 3-3 (Continued)

Day	GMT	Deep Space Station	Activities
177	11:52-15:55	12	a. MSFN/AGNQ
177/178	15:23-00:17	41	b. Selenodesy
178	08:52-09:26	12	Quick look
180	14:03-14:36	12	a. Quick look
			b. Comm processor evaluation
186	13:03-24:00	12	a. MSFN/AGNQ
186	15:27-17:22	62	b. Paint coupon / thermal test
186/187	21:08-06:00	41	c. Special star tracker test
			d. Selenodesy
188	19:07-19:50	12	a. Quick look
			b. Comm processor test
191	09:00-21:00	62	a. MSFN/AGNQ
191/192	19:46-04:50	12	b. Selenodesy
192	02:00-10:43	41	c. High-gain-antenna 360 degree rotation test
			d. Comm processor test
196	08:38-09:20	41	Quick look
198	05:57-06:30	41	Quick look
202			No contact

Table 3-4: Tracking Data Summary

Day of Pass	Station	Doppler					Ranging					**Syn-Freq
		*Type	Start Time	Stop Time	Amount (hrs)	Trans-mitter-on time	Start Time	Stop Time	Amount (hrs)	Station Delay	Trans-ponder Temp (°F)	
153	41	CC3	19:12	24:00	4.77	19:12	19:27	21:19	1.91	290.1	84	5930
155	12	CC3	11:22	23:04	12.05	11:22	11:22	23:03	9.78	309.2	85	5930
155	62	C3	11:22	15:29	4.01							5930
156	12	CC3	12:35	23:27	11.00	12:35	12:35	17:57	4.71	304.4	85	5930 → 22:00 5600 → 23:26
156	12	C3	23:28	23:55	0.42							5930
156	41	C3	20:27	23:27	3.02							5900 → 22:00 5560 → 23:30
156/7	41	CC3	23:28	06:16	6.75	23:28	01:17	06:16	4.40	288.3	86	5930
158/9	12	CC3	14:39	01:28	10.93	14:39	14:46	16:04	4.46	307.6	87.5	5930
							19:27	22:28			86	
158/9	41	C3	22:00	01:00	3.0							5930
159	12	CC3	18:03	23:42	5.6	18:03	18:37	20:23	1.83	299.6	86	5930 → 21:40 5640 → 23:10
159/60	12	C3	23:43	02:27	2.44							5930
159	41	C3	23:23	23:42	0.24							5930
159/60	41	CC3	23:43	08:00	8.3	23:43	00:29	08:00	7.5	288.3	86	5930
161	62	CC3	15:07	21:12	6.31	15:07			0			5930
161	62	C3	21:13	21:23	0.2							5930

Table 3-4 (Continued)

Day of Pass	Station	Doppler					Ranging					**Syn-Freq
		*Type	Start Time	Stop Time	Amount (hrs)	Trans-mitter-on time	Start Time	Stop Time	Amount (hrs)	Station Delay	Trans-ponder Temp (°F)	
161	12	C3	16:06	21:12	4.81							5930
161/2	12	CC3	21:13	04:10	6.9	21:13	23:13	04:05	4.88	302.0	86	5930
163	62	CC3	10:07	18:29	8.5	10:07	10:10	14:53	5.20	194.4	86	5930
							17:06	18:25			90	
163	62	C3	18:30	18:58	0.49							5930
163	12	C3	18:00	18:29	0.49							5930
163	12	CC3	18:30	20:45	2.25	18:30			0			5930
164	62	CC3	17:10	21:00	3.85	17:10	20:30	20:52	0.3	266.4	88	5930
												5930
164	62	C3	21:01	23:30	2.49							5930
164	12	C3	18:47	21:00	1.4							5930
164/5	12	CC3	21:01	06:47	8.7	21:01	04:26	06:12	1.8	306.0	89	5930
166	12	C3	20:21	23:15	2.9							5930
166/7	12	CC3	00:27	07:00	5.75	00:27			0			5930
167	62	CC3	19:01	23:43	4.75	19:01	19:01	21:44	2.1	280.0	81	5930
167	62	C3	23:44	24:00	.26							5930

Table 3-4 (Continued)

Day of Pass	Station	Doppler					Ranging					**Syn-Freq
		*Type	Start Time	Stop Time	Amount (hrs)	Trans-mitter-on time	Start Time	Stop Time	Amount (hrs)	Station Delay	Trans-ponder Temp (°F)	
167	12	C3	22:04	23:43	1.7							5930
167/8	12	CC3	23:44	07:00	7.25	23:44	00:20	01:10	2.8	298.0	85	5930
							04:46	06:50				
168	62	CC3	15:34	22:18	6.75	15:34	16:10	17:35	2.75	280.0	81	5930
							20:06	22:14			81	
168	62	C3	22:19	24:00	1.2							5930
168/9	12	CC3	22:19	09:24	10.6	22:19	22:50	09:24	10.6	298.0	81	5930
170/1	62	CC3	23:51	01:30	1.6	23:51			0			5930
172	62	CC3	20:29	24:00	3.3	20:29			0			5930
173	41	CC3	14:02	21:14	6.8	14:02	15:21	17:30	2.2	288.5	83	5930
173	41	C3	21:15	21:30	.25							5930
173/4	62	CC3	21:15	04:56	6.66	21:15	01:28	03:45	2.3	280.0	83	5930
177	12	CC3	11:56	15:10	2.75	11:56			0			5930
177/8	41	CC3	15:24	15:40	1.0	15:24			0			5930
			23:30	00:17								5930
186	12	CC3	13:06	14:26	1.35	13:06			0			5930

Table 3-4 (Continued)

Day of Pass	Station	Doppler					Ranging					**Syn-Freq
		*Type	Start Time	Stop Time	Amount (hrs)	Trans-mitter-on time	Start Time	Stop Time	Amount (hrs)	Station Delay	Trans-ponder Temp (°F)	
186	12	C3	23:01	24:00	1.0							5930
186/7	41	CC3	23:00	00:30	1.5	23:00			0			5930
191	62	CC3	09:03	13:30	4.4	09:03	12:12	13:25	1.2	298.4	72	5930
191	62	C3	20:00	21:00	1.0							5930
191/2	12	CC3	20:00	03:42	7.7	20:00			0			5930
192	12	C3	03:43	04:52	1.2							5930
192	41	CC3	03:43	05:00	1.3	03:43						5930

*CC3=Two way
C3 =Three way

**Syn-Freq=204XXXX0

Table 3-5:
Station Timing Synchronization

Day	Time (GMT)	Station Number	Timing Bias*
129	17:26	62	+379.6 μsec
131	00:32	41	+780.9 μsec
156	00:00	41	+834.0 μsec
156	00:01	62	+812.0 μsec
161	00:01	62	+859.0 μsec
164	20:48	62	+865.0 μsec

* Deviation from DSS – 12's clock.

Table 3-6:
Master File Tracking Data Tapes

Time Interval		Langley	JPL
Start Time GMT day:hr:min	Stop Time GMT day:hr:min	Tape Number	Tape Number
138:03:00	152:13:23	LT424	9918
153:19:14	159:23:01	LT425	9619 and 9664
159:22:00	162:04:10	LT427	
159:22:00	164:06:43	LT428	
159:22:00	165:06:46	LT429	
159:22:00	167:06:59	LT430	
159:22:00	169:09:34	LT431	
159:22:00	171:18:44	LT432	
159:22:00	173:03:49	LT433	
159:22:00	174:04:52	LT434	
159:22:00	192:10:45	LT435	9766 and 2249

Table 3-7: Lunar Harmonic Coefficients (LRC 11/11)

GM=4902.58	J20 =+2.07 E-4	J30=−0.446 E-4
J40 =−0.209 E-4	C21=+0.088 E-4	C31=+0.435 E-4
C41=−0.051 E-4	C22=+0.276 E-4	C32=−0.052 E-4
C42=+0.028 E-4	C33=+0.0091 E-4	C43=−0.0047 E-4
C44=+0.00094 E-4	S21 =−0.411 E-4	S31 =+0.107 E-4
S41 =−0.102 E-4	S22 =−0.058 E-4	S32 =+0.0187 E-4
S42 =−0.083 E-4	S33 =−0.033 E-4	S43 =−0.026 E-4
S44 =+0.0017 E-4		

converges to a solution, the perilune data is to be restored, but a rejection sigma of 0.1 cycle per second effectively is to be used to keep this data from being used.

- Converge on a solution for state vector and doppler bias; then converge on a solution for state vector doppler bias and eight high-order harmonic coefficients.
- True anamoly of spacecraft at epoch as close to 180 degrees (apolune) as possible and keep sufficient data for a good orbit determination.

The Keplerian state vectors resulting from the orbit determination are summarized in Table 3-8. Table 3-9 describes the data used in each determination and the resulting data statistics. Figures 3-1 through 3-3 show the calculated orbital elements versus time. Figure 3-4 is a plot of predicted perilune altitude (lifetime) using the results of the last orbit determination (OD 7009-9) and the lunar harmonic coefficients listed in Table 3-7.

3.2.3 Guidance Maneuvers

When the orbit determination process defines a trajectory, the trajectory is analyzed to determine if a maneuver is required. The need for a maneuver can result from many requirements (e.g. to offset the effects of a solar or lunar eclipse, to extend spacecraft life, or to fulfill planned or functional objectives). The process of designing the maneuver during the extended mission did not differ from the primary mission; basically the purpose of the maneuvers was different. During Extended Mission IV there were two guidance maneuvers planned and conducted to simulate the orbit for Mission V. Because Mission V design specified photographic coverage of many discreet sites with few frames to be used for each, precise determination of the photo times was necessary; hence, a more refined definition of the lunar gravitational field in the vicinity of the targets was required. To increase the possibility of a successful Mission V, it was decided to transfer Lunar Orbiter IV into an orbit that simulated the next mission orbit as closely as possible. From the tracking data obtained in this orbit, better estimates of the lunar gravitational harmonic coefficients could be derived. Consequently, an improved photo prediction capability would be available. Several objectives were incorporated into the transfer design:

- Lower the altitudes of perilune and apolune to levels at which significant selenodetic data could be obtained.
- Alter other orbital parameters, if necessary, to obtain a natural impact on the Moon's nearside after a lifetime of 150 days.
- Phase the spacecraft so that direct pas-

Table 3-8: Orbit Determination Summary

State Vector (selenographic true of date)								
O.D. Identification No.	Epoch GMT yr/m/d	Time (GMT) d h m	a (km)	e	ω°(deg)	Ω(deg)	z (deg)	Tp (sec)
5005-9	67/06/02	19 25 00	6145.65	0.294785	9.74937	158.612	83.4483	3809.35
5006-9	67/06/04	11 20 00	6150.62	0.295864	9.567.90	136.653	85.4689	17587.4
5007-9	67/06/05	12 35 00	6149.77	0.296145	9.78489	122.760	85.2113	-21343.1
6000-9	67/06/05	23 30 00	4820.58	0.623894	354.601	116.812	85.0816	13997.3
6001-9	67/06/07	14 55 00	4820.58	0.623432	354.325	95.1321	84.5838	5799.99
7000-9	67/06/08	23 00 00	3751.21	0.516238	354.464	77.4458	84.3990	1241.32
7001-9	67/06/10	16 00 00	3752.39	0.516926	354.179	54.8363	84.6541	4465.94
7002-9	67/06/12	10 05 00	3752.92	0.517896	354.213	31.6310	85.0578	-9074.19
7003-9	67/06/13	18 15 00	3751.85	0.518490	354.687	13.9424	85.3345	3548.09
7004-9	67/06/15	18 45 00	3753.11	0.518437	355.548	347.318	85.3518	-7599.34
7005-9	67/06/16	19 00 00	3751.35	0.518110	355.993	334.012	85.2928	-2851.39
7006-9	67/06/17	15 30 00	3752.98	0.517498	356.730	322.730	85.0550	9043.02
7007-9	67/06/22	16 20 00	3752.32	0.516673	355.408	256.215	84.8621	-9721.86
7008-9	67/07/05	13 05 00	3752.50	0.517367	356.374	86.3748	84.3678	8320.94
7009-9	67/07/10	20 00 00	3753.21	0.519875	356.314	16.4509	85.3312	-9237.13

Table 3-9: Orbit Determination Data Summary

O.D. Identification No.	Station Number	Data Type	Start Time	Stop Time	Number of Points	Standard Deviations
5005-9	41	CC3	6/2 1925	6/2 0000	262	0.0284
		3RU	6/2 1927	6/2 2119	108	7.26
5006-9	62	C3	6/4 1122	6/4 1528	192	0.0270
	12	CC3	6/4 1123	6/4 2303	696	0.0351
5007-9	12	CC3	6/5 1236	6/5 2259	562	0.0247
	41	C3	6/5 2027	6/5 2259	113	0.0304
6000-9	41	CC3	6/5 2332	6/6 0614	370	0.273
	12	C3	6/5 2335	6/5 2353	17	0.0303
6001-9	12	CC3	6/7 1455	6/8 0123	608	0.149
	41	C3	6/7 2200	6/8 0058	175	0.183
7000-9	12	CC3	6/8 2300	6/8 2339	33	0.0506
		C3	6/8 2343	6/9 0225	132	0.0117
	41	C3	6/8 2323	6/8 2336	14	0.0169
		CC3	6/8 2343	6/9 0759	443	0.0479
7006-9	62	CC3	6/17 1536	6/17 2217	310	0.0251
		C3	6/17 2232	6/17 2359	73	0.0425
	12	CC3	6/17 2251	6/18 0550	386	0.0365
7007-9	41	CC3	6/22 1620	6/22 2112	214	0.0142
		C3	6/22 2119	6/22 2128	10	0.0103
	62	C3	6/22 2057	6/22 2108	12	0.0076
		CC3	6/22 2118	6/23 0450	364	0.0150
7008-9	12	CC3	7/5 1305	7/5 2258	381	0.0164
		C3	7/5 2305	7/5 2356	48	0.0129
	41	C3	7/5 2109	7/5 2256	66	0.0116
		CC3	7/5 2305	7/6 0028	79	0.0088
	62	C3	7/5 1719	7/5 1720	2	0.0006

Table 3-9 (Continued)

Standard Deviations	Number of Points	Stop Time	Start Time	Data Type	Station Number	O.D. Identification No.
7009-9	62	C3	7/10 2003	7/10 2058	46	0.0330
	12	CC3	7/10 2003	7/11 0339	357	0.0244
		C3	7/11 0343	7/11 0450	26	0.0512
	41	C3	7/11 0200	7/11 0334	88	0.0153
		CC3	7/11 0343	7/11 0458	31	0.0499
7001-9	62	CC3	6/10 1606	6/10 2109	261	0.106
		C3	6/10 2113	6/10 2123	11	0.0047
	12	C3	6/10 1607	6/10 2107	270	0.106
		CC3	6/10 2113	6/11 0409	395	0.0833
7002-9	62	CC3	6/12 1008	6/12 1828	391	0.0468
		C3	6/12 1835	6/12 1857	21	0.0348
	12	C3	6/12 1759	6/12 1826	13	0.199
		CC3	6/12 1834	6/12 2158	151	0.0107
7003-9	62	CC3	6/13 1815	6/13 2039	116	0.0176
		C3	6/13 2103	6/13 2328	115	0.0743
	12	C3	6/13 1846	6/13 2057	77	0.0059
		CC3	6/13 2103	6/14 0644	433	0.0512
7004-9	62	CC3	6/15 1848	6/15 2313	181	0.0357
	12	C3	6/15 2021	6/15 2313	128	0.0385
		CC3	6/16 0028	6/16 0658	289	0.0342
7005-9	62	CC3	6/16 1901	6/16 2339	207	0.0427
		C3	6/16 2346	6/16 2358	13	0.0065
	12	C3	6/16 2203	6/16 2336	91	0.0164
		CC3	6/16 2348	6/17 0659	384	0.0400

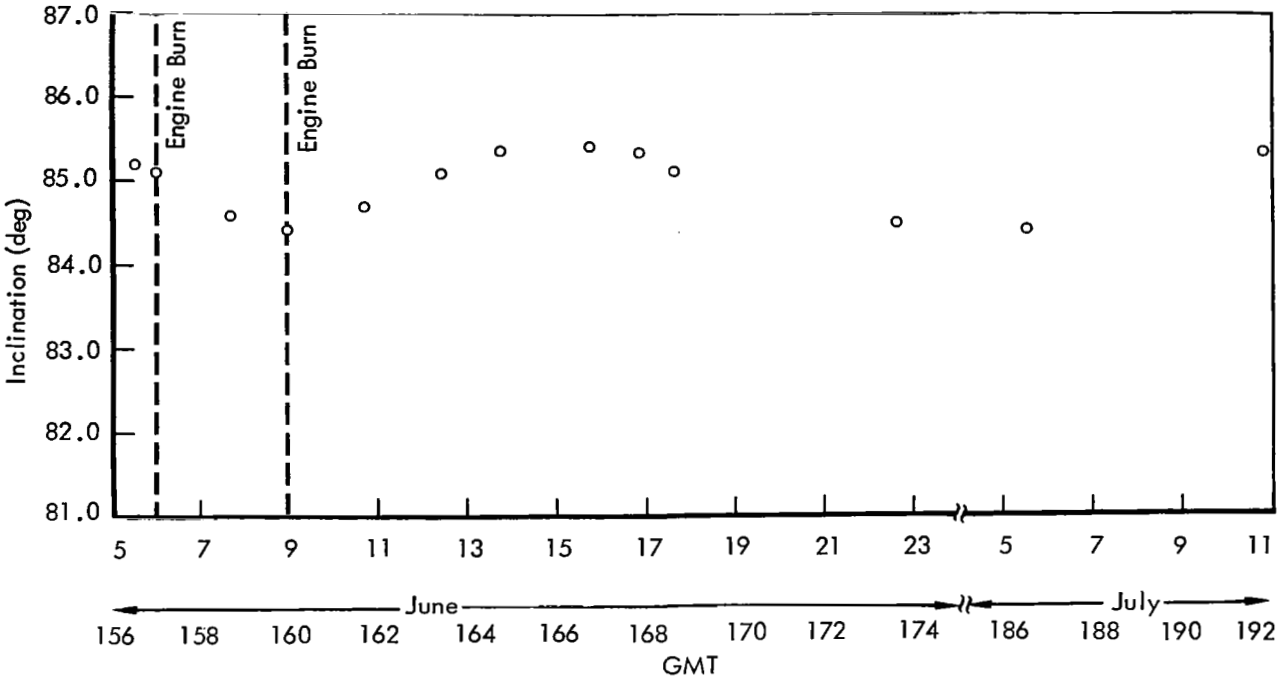

Figure 3-1: Orbit Inclination

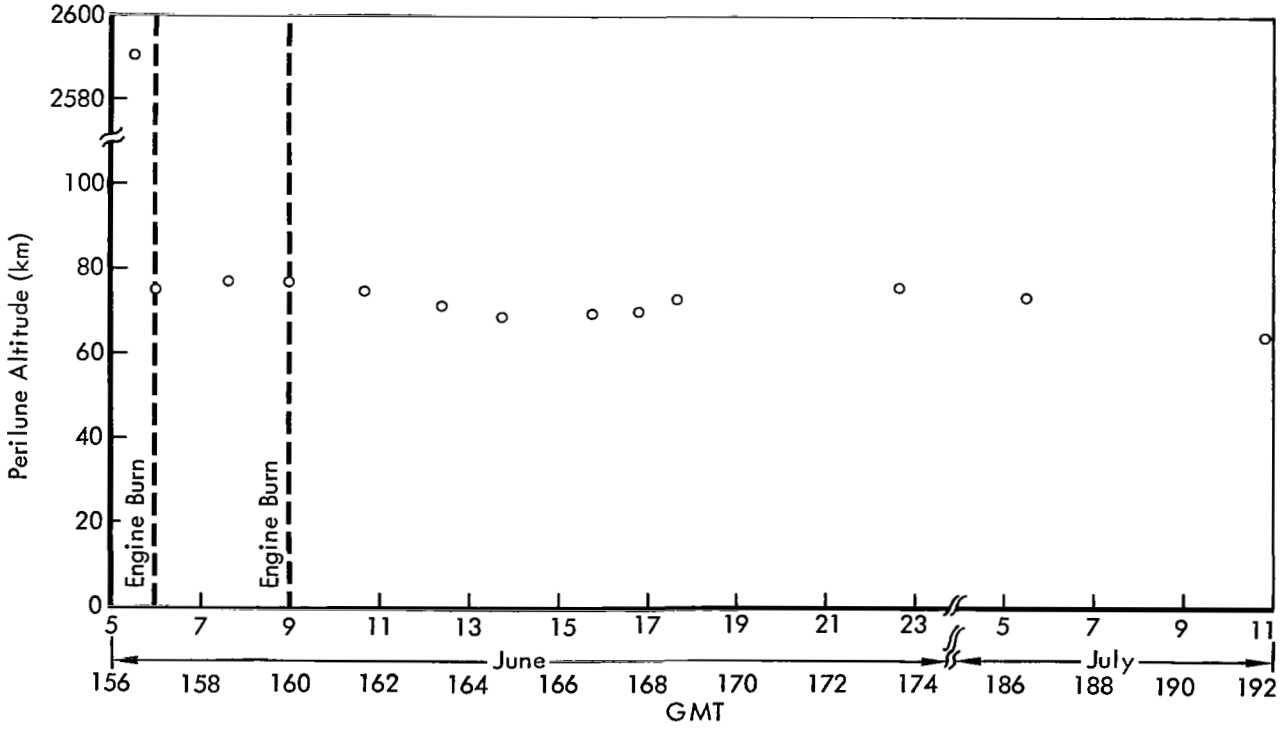

Figure 3-2: Orbit Perilune

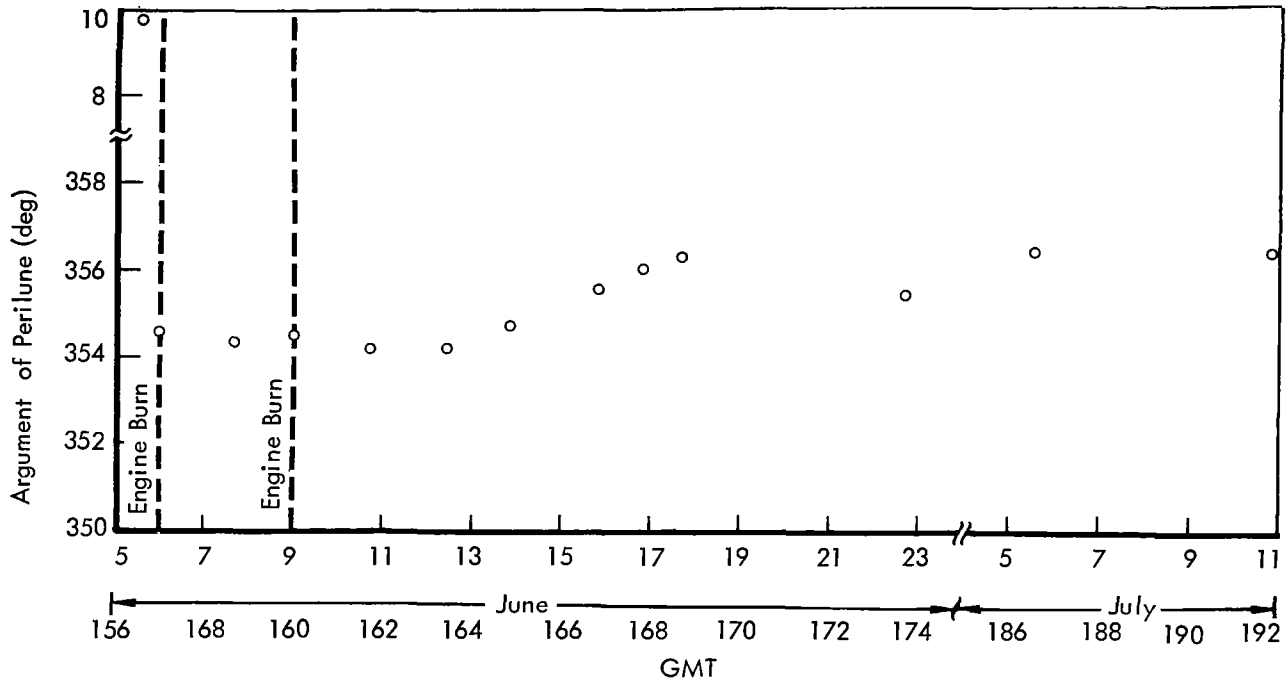

Figure 3-3: Argument of Perilune

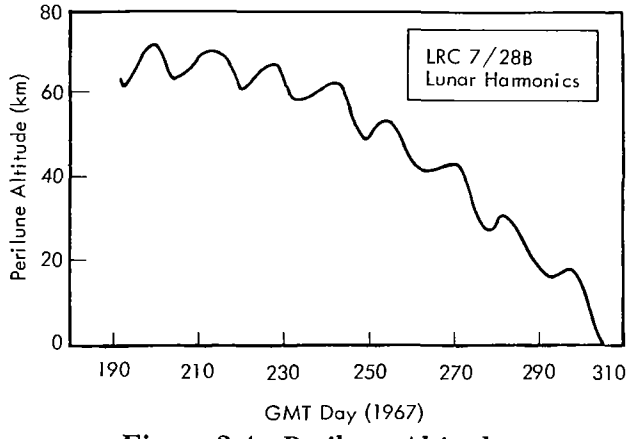

Figure 3-4: Perilune Altitude

sage over Mission II Site IIP-2 (34°E, 2.45° N) occurred in July, allowing a controlled crash into that area if desired.

- Maintain sufficient ΔV in the spacecraft to permit future phasing and impact maneuvers.

3.2.3.1 Maneuver Design

Analysis indicated that a perilune altitude of 75 kilometers would be desirable for lunar harmonic determination. With this selection, lifetime and ΔV considerations necessitated a rotation of the argument of periapsis, ω, to -5.0 degrees, and constrained apolune altitude to be above 3,950 kilometers. Two maneuvers were chosen to satisfy the design objectives. The first was selected to accomplish lowering of perilune altitude and rotation of the line of apsides. The second was to lower apolune altitude while phasing the spacecraft for passage over Mission II Site IIP-2. The resulting maneuver designs are shown in Table 3-10.

Maneuver Monitoring – Monitoring of Maneuver 1 was accomplished using DSS-12. Figure 3-5 shows the predicted and actual doppler shift during engine burn. Agreement was good; only a slight difference was evident near the end of the burn, due probably to a slight change in the engine thrust level.

After cutoff, the actual doppler was 3 to 4Hz above predicted but remained parallel, indicating a successful execution. Data was unavailable for approximately 50 seconds during the burn due to a temporary loss of signal caused by an antenna null condition.

Table 3-10: Maneuver Design

Requirement	Maneuver I*	Maneuver II**
ΔV	186.7 m/sec	70.54
Attitude (deg)		
Roll	+ 5.72	-88.80
Yaw	-83.78	0
Pitch	0	-91.79
Ignition time (GMT)	156:23:16:77	159:22:39:27
True anomaly (deg)	158.67	0.0
Spacecraft Constraints		
Thrust (lb)	100	100.3
Initial weight (lb)	648.3	605.0
Weight flow rate (lb/sec)	0.3623	.3634
Average acceleration (m/sec^2)	1.5648	1.674
Burn duration (sec)	119.3	42.8

Orbit Elements	Maneuver I*		Maneuver II**	
	before	after	before	after
a (km)	6148.50	4821.67	4819.67	3753.48
e	0.296444	0.624115	0.623155	0.516112
ω (deg)	9.801	354.996	353.988	354.272
Ω (deg)	116.853	116.869	77.656	77.673
i (deg)	85.147	85.071	84.562	84.395
T (min)	721.06	500.74	500.43	343.92
ha (km)	6233.09	6092.86	6084.98	3952.60
Hp (km)	2587.72	74.3	78.18	78.18

* Maneuver design used O.D. 5007-9 (Table 3-8)
** Maneuver design used O.D. 6001-9 (Table 3-8)

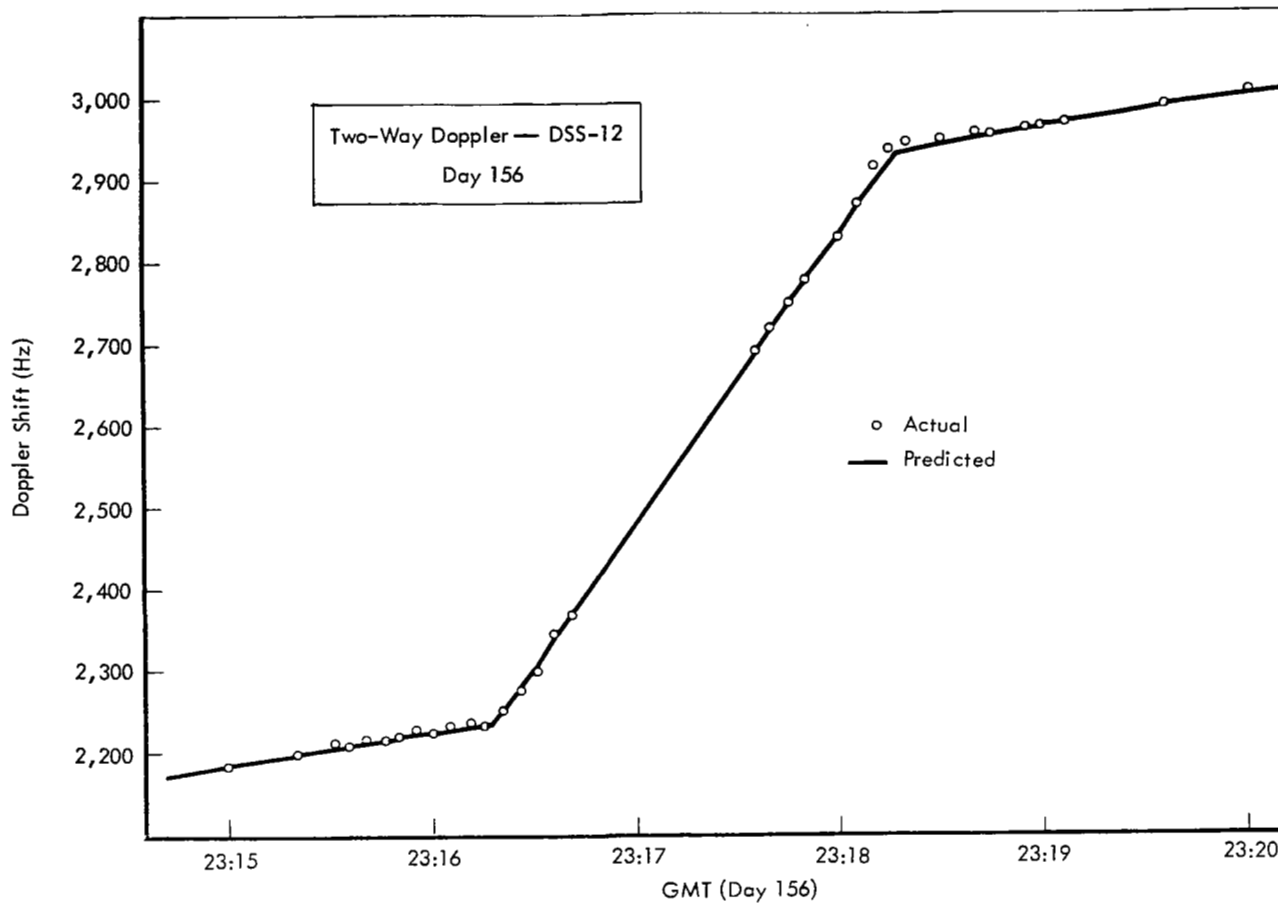

Figure 3-5: Apolune Decrease Maneuver

DSS-12 was also used to monitor Maneuver 2; the doppler plot is presented in Figure 3-6. Although predicted and actual doppler points are not coincident, the two parallel each other and indicate a successful maneuver execution. The 30-Hz bias seen before the burn was caused by epoch forwarding O.D. 6001-9 a period of 32 hours. However, only a 24-Hz bias was present after the burn. An early (approximately 1 second) engine cutoff is indicated.

Postmaneuver Analysis – Orbit determinations 6000-9 and 7000-9 show the results of Maneuvers 1 and 2, respectively. Table 3-11 is a tabulation of predicted and actual orbital elements for each engine burn.

To assess the success of the transfers, perilune altitude variations (based on the LRC 11/11 lunar gravitational model) were calculated (see Figure 3-7). The plot indicates an impact on the nearside of the Moon on October 30, 1967. Furthermore, Figure 3-8 shows the expected miss distance of Site IIP-2 on July 9, 1967. Finally, the available ΔV on board the spacecraft is 20 meters/second, sufficient to cause an impact into this area if desired.

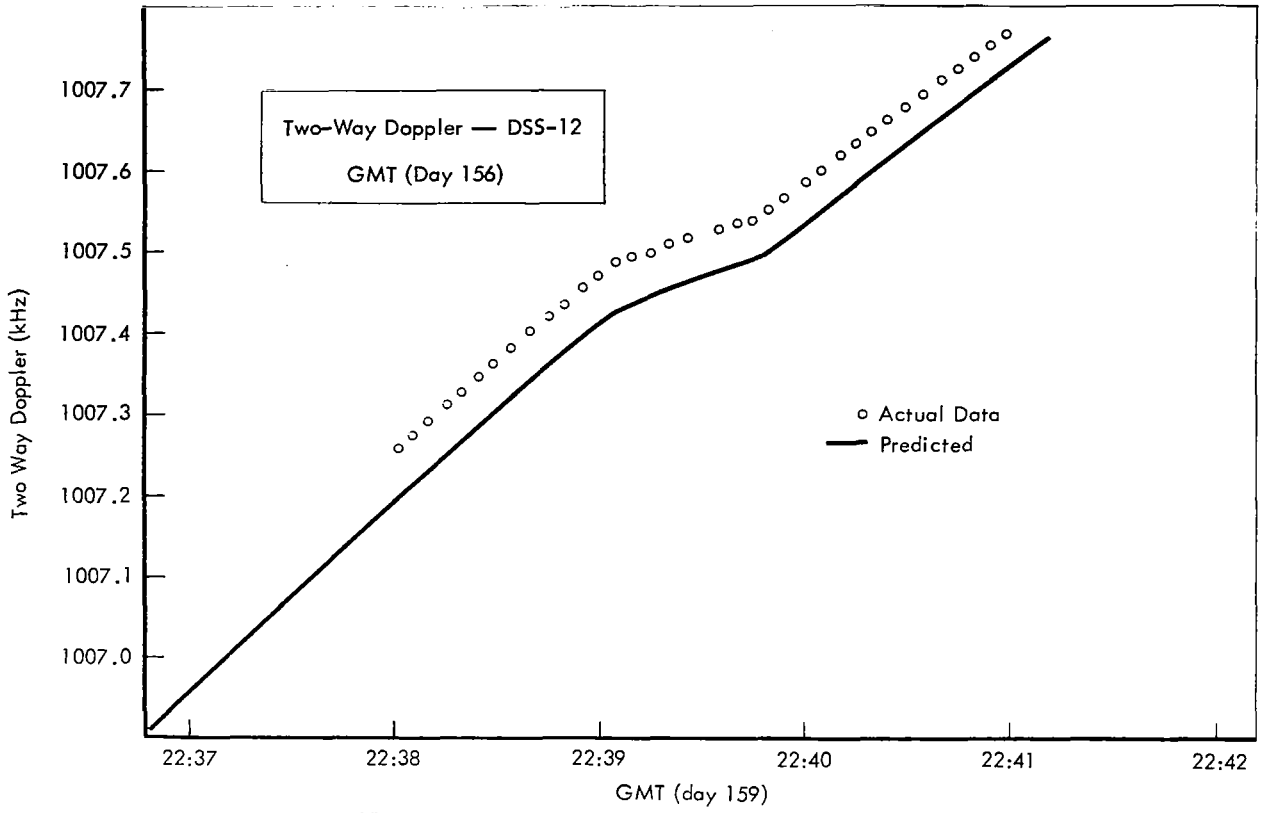

Figure 3-6: Perilune Decrease Maneuver

Table 3-11: Comparison of Predicted vs. Actual Postmaneuver Orbital Elements

	Maneuver I		Maneuver II	
	Predicted	Actual (OD 6000-9)	Predicted	Actual (OD 7000-9)
Semimajor axis (km)	4821.67	4820.58	3753.48	3751.21
Eccentricity	0.624115	0.623894	0.516112	0.516238
Argument of perilune (deg)	354.996	354.600	354.27	354.46
Longitude of ascending node (deg)	116.869	116.812	77.673	77.446
Inclination (deg)	85.071	85.082	84.395	84.399
Period (min)	500.74	500.57	343.92	343.62
Apolune altitude (km)	6092.86	6090.03	3952.60	3949.64
Perilune altitude (km)	74.30	74.96	78.18	76.61

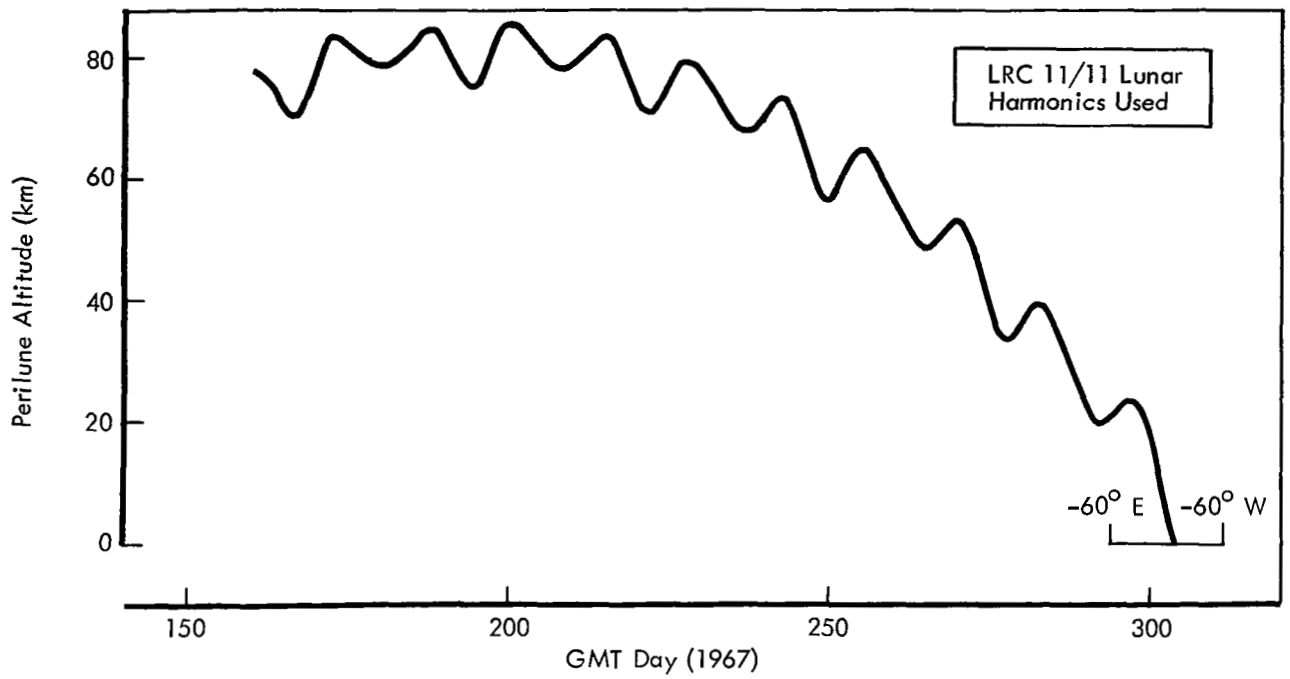

Figure 3-7: Predicted Perilune Altitude Following Perilune Decrease Maneuver

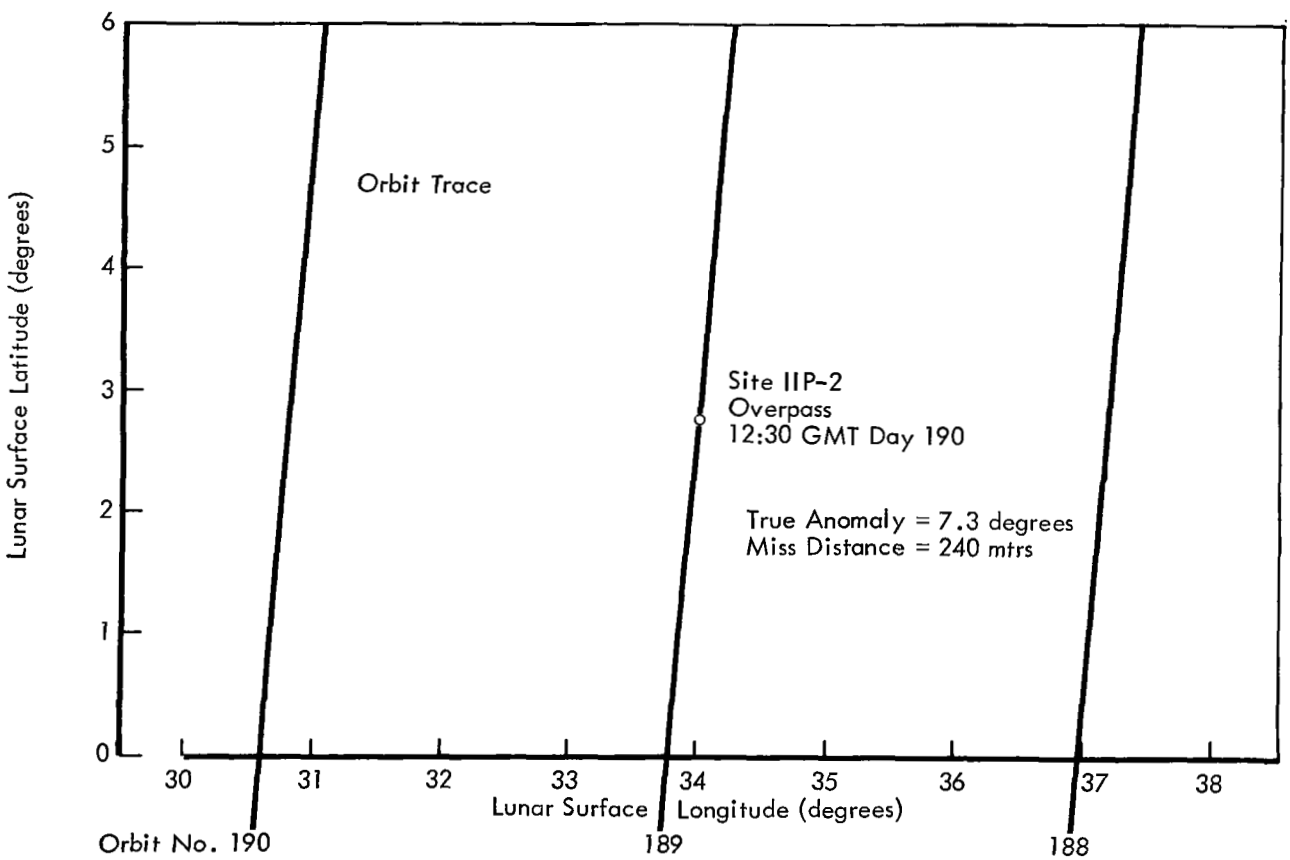

Figure 3-8: Site IIP-2 Coverage Following Perilune Decrease Maneuver

4.0 Flight Data

4.1 ENVIRONMENTAL DATA

A prime objective of the extended mission is to collect lunar environmental data during long periods of lunar flight. Spacecraft telemetry is monitored during each tracking period to determine if there has been any increase in radiation flux or micrometeoroid activity. Because the activity is frequently monitored in real time, however, the *exact* location or time is unknown.

4.1.1 Radiation

Table 4-1 shows radiation data collected during the extended mission. The scintillation counter located near the film cassette recorded 8.00 rads; the one located near the film looper recorded 66.0 at the beginning of the extended mission. Figure 4-1 illustrates the increasing radiation trend.

4.1.2 Micrometeoroids

The micrometeoroid detection system had received two hits during the prime mission; no further activity was recorded.

4.2 SPECIAL EXPERIMENTS

During the extended mission, the spacecraft was used to obtain scientific data and as a tool to conduct special experiments. Only the purpose of the experiment and the type of data collected are given in this report. Data analysis is the responsibility of the requesting agency.

4.2.1 Lunar Surface Conductivity Experiment

The purpose of this experiment was to obtain data (recordings of ground signal strength as the spacecraft occulted behind the Moon and the orbital geometry at that time) to determine the Moon's surface conductivity. The spacecraft was operating in the high-power mode at the time the data was recorded (see Table 4-2).

4.2.2 Manned Space Flight Network/Apollo Goss Navigational Qualification (MSFN/AGNQ) Support

The experiment was conducted with the Manned Space Flight Network in an effort to qualify the tracking stations for the Apollo missions. The spacecraft, used in support of Phase B of the MSFN/AGNQ program, was

Table 4-1: Radiation Data

Track Period GMT Days	Cassette Radiation (rads)	Looper Radiation (rads)
153	8.00	66.0
155	8.00	66.0
156-157	8.00	66.0
158-159	8.25	67.5
159-160	8.25	68.0
161-162	8.50	68.0
163-164	8.50	68.5
164-165	8.50	68.5
166-167	8.75	68.5
167-168	8.75	68.5
168-169	9.00	69.0
170-171	9.00	69.0
172-172	9.00	69.0
173-174	9.00	69.0
176	9.25	69.0
178	9.25	69.0
180	9.50	69.5
186-187	9.75	69.5
188	9.75	69.5

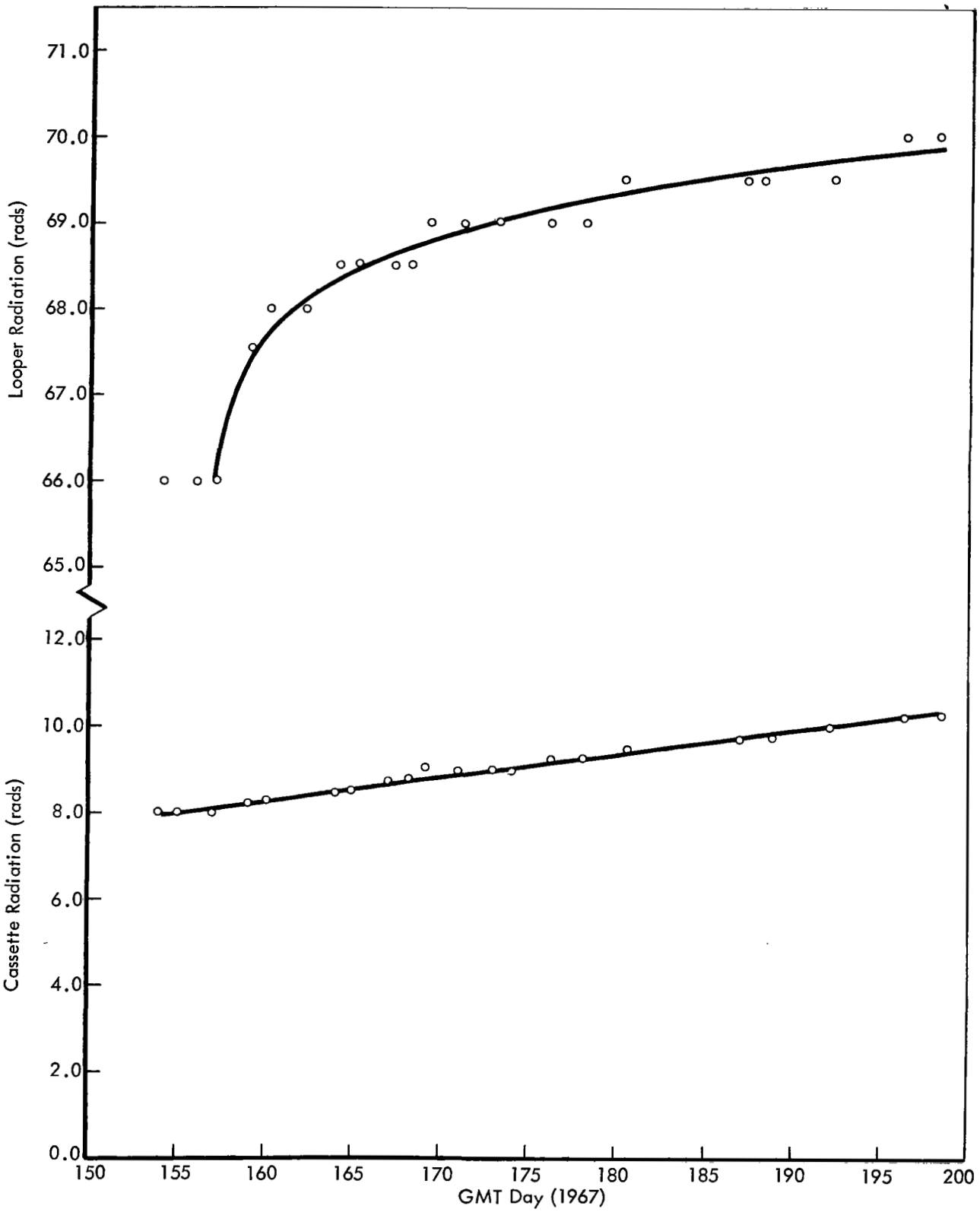

Figure 4-1: Radiation Dosage Measurement, Looper and Cassette

Table 4-2:
Lunar Surface Conductivity Data Periods

Day	GMT	DS
May 19, 1967	10:37 - 11:47	41
May 31, 1967	05:33 - 06:21	62
May 31, 1967	17:34 - 18:24	12
June 13, 1967	19:38 - 20:25	12
June 13, 1967	19:46 - 20:19	62
June 14, 1967	01:15 - 02:20	12

operated in the high-power mode with the TWTA on during the tracking exercises. The network stations tracked the spacecraft in two-way lock and practiced station-to-station handovers (see Table 4-3).

4.2.3 Voice Relay Experiment

The experiment was conducted to investigate the feasibility of relaying voice communications by a lunar orbiting spacecraft. Voice data was transmitted to the spacecraft, detected by the transponder receiver, passed through the ranging module, retransmitted to Earth, and received by the DSIF. Three male and one female voices were recorded on tape prior to the experiment to observe the reproduction quality of the voice characteristics and to maintain proper modulation index.

Two transmission methods were used during the experiments.

FM/PM — Voice from the test tape was frequency modulated onto a 40-kHz subcarrier with a peak frequency deviation of 6 kHz. The output of the 40-kHz VCO was phase-modulated onto the S-band uplink with modulation index of 1.5 radians and transmitted to the spacecraft. After turnaround by the spacecraft transponder, the S-band downlink was received by the DSIF Receiver 1. The output of Receiver 1 was fed to FR-1400 Track 3 and also to a 40-Hz discriminator. The received voice output from the subcarrier discriminator was recorded on FR-1400 Track 5 and also fed to a speaker for real-time monitoring.

PM/PM — The audio from the voice test tape was phase-modulated onto the 40-kHz subcarrier with a modulation index of 1.8 radians. The output of the 40-kHz VCO was phase-modulated onto the S-band uplink and transmitted to the spacecraft, which in turn retransmitted back to Earth. Receiver 2 was locked to the 40-kHz sideband, and the receiver phase detector output fed to a speaker and recorded on FR-1400 Track 5. The output of Receiver 1 was recorded on Track 3.

Table 4-3 MSFN/AGNQ Tracking Summary

Day	Total Tracking Time (GMT)	MSFN Three-Way Tracking (GMT)	MSFN Two-Way Tracking (GMT)	MSFN Ranging (GMT)	Number of Handovers
163/4	10:00-07:00	17:00-20:45	20:45-06:00		5
170/1	23:30-18:45	23:30-01:30	01:30-17:30	02:30-05:00	17
177/8	11:52-00:17	12:00-15:40	15:40-23:30		4
186/7	13:00-06:00	13:00-14:30	14:30-17:00	14:45-16:30	5
		17:00-00:30	00:30-05:30		
191/2	09:00-10:46	09:00-13:30	13:30-20:00	13:42-16:50	7
		02:00-05:00	05:00-10:20		

4.2.4 Ionosphere Effects Experiment

The experiment, performed to determine the effect of the Earth's ionosphere on doppler and ranging data obtained by the spacecraft, consisted of obtaining two-way doppler and ranging data on eight horizon-to-horizon passes. Lunar Orbiter IV was used for two of these tracking periods – on Day 155 from 10:59 to 23:15 GMT, and on Days 169/170 from 22:23 to 09:21 GMT. The data was compiled and transmitted to the requesting agency, Jet Propulsion Laboratory, Pasadena, California.

The spacecraft communications subsystem was in the following condition.

- TWTA on;
- Ranging modulation on;
- High-gain antenna pointed at DSS-12.

The test consisted of 10 transmission sequences. The data was collected at DSS-12 by the requesting agency.

5.0 Spacecraft Subsystem Performance

Periodic monitoring of spacecraft telemetry data provided information that was used to determine subsystem performance. The data was analyzed to show trends in performance in an attempt to establish detrimental effects on components or subsystems after exposure to space environment. The data and results are presented in this section.

5.1 SUMMARY

Individual subsystem performance was generally within design requirements; there was very little evidence of subsystem or component degradation. The *attitude control subsystem* operated normally during the extended mission, with the exception of a suspected anomaly in the plus-pitch jet one-shot, and the gyro heater loop oscillations which were evident when the EMD temperature rose above 82°F. An erratic change of yaw gyro wheel current was also noted at this time. Performance and operational parameters were unaffected and remained within design specifications. Sixty maneuvers and 17 Sun acquisitions were performed. Gyro drift and limit cycle rates were low and the limit cycle nominal. Gyro temperature was generally normal and remained close to nominal. The star tracker operated as expected – star map voltage slowly deteriorated from 2.4 to about 1.9 volts. Sun sensor operation was normal, with output variations close to that found on other missions. The control assembly performed correctly throughout the extended mission; clock error remained the same as observed during the primary mission.

The *communications subsystem* met all performance requirements. During Sun occultation with the TWTA operating, normal TWTA output was obtained at input bus voltages 1.1 volts below the minimum specification requirement of 26 v.d.c. No permanent degradation of TWTA characteristics occurred subsequent to TWTA operation at input bus voltages as low as 23.5 v.d.c. *Power subsystem* performance was normal with adequate power available at all times. Solar panel and battery degradation was less than specified in the design requirements.

The *photo subsystem* was not used during extended-mission experiments; however, a film rewind sequence was initiated. The leakage rate from the pressurization system was very low. Telemetry data from the pressure bottle indicated no leakage.

With the exception of the EMD thermal control coating, the *structures and mechanisms subsystem* performed as predicted. Degradation of the EMD thermal control coating occurred as anticipated, requiring that the spacecraft be oriented "off-Sun" to maintain proper spacecraft thermal control.

The *velocity and reaction control subsystem* performed satisfactorily. Over 33,000 thruster cycles were recorded in the pitch, yaw, and roll axes with no evidence of degraded attitude control performance. Nitrogen usage was within predicted limits for the actual maneuvers and limit cycle mode maintained. The velocity control subsystem was operated four times during the mission in accumulating a total engine burn time of 715.1 seconds. Two of these maneuvers were during the extended mission, accounting for 160.7 seconds. Each thrust vector control actuator was cycled an estimated 1,070 times in maintaining pitch and yaw attitude control in a limit cycling mode during the four engine burns. The final velocity maneuver to lower the orbit apolune was accomplished after 35 days exposure to space environment.

5.2 SUBSYSTEM PERFORMANCE

5.2.1 Attitude Control Subsystem

The attitude control subsystem consists of inertial reference, control assembly, star tracker and Sun sensor units, and a switching assembly. The inertial reference unit is a three-axis, strapdown gyro system with an accelerometer for differential velocity derivation. Inertial reference outputs consist of angular rates and position data about each of the spacecraft's three orthogonal axes, and spacecraft velocity change in line with the X axis. Subsystem control and integration is furnished by the control assembly,

which consists of a memory core, a clock oscillator, a logic system, input circuitry, and closed-loop electronics. Its primary purpose is to command the spacecraft either from stored commands or real-time commands and, through the logic system and closed-loop electronics, control the position thrusters and the engine pointing angle. The star tracker contains a photo multiplier tube for sensing Canopus presence; a bright-object sensor to operate a sun shade for protection of the photo multiplier tube; light baffles and optics; and associated electronics. Its purpose is to furnish spatial roll axis references. The sun sensors are silicon solar cells which provide spatial yaw and pitch axis reference. The switching assembly contains high-power switching circuitry and is controlled by the control assembly (see Figure 5-1). A summary of extended-mission maneuvers is given in Table 5-1.

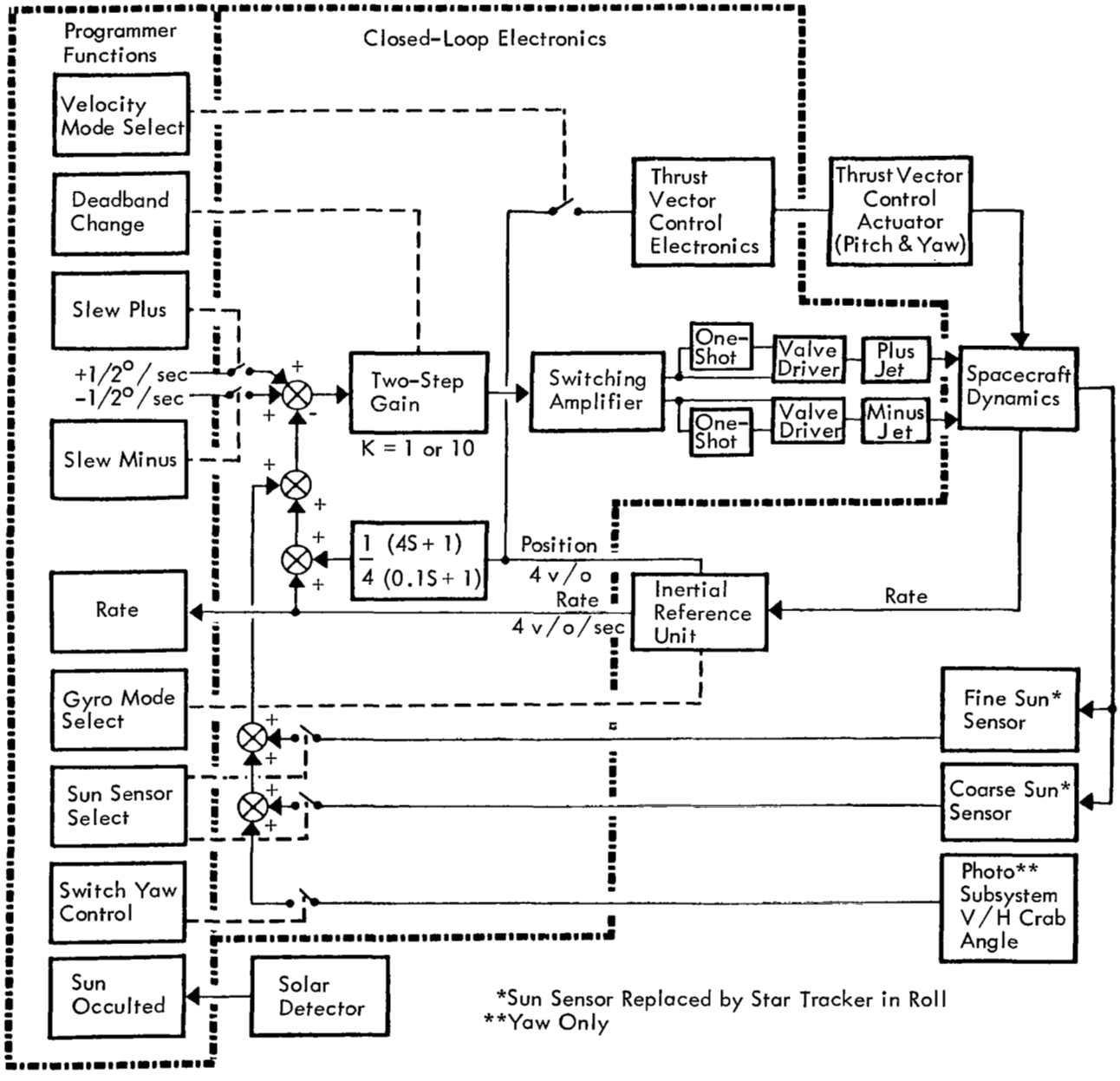

Figure 5-1: Attitude Control Subsystem

Table 5-1: Extended-Mission Maneuvers

Time D:H:M:S	Event	Magnitude (deg)	Command	Remarks
150:20:12:42	PIP	7.8	RTC	
152:12:22:41	PIM	40.5		
12:29:27	ASU			
12:45:35	ROM	1.8	RTC	
12:49:36.5	PIP	40.0	RTC	
12:28:26.5	ROP	3.24	RTC	
155:12:11:47	ASU		RTC	
13:10:32	PIP	95.0		Battery deepdischarge test
14:08:08	PIM	95.0		
14:12:12	ASU			Spacecraft three-axis drift test
14:20:48	PIP	0.011	RTC	
16:52:29	ROP	3.35		
17:08:14	PIP	40.0		
156:15:25:19	PIM	37.5		
15:28:00	ASU			
15:51:00	ROM	0.55	RTC	
16:05:15	PIP	40.0		
21:50:28	PIM	39.3		
21:52:46	ASU			
23:01:35	ROP	5.7		Attitude change for orbit transfer
23:02:27	YAM	83.78		
23:16:16	CDZ			
23:16:16	ΔV			186.72 m/sec
23:19:10	CDZ*			

Table 5-1 (Continued)

Time D:H:M:S	Event	Magnitude (deg)	Command	Remarks
23:19:10	YAP	83.78		
23:22:49	ROM	5.7		
23:25:19	ASU			
23:45:40	ROP	3.2	RTC	
157:00:03:20	YAP	0.5	RTC	
00:07:57	PIP	40.0		
158:17:32:25	PIM	36.0		
17:36:39	ASU			
18:00:19	ROP	0.4	RTC	
18:16:12	PIP	40.0		
159:18:10	PIM	37.4		
18:12:07	ASU			
18:34	PIP	40.0	RTC	
21:00:00	PIM	39.5		
21:19:00	ROM	0.33		
22:22:09	ROM	88.8		Attitude change for orbit transfer
22:25:58	PIM	91.78		
22:39:03	CDZ			
22:39:46	ΔV			70.53 m/sec
22:40:37	CDZ*			
22:43:41	PIP	91.8		
22:44:32	ROP	88.8		
159:22:49:13	ASU			
23:19:56	PIP	45.1		

Table 5-1 (Continued)

Time D:H:M:S	Event	Magnitude (deg)	Command	Remarks
161:23:00	PIP	5.0	RTC	
163:15:15	CDZ			(BOS-glint test)
15:15	PIM	36.0		
15:26	ASU			
15:30	YAM	15.0		
15:38	YAP	15.0		
15:41	ASU			
15:44	YAP	17.0		
15:53	PIM	20.0		
16:02	PIP	40.0		
16:12	PIM	20.0		
16:21	YAM	17.0	.0	
16:27	ASU			
16:30	PIP	45.1		
164:23:42	ROP	4.0	RTC	
165:06:14	PIP	10.0	RTC	
167:04:20	ASU		RTC	
04:28	ROP	5.0	RTC	
04:50	PIM	40.0	RTC	
22:14	ASU		RTC	
22:54	PIM	40.0	RTC	
171:00:27	ASU		RTC	
00:48	PIM	40.0	RTC	
177:13:10	ROP	14.0	RTC	

Table 5-1 (Continued)

Time D:H:M:S	Event	Magnitude (deg)	Command	Remarks
186:13:15	ROP	10	RTC	
13:59	YAM	4	RTC	
14:09	ROP	5	RTC	
17:40	ASU			Thermal test and Canopus tracker test
17:57	ROP	10	RTC	
18:29	ROP	7	RTC	
18:58	ROM	5	RTC	
19:07	YAP	3	RTC	
19:18	ROM	5	RTC	
19:34	CDZ*		RTC	
19:42	ROP	10	RTC	
20:16	ASU		RTC	
22:11	CDZ		RTC	
22:15	PIM	45	RTC	
191:10:53	YAM	4	RTC	
▷ 202:09:00				DSS unable to acquire
▷ 202:11:22	ROM	50		To correct possible antenna null
▷ 202:21:23	ASU			
▷ 202:23:11	ASU			
▷ 202:23:24	PIM	45		
202:23:26	CDZ			

▷ There is no indication that commands were performed by spacecraft.

5.2.1.1 Inertial Reference Unit

Performance of the inertial reference unit was nominal, although a heater loop oscillation was observed when the EMD temperature exceeded 82°F. An erratic change in the yaw gyro wheel current telemetry signal was also observed. The temperature oscillation, which was noted during the photographic mission and apparently had no effect on IRU performance parameters, was noted during test on other units and is attributed to interaction between the internal telemetry signals of the accelerometer heater loop and gyro heater loop. An erratic oscillation of yaw gyro wheel current appeared on Day 171, 14:42 GMT when the current jumped two bits between successive telemetry frames. Heretofore, the maximum change noted had been the normal one-count variation due to the analog value being at the decision point of the analog-to-digital converter. The same phenomenon was also observed on Day 186 at 13:20 GMT when it appeared as a continuous oscillation and persisted for most of the tracking period over a wide range of spacecraft conditions and temperatures. A time history of wheel currents, gyro temperature, and EMD temperature during the tracking period is shown in Figures 5-2 and 5-3. The oscillation in Figure 5-2 appears to be sensitive to EMD temperatures, particularly to the abrupt changes in heat flow conditions resulting from Sun acquisition (186:17:40) and the two sunset

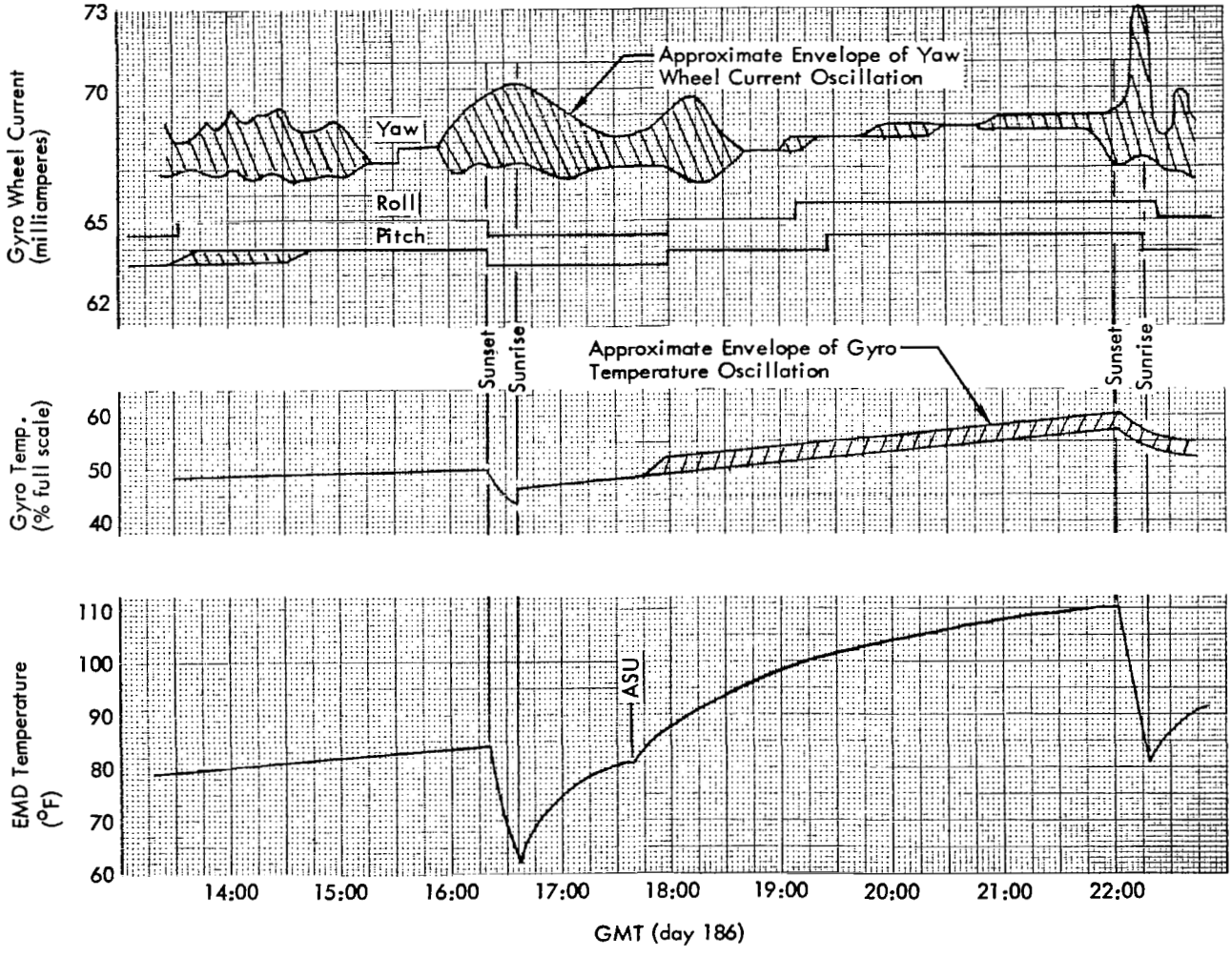

Figure 5-2: Gyro Wheel Current

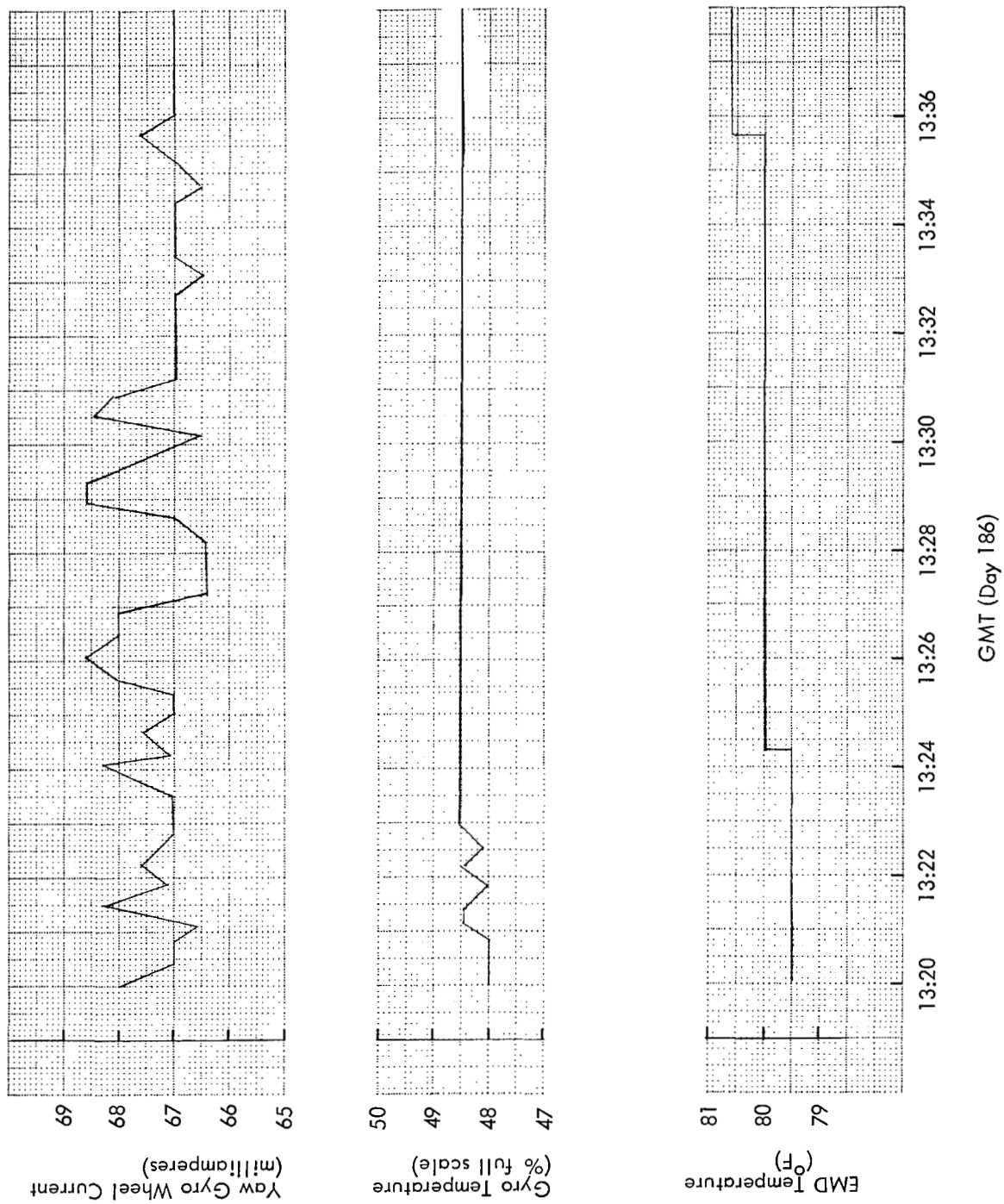

Figure 5-3: Yaw Gyro Wheel Current

periods. The maximum oscillation envelope occurs when telemetry point STO3 reaches 110°F.

Figure 5-3 shows the oscillations on an expanded time scale. A similar pattern was observed during test. The oscillations occurred during 100% heater operation; the cause was attributed to heater loop oscillation coupling into the wheel current telemetry. However, the yaw gyro wheel current oscillations had no discernible effect on gyro performance and the wheel current telemetry returned to normal after Day 186. Wheel current data was normal throughout the remainder of the extended mission. Table 5-2 depicts initial and final values of wheel current for each axis over the extended mission.

Table 5-2:
Wheel Currents (milliamps)

	Initial	Final	Maximum Variation
Roll	64.9	64.4	1.5
Pitch	62.8	63.0	1.5
Yaw	66.0	65.4	8.1

A plot of IRU temperature versus time is shown in Figure 5-4 along with the EMD temperature closest to the gyro. Gyro temperature is a pseudotemperature output signal derived from the addition of error signals in the roll, pitch, and yaw gyro heater control circuits plus the accelerometer heater circuits, and is somewhat dependent on spacecraft bus voltage. The temperature control circuits are used to stabilize the viscosity and density of the gyro and accelerometer flotation fluid. The measurement is expressed in percent of full scale from 0 to 100%, corresponding to the telemetry range of 0 to 5 volts. The approximate indicated IRU temperature range for 0 to 100% is 142.5 to 147.5°F. The gyro heater control circuits are normally off when the IRU temperature goes above 100% and the IRU temperature increases at a 1:1 rate with increase in spacecraft EMD temperature.

Figure 5-4 shows there is a wide temperature variation as the EMD oscillates into and out of sunlight. Despite these large variations, the gyro temperatures are controlled within a rela-

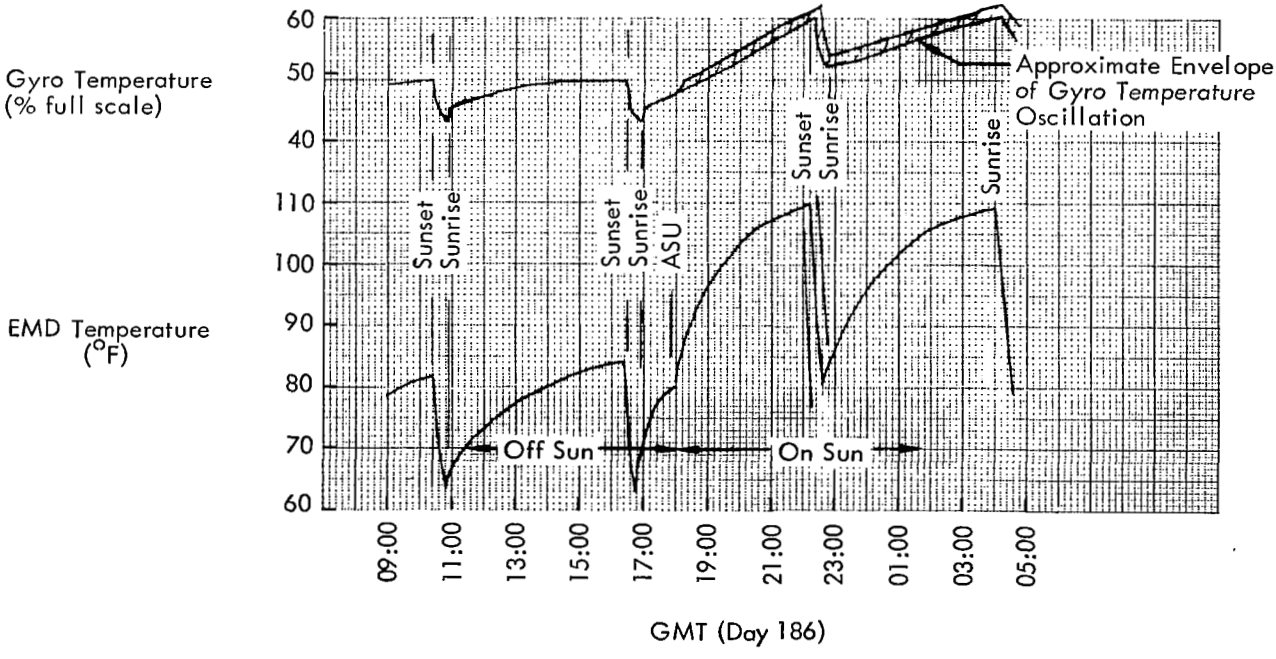

Figure 5-4: IRU and EMD Temperature vs Time

tively constant range by the gyro heater circuits; however, high EMD temperatures resulted in small gyro temperature oscillations on telemetry only. Gyro temperature throughout the extended mission was consistent and corresponded with EMD temperature changes.

Low and stable IRU drift rates contributed to a successful photographic mission and efficient nitrogen gas usage throughout the extended mission. Figure 5-5 depicts the trend of IRU drift from launch through the extended mission.

There is close correlation between test values at launch and those obtained in space. The extremely low values of drift permitted the use of long wait times between Sun and Canopus updates during the extended mission; this conserved gas and reduced the number of programmer updates and amount of DSN observation time.

The attitude control subsystem performed 60 maneuvers and 17 Sun acquisition sequences during the extended mission (see Table 5-3). Maneuver and Sun acquisition rates were within design tolerances. The limit cycle was observed to be accurately controlled within nominal limits, depending on the operational mode at the particular line. The ±12-degree deadband (2-degree deadband, coarse sun sensors only) was not used. There were no maneuvers attempted that would allow calculation of maneuver accuracies (an attitude gas savings criteria, not a performance constraint).

Drift rates while pitched off the Sun in wide deadband appeared to be significantly different from narrow deadband rates; this is explained by the larger gyro error encountered in wide deadband operation due to being farther away from gyro null. Table 5-4 summarizes the measured narrow deadband drift rates and the estimated wide deadband drift rates during off-Sun operation.

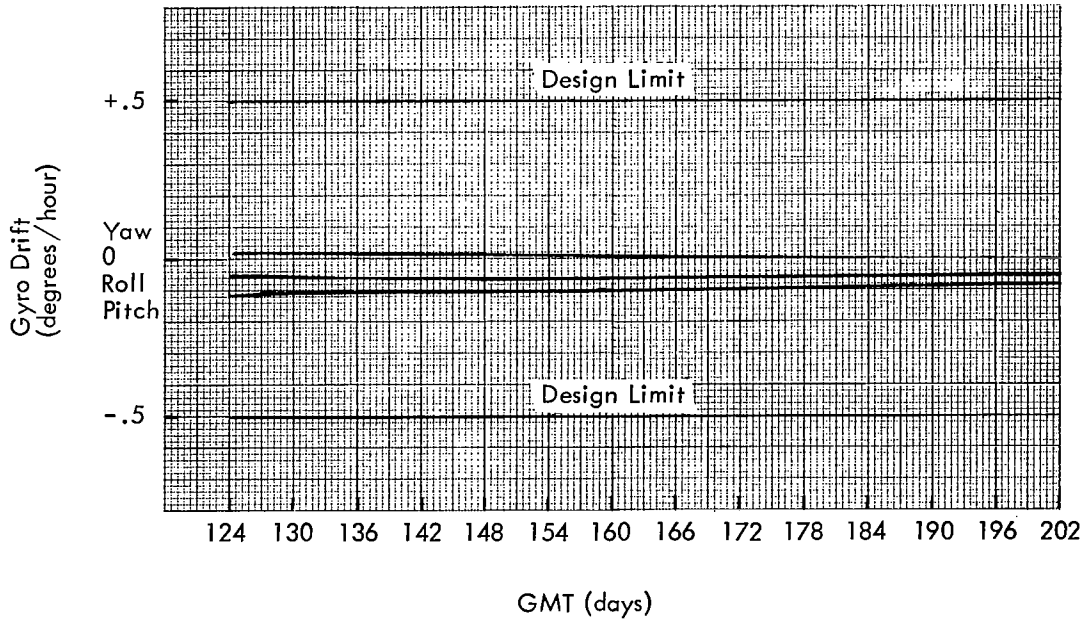

Figure 5-5: IRU Drift

Table 5-3: Maneuver Summary

0.2-Degree Deadband		2.0-Degree Deadband	
Number Maneuvers	Typical Rate (degree/sec)	Number Maneuvers	Typical Rate (degree/sec)
Roll 12	0.55 ± 0.05	Roll 9	0.050-0.059
Pitch 19	0.55 ± 0.05	Pitch 10	0.066-0.093
Yaw 3	0.55 ± 0.05	Yaw 7	0.050-0.094
ASU 10	0.55 ± 0.05	ASU 7	0.16

Table 5-4: Drift Rates

	0.2-Degree Deadband	2.0-Degree Deadband	
		Pitch + 40 degrees	Pitch −40 degrees
	(degree/hr)		(degree/hr)
Roll	−0.065		−0.11
Pitch	−0.10	−0.11	0.00
Yaw	+0.01	−0.03	+0.03

Figure 5-6 depicts the steady-state attitude history of the spacecraft during the extended mission. Because of axis cross-coupling and changing solar pressure conditions, the attitude-versus-time-curve slopes do not completely match the drift values in Table 5-4. The average drift rates during the extended mission were roll, -0.056 degree per hour; pitch, -0.055 degree per hour; and yaw, -0.004 degree per hour. The close correlation of these rates is shown in Table 5-4.

5.2.1.2 Star Tracker

The Canopus star tracker, which continued to operate satisfactorily for the extended mission, was cycled on and off 32 times for a total operating time of 11 hours, 3 minutes. Including the photographic mission, the tracker was on a total of 39 hours, 49 minutes and was operated through 145 on-off cycles. In most instances, the tracker was not normally used in the closed-loop mode; however, roll error was derived from star tracker telemetry data and updated in real time. The star tracker performed as designed when it was operated in the closed-loop mode (command "acquire Canopus" given). Table 5-5 summarizes star tracker operation during the extended mission.

Figure 5-7 contrasts star map voltage versus accumulated time for the Canopus tracker. The tracker ended the extended mission with a star map output of 2.4 to 2.30 volts. The initial star map voltage was 2.50 volts, which decayed to 2.1 volts at the start of the photographic mission, but recovered to 2.4 volts by the start of the extended mission. There is a small amount of degradation observable in star map output on Days 167 and 186 caused by the 2- to 3-hour exposure of the photomultiplier tube to stray light during the glint tests. This phenomena was detected during the qualification test of the

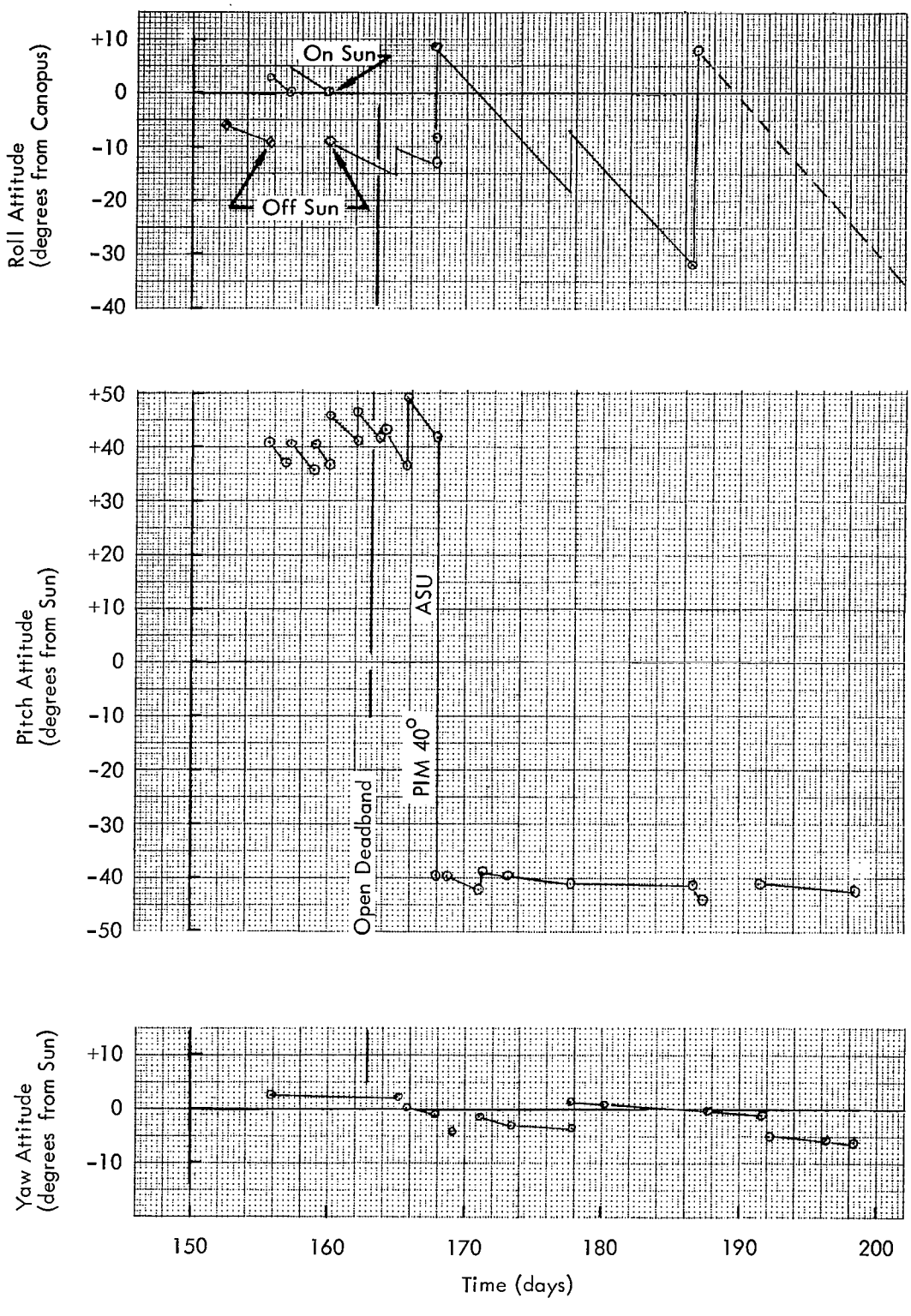

Figure 5-6: Spacecraft Attitude History

Table 5-5:
Star Tracker History

GMT Time On (day:hr:min)	Accumulated Time (hr:min)	Star Map Voltage (volts)	Accumulated (cycles)
155:12:14	00:08	2.24	1
14:13	2:54	2.36	2
17:02	2:57	2.32	3
156:15:29	3:30	2.32	4
21:56	4:19	2.32	5
23:28	4:44	2.30	6
23:55	4:56	2.10	7
158:17:40	5:28	2.38	8
159:18:13	5:45	2.40	9
21:05	5:59	2.38	10
22:53	6:26	BOS closed (test)	11
163:15:27	7:29	Glint (test)	12
167:04:26	7:36	Glint (test)	13
04:34	7:41	Glint (test)	14
04:42	7:46	Glint (test)	15
22:21	8:17	2.08 (test)	16
171:00:36	8:28	Glint (test)	17
186:17:50	8:53	Glint (test)	18
18:17	9:13	Glint (test)	19
18:39	9:37	Glint (test)	20
186:19:24	9:44	Glint (test)	21
19:32	10:09	Glint (test)	22
19:38	10:19	1.70 (test)	23
20:10	10:31	1.78 (test)	24
20:24	10:38	Glint (test)	25
20:45	10:42	1.90 (test)	26
21:05	10:46	Glint (test)	27
21:32	10:49	1.90 (test)	28
21:43	10:50	1.88 (test)	29
21:52	10:54	Glint (test)	30
21:59	11:03	1.80 (test)	31

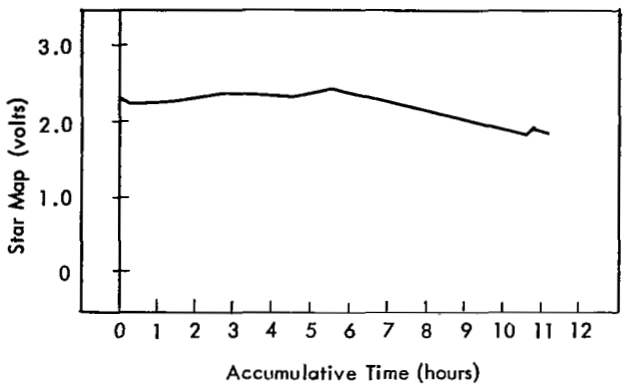

Figure 5-7: Canopus Tracker Performance

star tracker and is a temporary situation because the photomultiplier tube will recover when left off, or not exposed to stray light. The large number of times glint was evident (see Table 5-5) was caused by tests for glint affecting the tracker. The results of these tests are described later in the report.

5.2.1.3 Sun Sensors

Yaw sun sensor output voltage at a pitch angle of 30 degrees was approximately 75% of the voltage when oriented on the Sun. The values corresponded with those of previous missions; however, the predicted change was 86%. The difference of 11% was masking effect due to sensor construction and was not detrimental to the mission. The sun sensor narrow- and wide-deadband limits (see Table 5-8) are within specification.

Figure 5-8 shows calibration values for the plus coarse pitch limits at + 31.5 degrees and minus

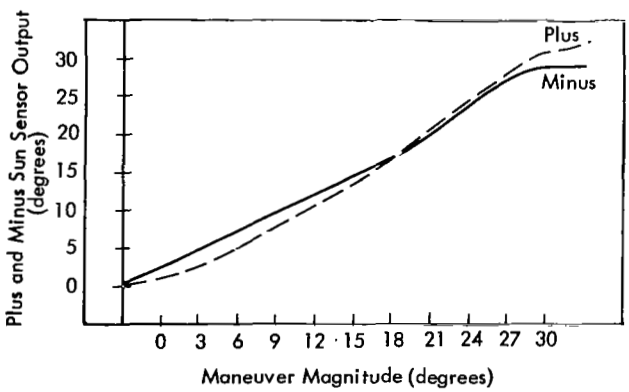

Figure 5-8: Coarse Sun Sensor Calibration

Table 5-6: Sun Sensor Limit

Mission	+ Pitch (degrees)	– Pitch (degrees)
I	Not available	26 (hard)
II	29 (soft)	26 (hard)
III	29 (soft)	29 (hard)
IV	31.5 (soft)	28 (hard)

coarse pitch limits at −27.8 degrees. The expected limit is 25 ± 3.75 degrees. The plus curve shows a softer limit than the minus curve, as was the case for Missions II and III. The fact that the limiting value is high leads to slightly higher pitch rates during the Sun acquisition, but any increase in nitrogen consumption at the higher rate is negligible. A calibration curve for the coarse yaw sun sensor was not made because maneuvers were not required where this data was available. A comparison of pitch limits with previous missions is shown in Table 5-6.

5.2.1.4 Closed-Loop Electronics

The closed-loop electronics performed satisfactorily. The thrust vector control actuator position during the extended-mission velocity maneuvers was normal. Table 5-7 shows the starting and ending positions, and the total range of commanded actuator position.

Table 5-7: Commanded Actuator Position

Day		156:23:16	
	Start	End	Range
Pitch	+ 0.003	+0.003	−0.042/+0.249
Yaw	+0.198	+0.033	+0.198/+0.060
Day		159:22:40	
	Start	End	Range
	−0.019	−0.019	+0.003/−0.019
	+0.060	+0.083	+0.060/+0.129

The accuracy of position error deadbands is shown in Table 5-8 for the various position error channels of the attitude control subsystem. There was no offset (except when solar pressure due to off-Sun operation resulted in the spacecraft staying on one switching line). There is extremely close agreement with the design values with no evidence of degradation during flight.

One-Shot Multivibrator Anomaly – The failure of the one-shot multivibrator noted during the primary mission continued into the extended mission without detrimental effects on either subsystem performance or nitrogen gas utilization. Typical examples of the phenomena which are characterized by indications of thruster firings without detectable changes in spacecraft attitude are shown in Figures 5-9 and 5-10.

5.2.1.5 Control Assembly

During the extended mission the control assembly responded correctly to every received and stored-program command.

A total of 656 commands was transmitted and executed during the extended mission. Since many of these are repetitive, the programmer actually executed some 3,200 commands. Moreover, the programmer cycled 40 million times and accumulated 4 million clock incrementations while directing spacecraft operation. The total clock error as of Day 198 was plus 2.30 seconds for a slope of 1.32 milliseconds per hour. This drift is well within the design tolerance of 3.4 milliseconds per hour.

5.2.1.6 Switching Assembly

The switching assembly was not used during the extended mission except for velocity maneuvers and firing of the nitrogen isolation squib. Performance was normal. No anomalies were observed in the spacecraft telemetry data that would indicate a switching assembly problem.

5.2.1.7 Nitrogen Isolation Squib Firing

The nitrogen isolation squib was fired on Day 156. The star tracker was left on during this event and telemetry monitored. Figure 5-10 shows the roll attitude, tracker outputs, and yaw and pitch rates. The tracker roll error shows a disturbance sometime after the squib was fired (the exact time of the disturbance is impossible to fix due to the 23 seconds between signals). The star map shows a disturbance approximately 12 seconds after the squib was fired. There also appears to be a related disturbance on the yaw axis. While no definite cause-effect relationship has been substantiated explaining the squib-tracker interaction, the observed delay along with data from Mission V where nothing occurred during squib firing, suggests something such as particles emitted into the view of the tracker could account for the problem.

Table 5-8: Position Error Deadband Limits

Position Error	Deadband Limits (degrees)			
Channel Designation	Narrow Deadband		Wide Deadband	
	Plus	Minus	Plus	Minus
Attitude Control Specification	0.18 ± 0.03	0.18 ± 0.03	1.90 ± 0.19	1.90 ± 0.19
Roll Position	0.165 ± 0.005	0.178 ± 0.01	1.96 ± 0.05	1.97 ± 0.03
Pitch Position	0.162 ± 0.01	0.195 ± 0.01	1.90 ± 0.05	1.97 ± 0.03
Yaw Position	0.19 ± 0.01	0.18 ± 0.02	1.93 ± 0.05	2.02 ± 0.06
Sun Sensor Pitch Position	0.20 ± 0.01	0.198±0.05	1.98 ± 0.04	1.97 ± 0.02
Sun Sensor Yaw Position	0.029±0.04	0.198 ± 0.02	1.98 ± 0.03	1.92 ± 0.03

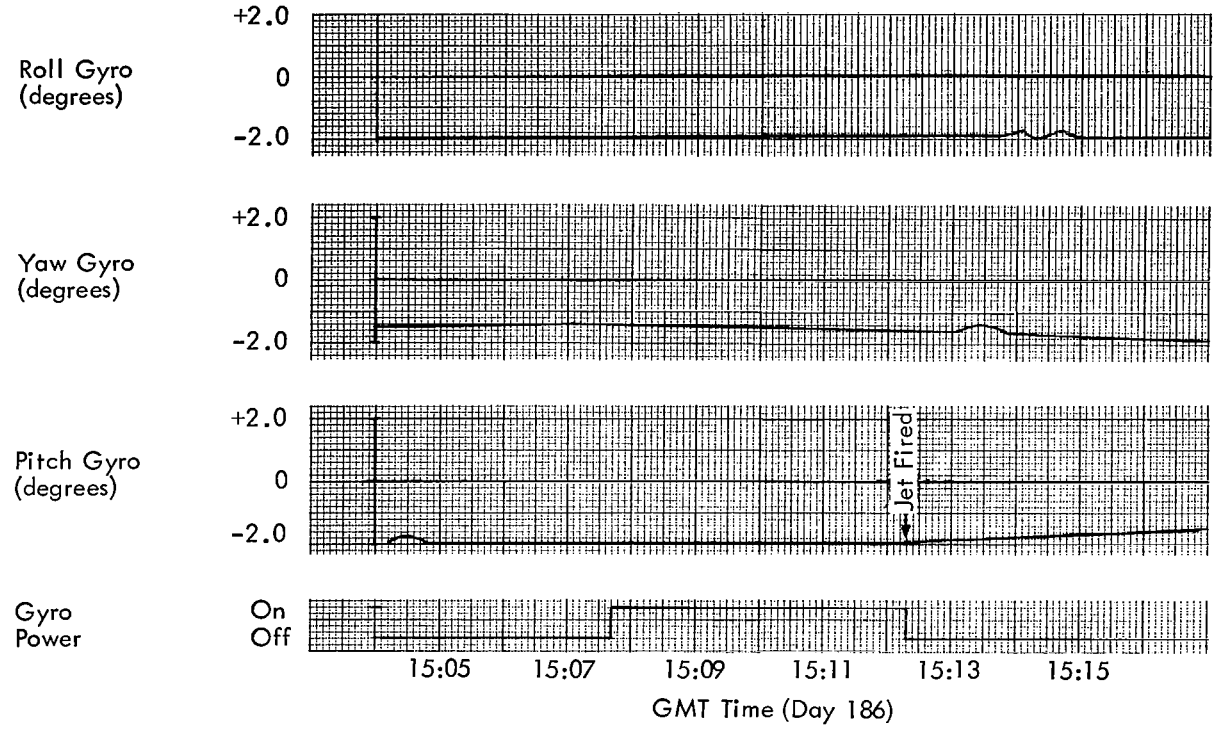

Figure 5-9: Pitch Jet Firing

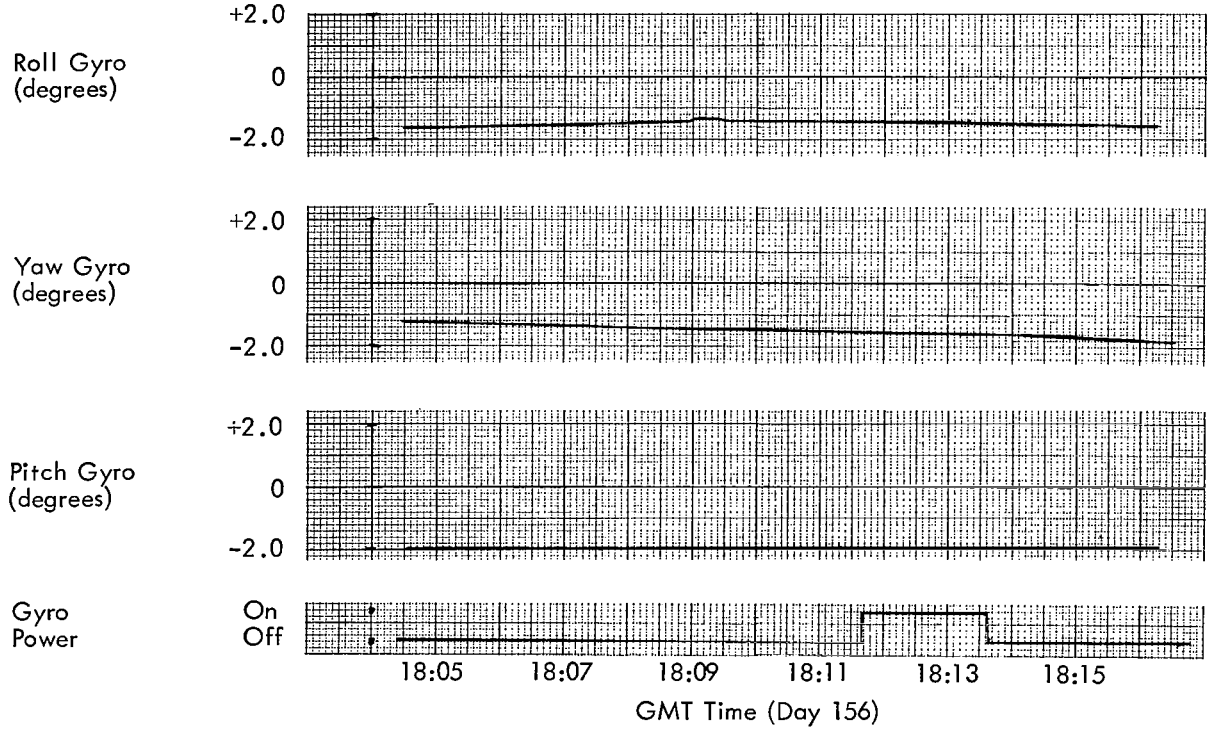

Figure 5-10: Pitch Jet Anomaly

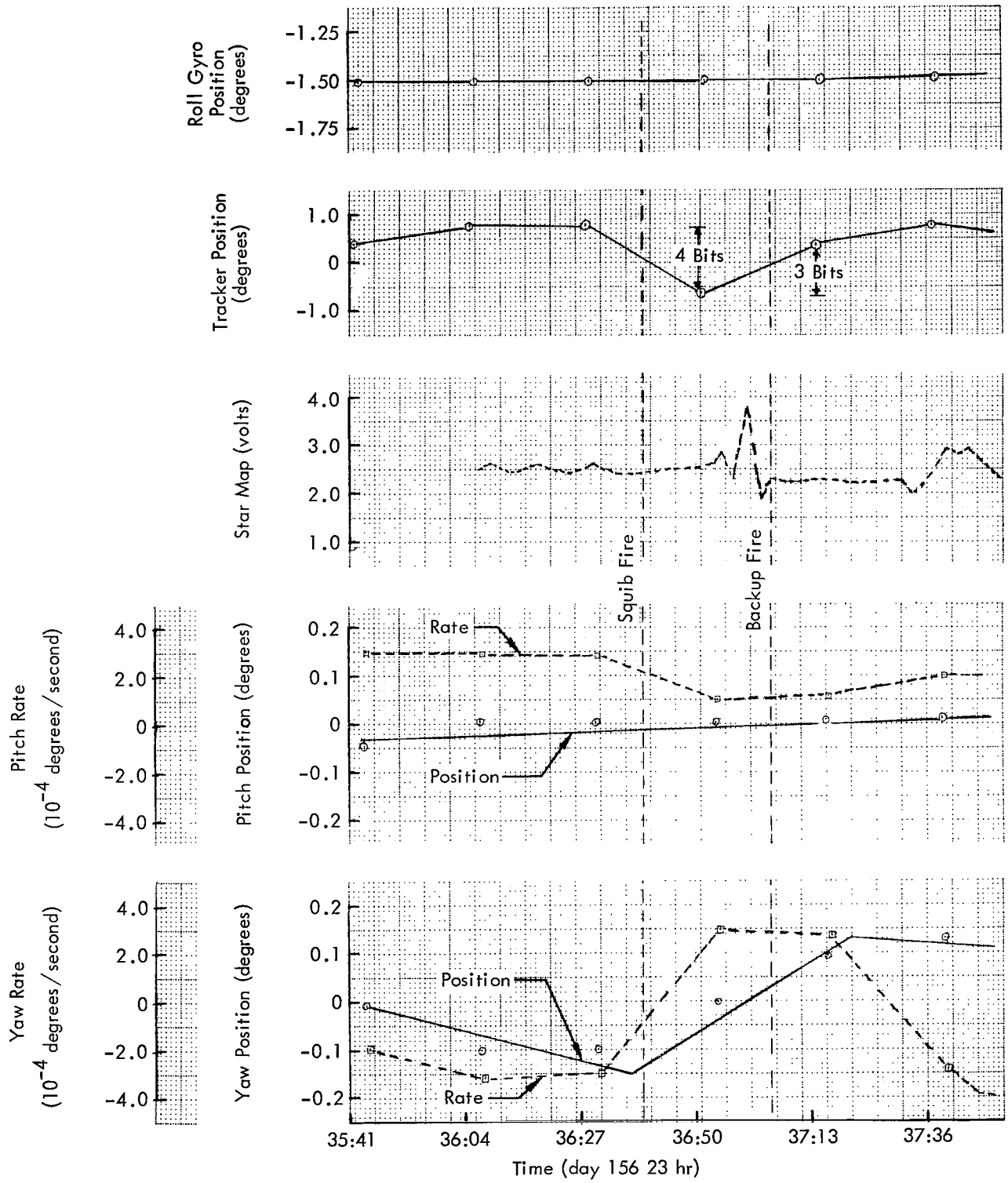

Figure 5-11: N_2 Isolation Squib Firing

5.2.1.8 Spacecraft Loss

The last observation was on Day 198. Several attempts were made by the DSN to establish communication; however, the spacecraft could not be acquired as of Day 202. Table 5-9 depicts the state of the attitude control subsystem at the time of last contact.

Table 5-9:
Attitude Control Subsystem Condition

Attitude	
Roll	= −24 degrees
Pitch	= −40 degrees
Yaw	= − 6 degrees
Inertial Reference Unit	
Gyro Drift Rate	
Roll	= −0.11 degree/hour
Pitch	= Negligible
Yaw	= +0.03 degree hour
Wheel Current	
Roll	64.4 milliamps (Inertial Hold)
Pitch	63.8 milliamps (Inertial Hold)
Yaw	65.4 milliamps (Inertial Hold)
Temp.	48.8% Full Scale
Canopus Tracker	Off
Sun Sensors Coarse	On
Fine	On
Control Assembly Wait Time	= 29 hours
Deadband	= 2.0 degrees

5.2.2 Communications Subsystem

The communications subsystem (see Figure 5-12) consists of the equipment which: (1) receives information from the ground via an rf link and converts this information to a form suitable for use by the spacecraft; (2) receives information from the spacecraft (telemetry and video), converts this information to modulation on an rf carrier, and transmits this modulated rf carrier to the ground; (3) receives ranging information from the ground via rf link, modulates this information on an rf carrier, and retransmits this to the ground for use in range determination; and (4) establishes a specific ratio between the received rf frequency from the ground and the spacecraft transmitted frequency for accurate determination of the spacecraft velocity using doppler information.

The communications subsystem operated nominally throughout the extended mission while performing the following functions.

Command Capability — The command loop received, verified, and executed 656 commands without error; the use of command decoder redundant command register was never required. The communications subsystem responded to all operational commands as directed.

Spacecraft Performance Information — Telemetry data from all spacecraft subsystem transducers were compiled and transmitted with desired accuracy.

Lunar Environment Information — As a primary objective of the extended mission, radiation and micrometeoroid data were provided by the communications subsystem throughout the extended mission.

Photographic Information — Although the communications subsystem maintained this capability, no video data was transmitted during the extended mission.

Selenodetic Information — Ranging and coherent doppler data with one and two tracking stations were successfully provided throughout the extended mission. Time correlation between tracking stations was accomplished using the ranging system.

5.2.2.1 Transponder

The transponder operated satisfactorily throughout the extended mission. Telemetry indication of transponder rf power output variations with transponder temperature and equipment mount-

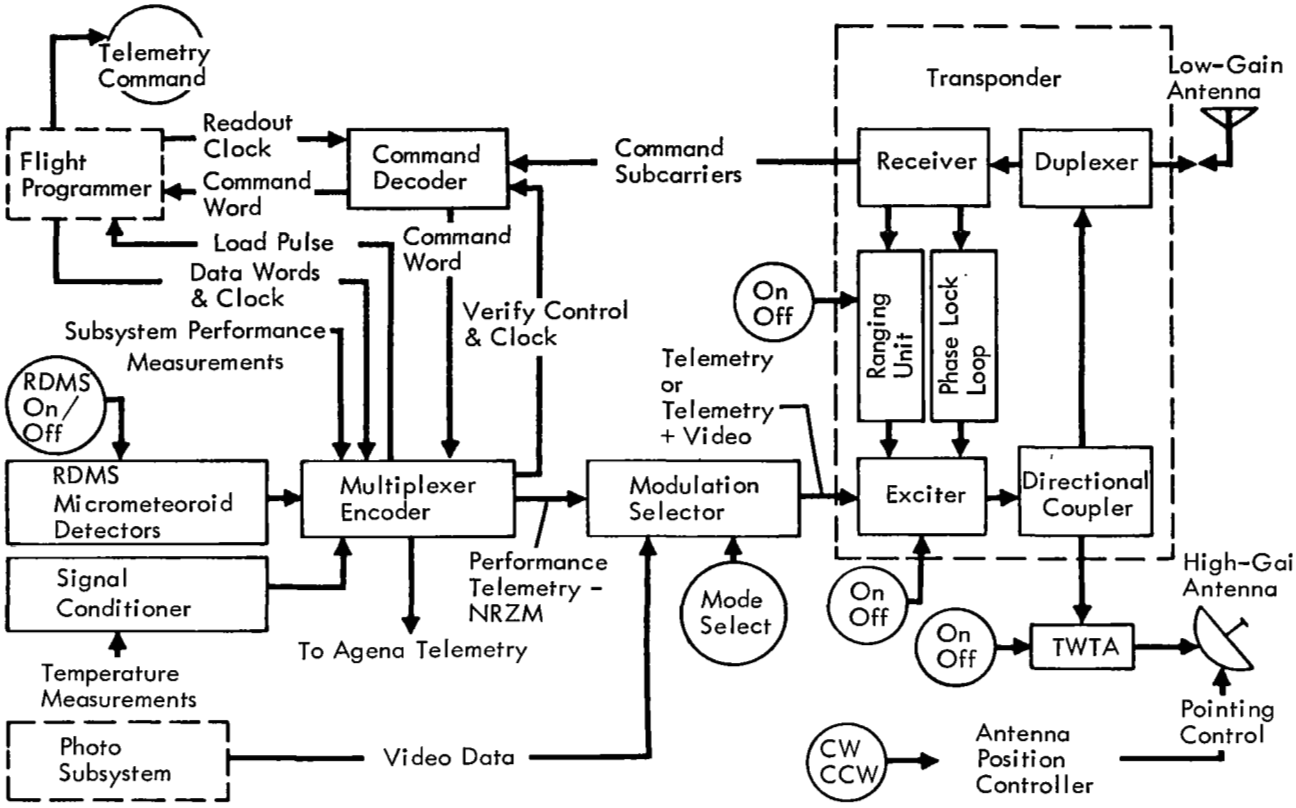

Figure 5-12: Communication Subsystem

ing deck temperature is shown in Figures 5-13 and 5-14, respectively. The decrease in power output with increasing temperature is normal and compares favorably with the flight acceptance test (FAT) data. Actual power output variation is only about one-third to one-half that indicated by telemetry due to the temperature sensitivity of the transponder power output signal sampler. Figure 5-15 portrays typical transponder rf power output versus transponder temperature during the extended mission. Exceptional correlation exists between telemetry indicated power output and temperature.

For constant uplink rf carrier power with no command or ranging modulation present, trans-

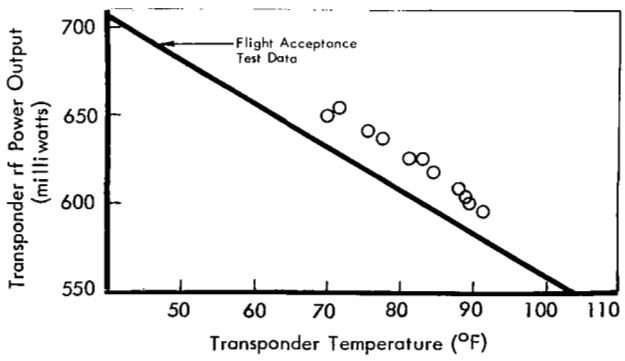

Figure 5-13: Transponder Temperature

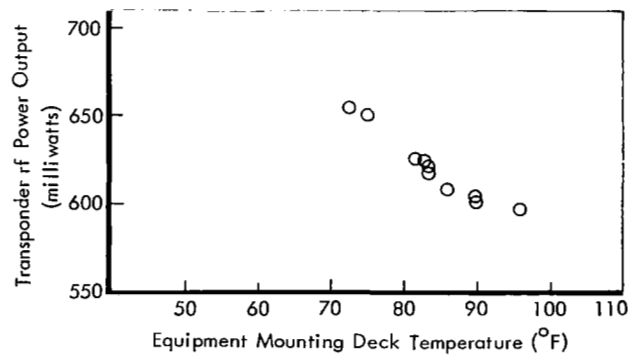

Figure 5-14: Equipment Mount Deck Temperature

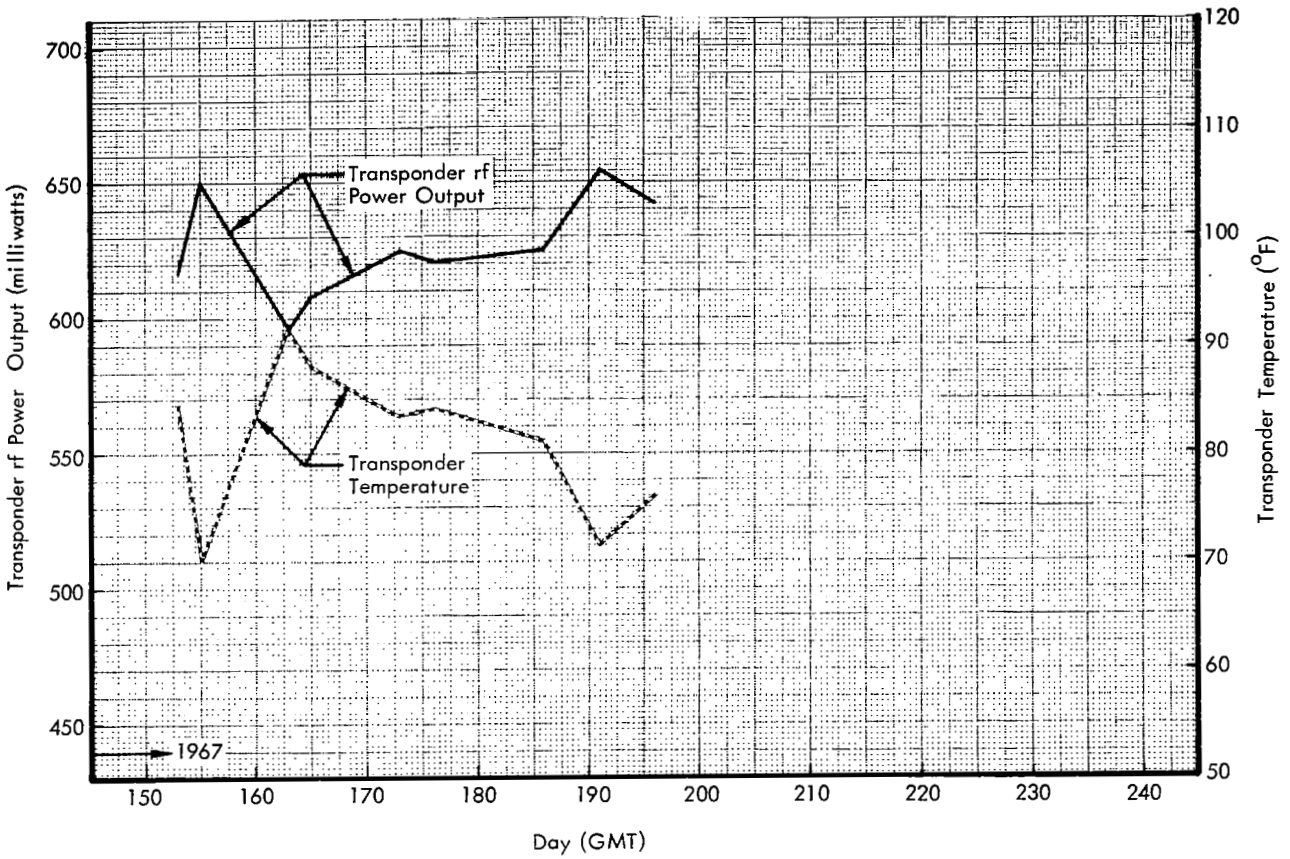

Figure 5-15: Transponder Power

ponder AGC remained within ± 2 dbm during this extended mission. The transponder ranging module was "on" throughout the extended mission and approximately 80 hours of ranging data were obtained.

No problems were encountered with ground received signal strength and the transponder fulfilled all design requirements.

5.2.2.2 Traveling-Wave-Tube Amplifier
The TWTA provided a high-power signal for extended-mission exercises and tracking data for MSFN stations. The TWTA was operated in an "on" state during seven Sun occultation periods. Two of these periods lasted about 14 minutes; five lasted about 18 minutes. At the end of the extended mission on Day 198, the TWTA had been cycled on and off four times and had accumulated an operating time of 494 hours, totaling 1,010 hours during the spacecraft life. TWTA operation throughout the extended mission was nominal as indicated by Figure 5-16. Additional data on TWTA performance at reduced input voltage are presented in Section 5.3.

5.2.2.3 Command Decoder
The command decoder performed as planned throughout the extended mission; there were no errors in any of the verified words that were executed into the flight programmer.

5.2.2.4 Modulation Selector
Operation of the modulation selector was very satisfactory. The subcarrier frequencies for Modes 1 and 3 and Mode 2 were 30,012 and 30,006 cps, respectively, well within the specification limits of 30,000 ± 90 cps. All design and operation requirements for the modulation selector were fulfilled.

5.2.2.5 High-Gain-Antenna Position Controller
The antenna position controller rotated the

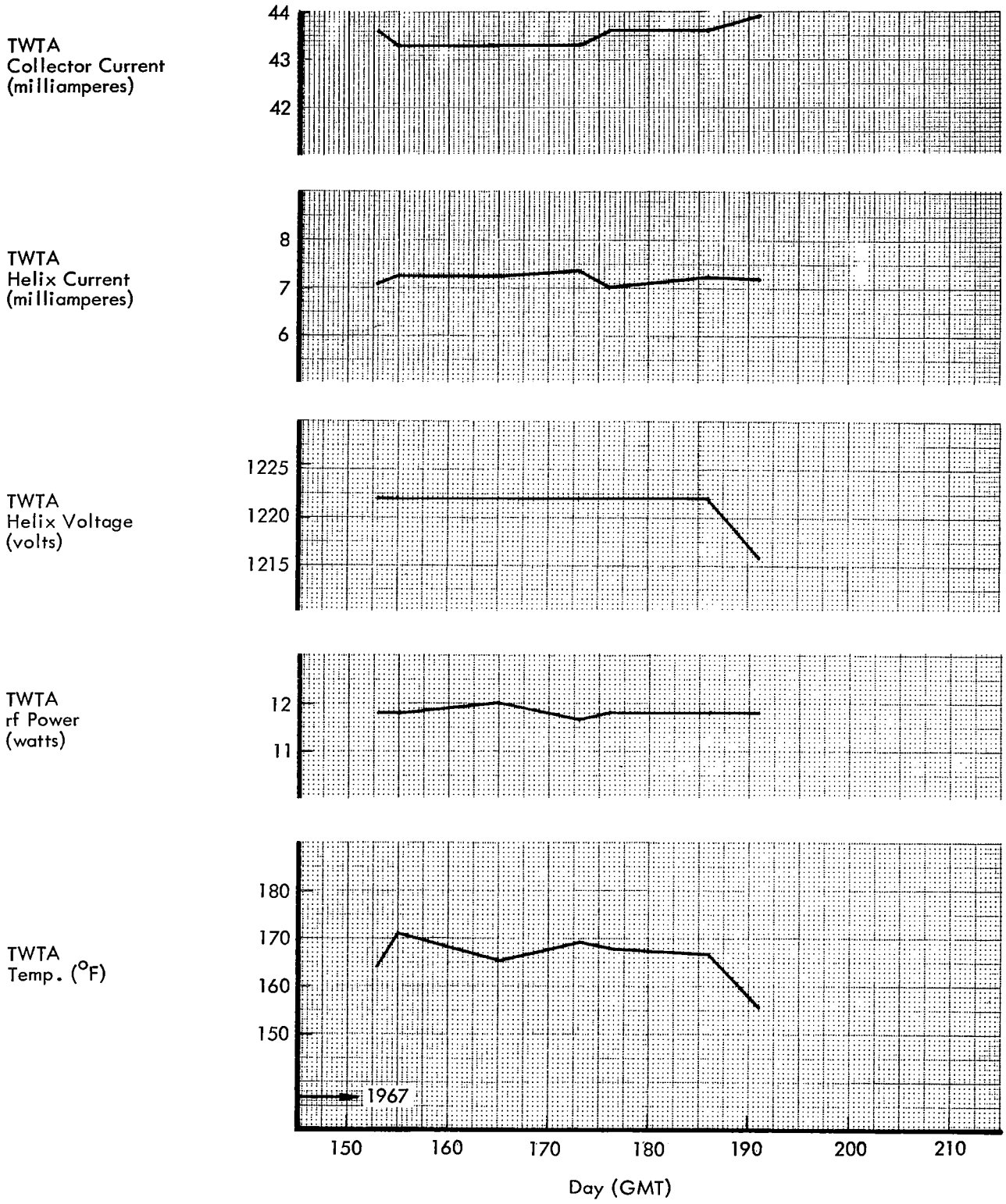

Figure 5-16: TWTA Operation

high-gain antenna in either direction as commanded.

5.2.2.6 Radiation Dosage Measurement System (RDMS)
The RDMS continued to function normally during the extended mission.

5.2.2.7 Micrometeoroid Data
Micrometeoroid bits had been sustained on Detectors 5 and 17 prior to the extended mission. Additional micrometeoroid hits were not detected during the extended mission.

5.2.3 Power Subsystem
The electrical power subsystem is the sole source of all electrical power used by the spacecraft as it performs all phases of its space mission. Radiant solar energy is collected by 2,714 N-on-P solar cells mounted on each of four solar panels and is converted into electrical energy. This energy supplies all spacecraft loads, power subsystem losses, and charging current to the nickel-cadmium battery. The shunt regulator dissipates excessive electrical energy in power dissipating elements mounted external to the spacecraft thermal shield. The shunt regulator also limits the bus voltage to less than 31 volts. A charge controller protects the battery from overvoltage and overtemperature conditions by regulating the charging current. The 12-ampere-hour battery provides electrical power to the spacecraft loads during periods of Sun occultation. Refer to Figure 5-17 for a functional schematic of the subsystem.

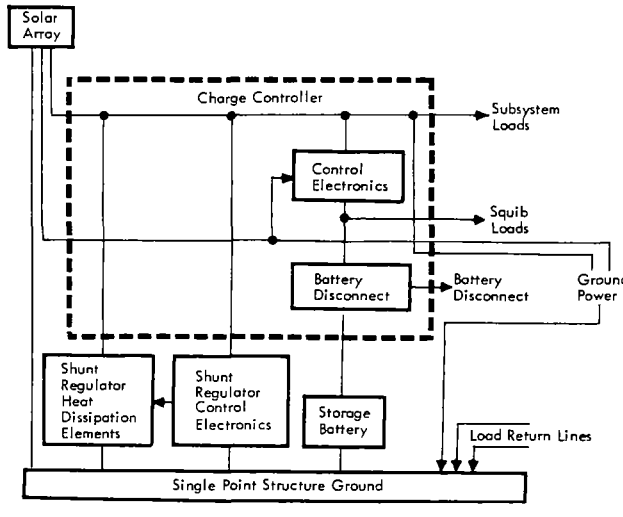

Figure 5-17: Power Subsystem

5.2.3.1 Solar-Array Performance
The solar array operated normally throughout the extended mission. Sufficient power was provided to maintain a constant bus voltage of 30.56 volts when in the sunlight. Solar panel degradation was minimal. Total solar panel output power at Lunar Orbiter IV launch was 12.85 amperes at 30.56 volts. As the mission progressed, the output power varied with time as a function of solar cell degradation and the changing solar constant (see Table 5-10), the figures are adjusted to an equal solar constant.

Table 5-10: Solar Panel Degradation

GMT Day	Measured Data at Solar Constant	Data Converted to Launch Day Solar Constant	Apparent Degradation
124 (Launch)	12.85 amps at 126.1 w/sq ft	12.85 amps	–
155	12.49 amps at 126.1 w/sq ft	12.57 amps	2.0%
186	12.37 amps at 126.1 w/sq ft	12.44 amps	3.0%

Solar panel degradation is in agreement with that measured on other Lunar Orbiter flights.

5.2.3.2 Battery Performance
Battery performance was as predicted during the extended mission. The higher battery temperatures, expected because of the flight plans, reached the qualification level of 105°F, thereby confirming the adequacy of the design to operate at elevated temperature.

These battery temperatures were above FAT limits and were attributed to elevated spacecraft deck temperatures under the battery, which were expected and considered acceptable for this flight.

Figure 5-18 reflects the battery discharge characteristics during a programmed exercise on Day 155 to discharge the battery following a long-term constant-charge condition during the primary mission. This discharge was normal. Later, on Day 192, the battery was discharged again (Figure 5-19) during a scheduled spacecraft maneuver. Again the discharge was normal. The lower end of discharge voltage on Day 192 is a direct result of the rate of discharge and is a

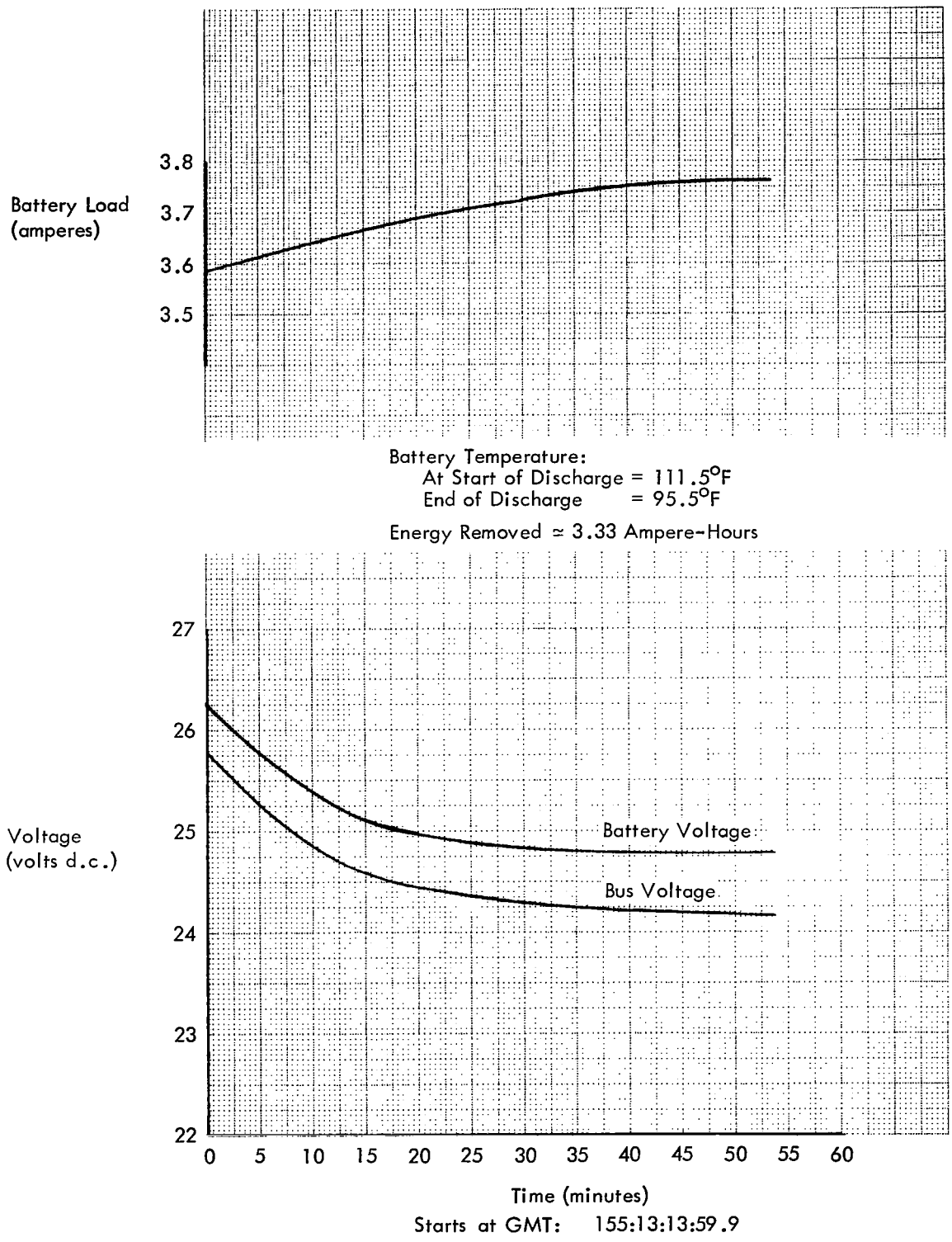

Figure 5-18: Battery Discharge Characteristic

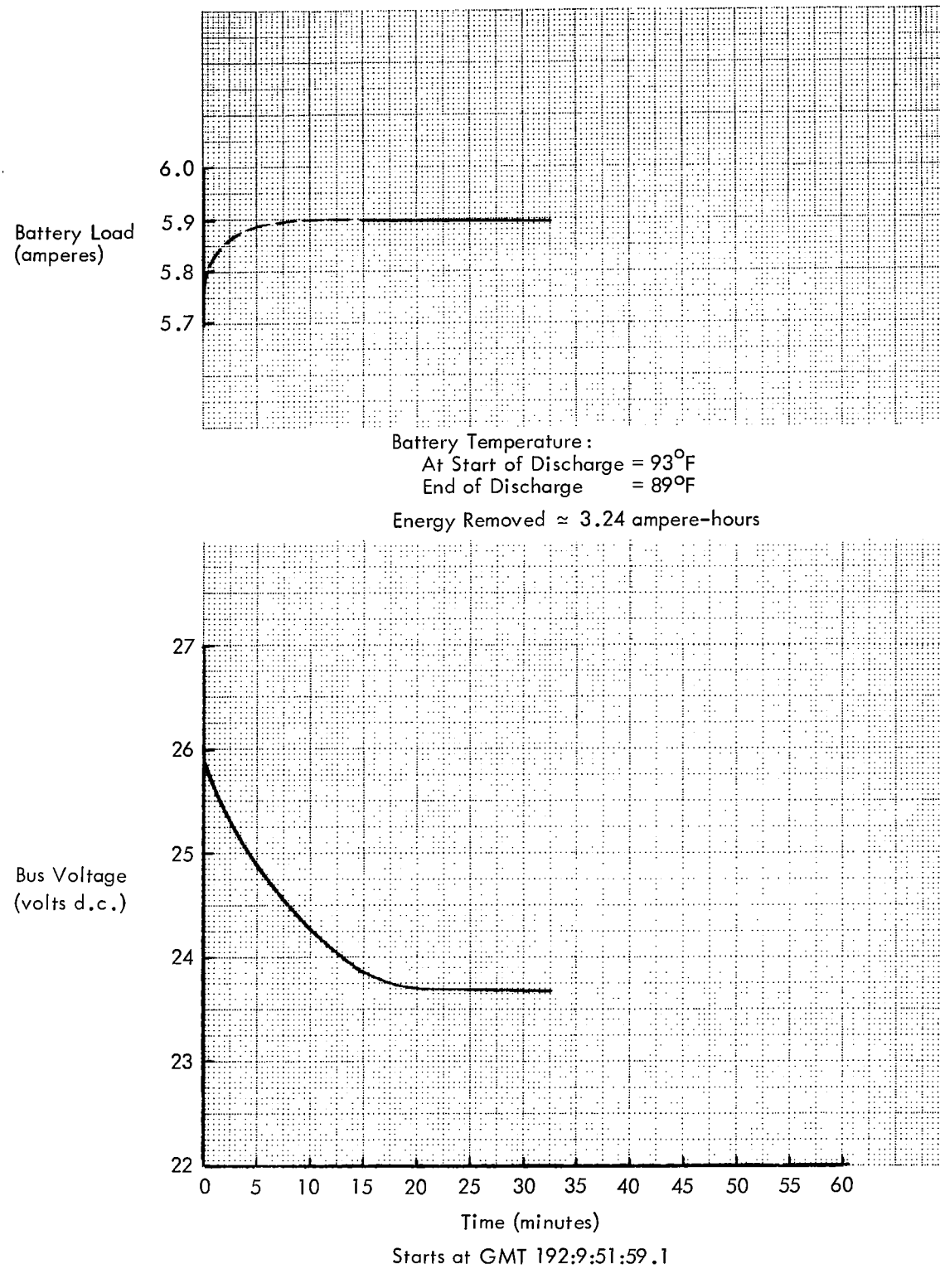

Figure 5-19: Battery Discharge Characteristic

normal characteristic. The discharge on Day 155 was at a C/3.2 rate, whereas the discharge on Day 192 was at a rate of C/2.1 (where C = battery capacity in ampere-hours).

5.2.3.3 Power Subsystem Performance

A comparison of power subsystem data from the first day of the extended mission and the last available data on Day 198 is shown in Table 5-11.

This data reveals that the power subsystem was operating normally when the spacecraft was last monitored. There was no indication of any impending failure that could have contributed to loss of the spacecraft.

The power subsystem response to an antenna rotation on Day 186 warrants explanation. The applicable data is shown in Figure 5-20. The antenna rotation started at 22:42:40.8 on Day 186 and lasted for six telemetry frames equaling a 39-degree antenna rotation. The spacecraft reacted to this antenna rotation by pitching on Sun 2.5 degrees during this same time interval, which is indicated by the increase in solar array output current and pitch position error. The bus voltage dip to 28.48 volts for one telemetry frame during antenna rotation is normal operation because the antenna drive requires a nominal 2-ampere current pulse. This additional load must come from the excess current in the shunt regulator. At this particular time interval, the shunt regulator had 2 amperes or less for several frames. The result was that each time the antenna current pulse initiated the shunt regulator turned off and the bus voltage dropped to a lower value as expected. Telemetry sampled the bus voltage during one of the antenna current pulses, accounting for the one reduced voltage reading. The battery voltage changes represent one telemetry bit change, indicating that the voltage was at the decision point in the analog-to-digital converter. The shunt regulator general rise in value reflects the increasing solar array output and the two dips in current represent antenna loading.

Table 5-11: Power Subsystem Data

	GMT	
	153:19:12:16.3	198:6:29:36.7
Bus voltage	30.56 volts	30.56 volts
Solar array current	9.84 amps	9.24 amps
Load current	5.37 amps	3.49 amps
Shunt regulator current	3.30 amps	4.61 amps
Battery charge current	1.025 amps	1.025 amps
Battery voltage	27.84 volts	28.48 volts
Signal conditioner supply	20.00 volts	20.00 volts
Battery temperature	103°F	85°F
Average solar panel temperature	65°F	70.5°F

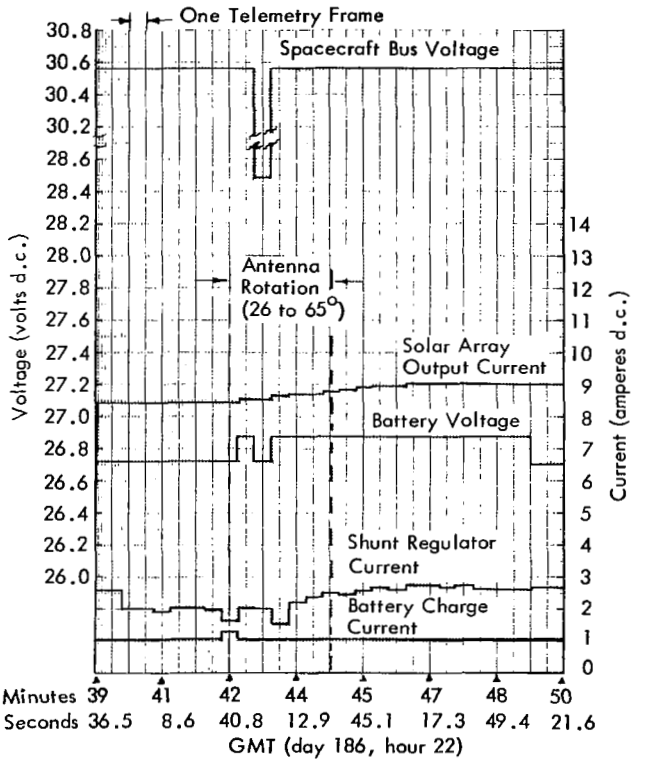

Figure 5-20: Power Response to Antenna Rotation

The single frame of increased battery charge current cannot be conclusively explained. It is of interest to note that the change occurred in the same frame when the antenna rotation started, which could have been caused by a small transient condition if the value of the battery charging current were close to the decision point in the analog-to-digital converter.

5.2.4 Photo Subsystem

The photo subsystem is housed in a pressurized, thermally controlled container, and includes camera, lens, film, film handling equipment, film processor, readout equipment, and environmental controls (see Figure 5-21). The subsystem is designed to expose, develop, and read out images for transmission to Earth via the communications subsystem.

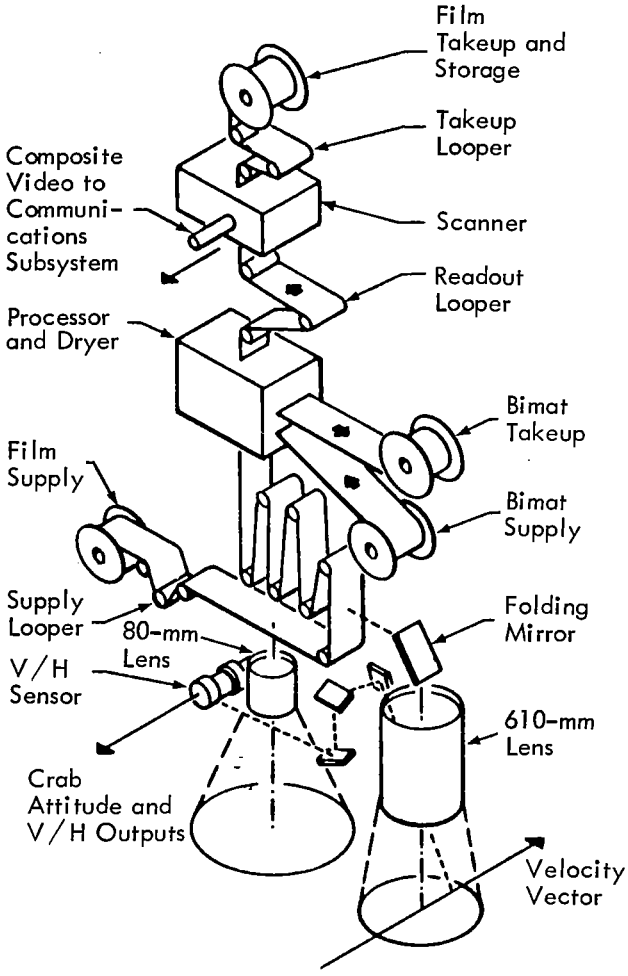

Figure 5-21: Photo Subsystem

One extended-mission objective was to read out photos that had been only partially read out during the prime mission while rewinding the exposed film onto the film supply, which would enable the subsystem to be used for various studies and tests.

The status of the various subsystems during the extended mission (from Day 152 and on) follows.

5.2.4.1 Camera and Lens

There was no activity during the extended mission because all photography was completed by Day 118.

5.2.4.2 Film Processor

There was no activity during the extended mission because processing and Bimat cut were completed on Day 118.

5.2.4.3 Film Handling

Normal mission film handling was considered complete at Readout Index 108.74; however, it was still necessary to transfer at least 108.74 frames from the takeup to the supply spool.

During the prime mission readout sequences, an intermittent circuitry caused the readout looper to indicate a full condition – thereby inhibiting takeup motor operation – and in turn prevented film from being advanced through the optical-mechanical scanner portion of the readout system. The condition of intermittent malfunctioning repeated itself during the extended-mission readout periods.

5.2.4.4 Readout Equipment

The readout equipment operated normally until Day 166, when normal command sequences failed to turn off the readout electronics. Subsequent command sequences of various combinations of "solar eclipse on and off," "readout drive off," and "readout drive on" were tried without success. A successful turnoff was finally achieved by a series of ten "readout drive on" commands spaced 23 seconds apart and further rewind or readout was not attempted. A complete analysis of this anomaly was not possible because video modulation had been previously turned off during the film readout

and GRE film was not available. A listing of the command sequences and a complete sequence of subsystem events for the rewind operation is given in the appendix.

During a normal readout turn-off sequence, the "readout drive off" command sets up the logic to stop the OMS motor and cam when the cam operates the encoder at the "spot stop" position, and resets the readout electronics and readout drive memories. During normal operation, the encoder sets the logic about 3 degrees before the cam dwell spot and the inertia of the drive train allows the cam to coast about 4 degrees, which places the cam dwell portion under the encoder, which in turn commands the video off. Analysis of this anomaly, failure to turn off video on the first command, indicates the following operation of the readout equipment.

The encoder operated at the proper timing; however, an increase in film tension was caused by the false readout looper encoder signal inhibiting the takeup motor brake from releasing film to the OMS. The OMS continued to pull on the film when the takeup looper was at mechanically empty, causing more drag on the OMS gearing due to the friction of film on the drive roller. As a consequence, the lower inertia caused the cam to stop slightly before the dwell portion. The pressure of the encoder on the cam at this point caused the cam to reverse, which changes the encoder to allow the readout electronics to come back on.

This anomaly is similar to a Mission II anomaly that necessitated a command sequence change. A spacecraft "readout drive on" command was programmed to follow the normal commands at "readout turnoff." The additional command normally pulsed the OMS long enough to drive the cam far enough so the encoder rode on the dwell portion. The Mission II anomaly, however, was considered to have occurred with normal film tension and was attributed to tolerance buildup because the occurrence was random. On Day 167, all indications point to the fact that the increased tension caused excessive drag on the OMS gear train. The continued commands eventually caused the OMS drive to slip on the film and allow the encoder to ride on the dwell portion.

5.2.4.5 Environmental Controls

The subsystem was not used for tests other than the rewind operation so the environmental conditions remained normal throughout the reporting period. Table 5-12 shows variations in the nitrogen bottle pressure with respect to subsystem temperature.

5.2.5 Structures and Mechanisms Subsystem

The structures and mechanisms subsystem consists of the support structure, thermal control coatings, thermal barrier, engine deck heat shield, solar panel and antenna deployment mechanisms, camera thermal door, rocket engine gimbal, bipropellant tank heaters, and the interconnecting electrical wiring.

With the exception of the camera thermal door and the rocket engine gimbal, this subsystem is in a passive state during the extended mission. Only the thermal control coating is discussed since the remainder of the subsystem performed as anticipated.

5.2.5.1 Equipment Mount Deck Thermal Control Coating

The EMD thermal control surface for Mission IV was S13G over B1056 with a 20%, uniform distribution of optical solar reflectors, mirrors. The combination of mirrors and S13G over B1056 resulted in a thermal improvement of approximately 25°F after 1,100 equivalent Sun hours over the Mission II and III spacecraft (see Figure 5-22). Degradation of the thermal coating (paint only) still required the spacecraft to be operated approximately 40 degrees off-Sun to maintain EMD temperatures at a safe level. Figure 5-23 shows the spacecraft angle off-Sun and Figures 5-24, 5-25, and 5-26 show the corresponding EMD temperature measurements near the TWTA, transponder, and the IRU, respectively. Additional discussion on this subsystem is contained in Section 5.3.

The camera thermal door test, Section 5.3.8, was designed to obtain additional information on the anomaly that occurred during the photo mission.

Section 5.3.9 discusses the paint degradation exercise designed to obtain temperature data

Table 5-12: Photo Subsystem Temperatures and Pressures

GMT Day	Internal Pressure (psia)	Nitrogen Bottle Pressure (psi)	Readout Thermal Fin Temp. (°F)	Lower Environ. Temp. (°F)	Upper Environ. Temp. (°F)
153	1.70	2,172	64.2	64.3	68.9
155	1.63	2,225	79.4	78.0	77.0
156	1.63	2,194	65.0	65.0	67.0
158	1.63	2,210	75.8	75.8	76.8
159	1.63	2,194	70.5	72.8	73.6
161	1.63	2,210	70.8	70.9	73.3
163	1.63	2,210	70.9	71.9	74.9
164	1.63	2,210	70.9	72.0	74.8
166	1.63	2,225	80.9	78.9	78.4
173	1.63	2,210	70.9	71.5	73.6
186	1.63	2,239	69.4	70.1	71.0
191	1.63	2,195	69.7	70.2	70.5
198	1.63	2,172	66.6	66.8	69.5

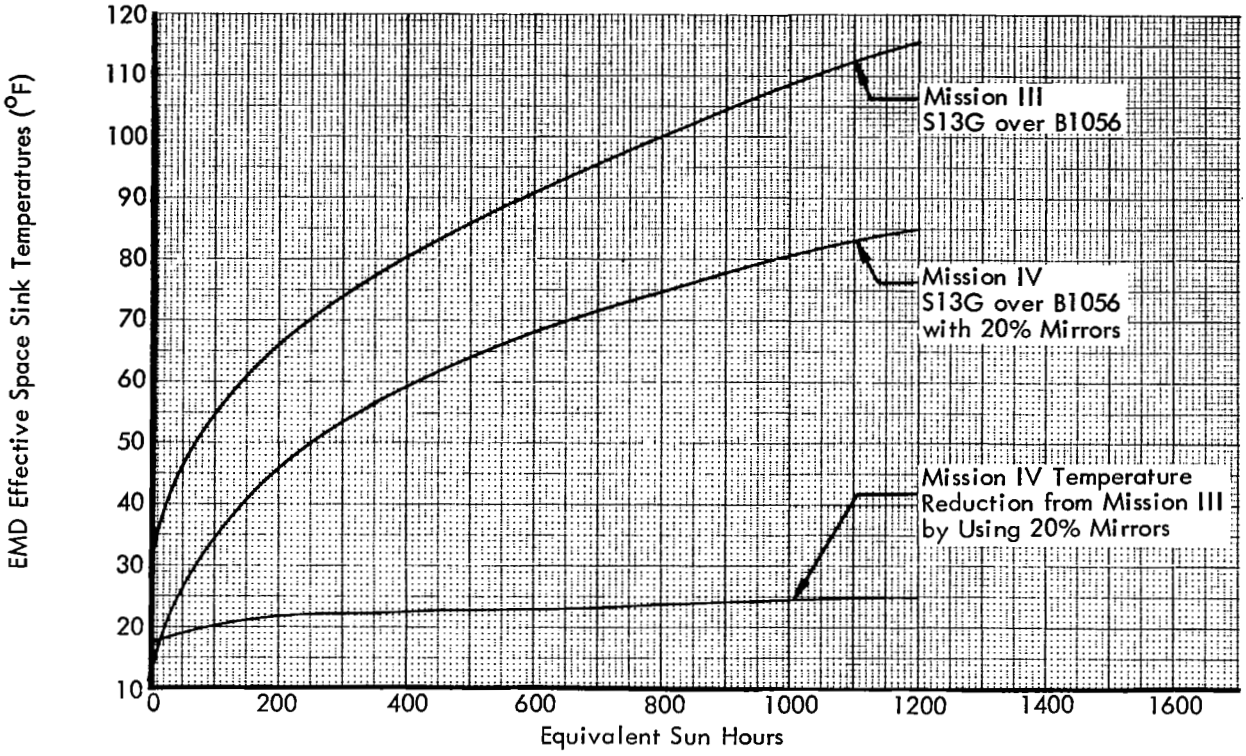

Figure 5-22: EMD Temperature Comparison

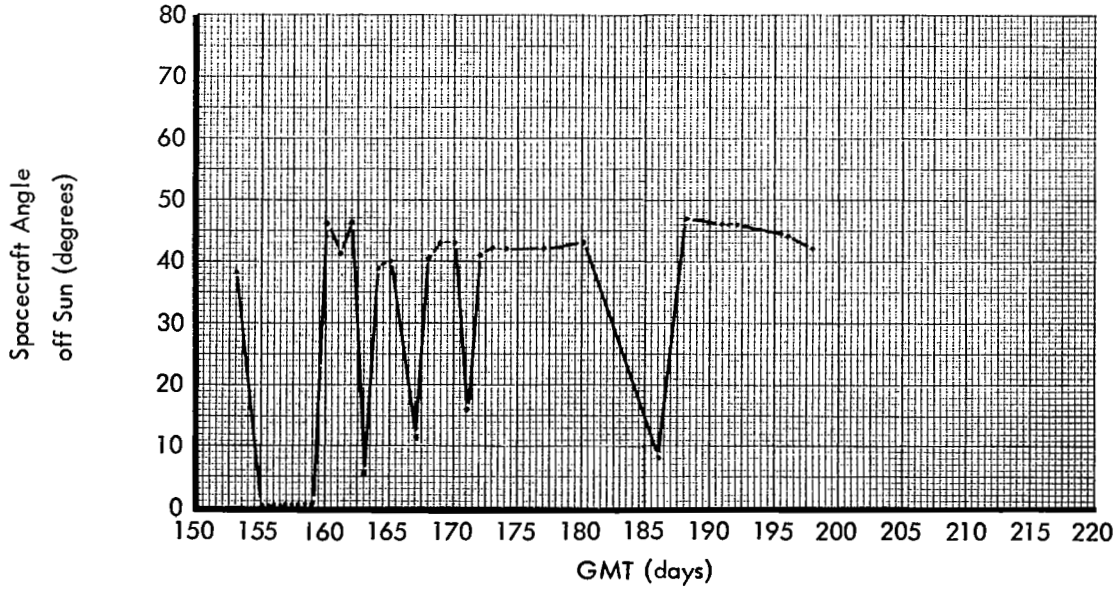

Figure 5-23: Spacecraft Pitch Angle History

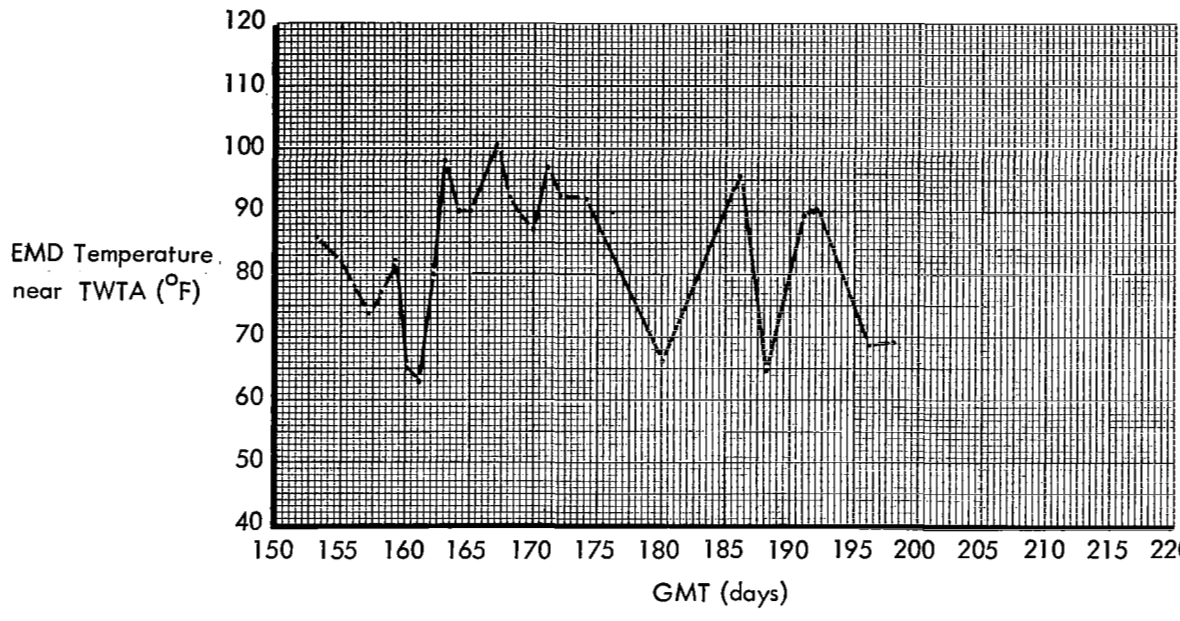

Figure 5-24: EMD Temperature History (TWTA)

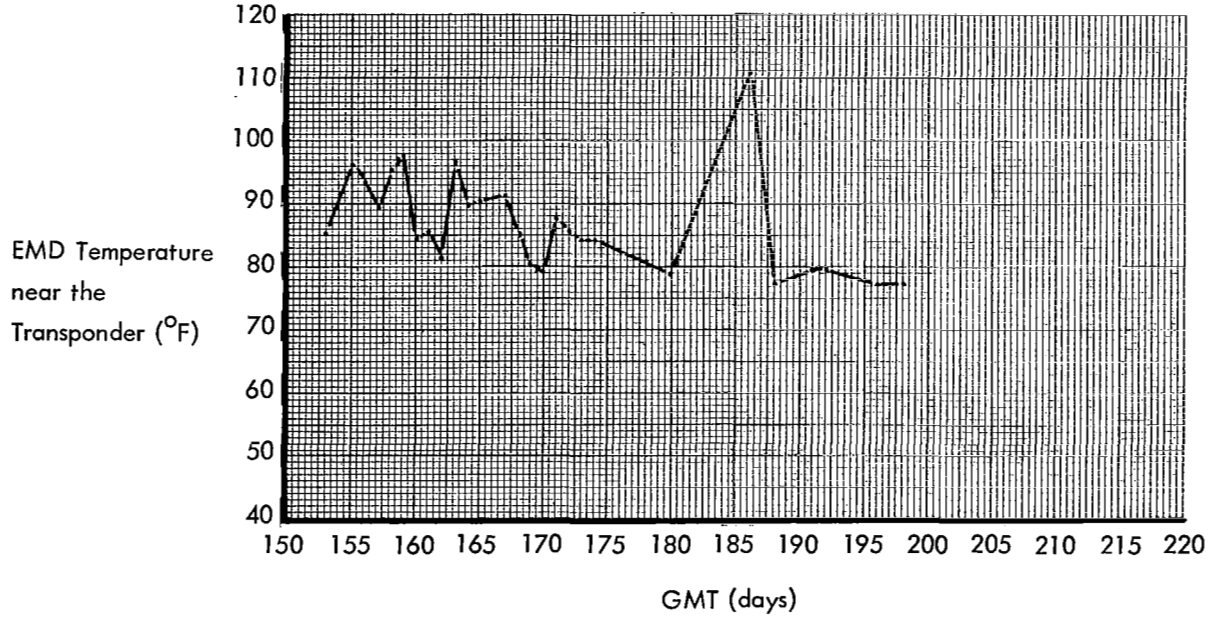

Figure 5-25: EMD Temperature History (Transponder)

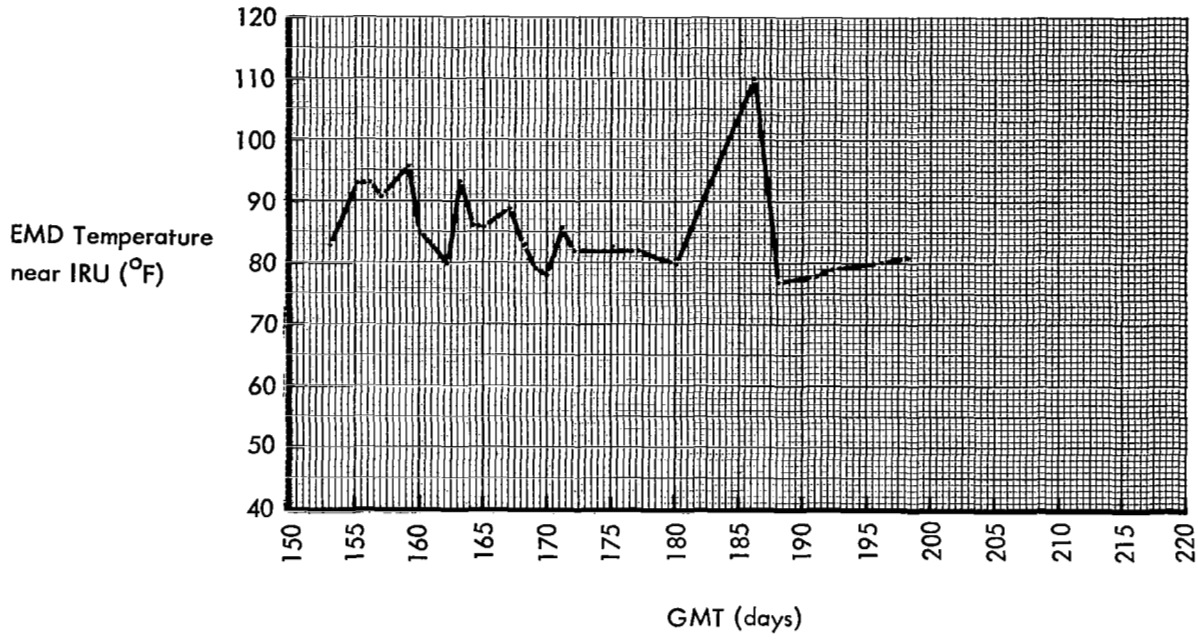

Figure 5-26: EMD Temperature History (IRU)

on the test paint coupons to determine the degradation characteristics of each paint. The test paint coupons were S13G over B1056 (STO9A), S13G (ST10A), B1060 (ST13), and Hughes' Inorganic White (ST14).

5.2.6 Velocity and Reaction Control Subsystems

The velocity control subsystem consists of the propellant pressurization equipment, propellant storage tanks and feed system, bipropellant rocket engine, and thrust vector control actuators. The reaction control subsystem (Figure 5-27) includes the nitrogen storage tank that is common to the velocity control subsystem, thrusters and interconnecting plumbing, filter, and regulator, and provides the impulsive force to maintain attitude control and perform attitude maneuvers about the pitch, roll, and yaw axes of the spacecraft.

5.2.6.1 Reaction Control Subsystem Performance

The reaction control subsystem performed satisfactorily throughout the extended mission. The subsystem maintained spacecraft attitude control in wide (2-degree) deadband while in

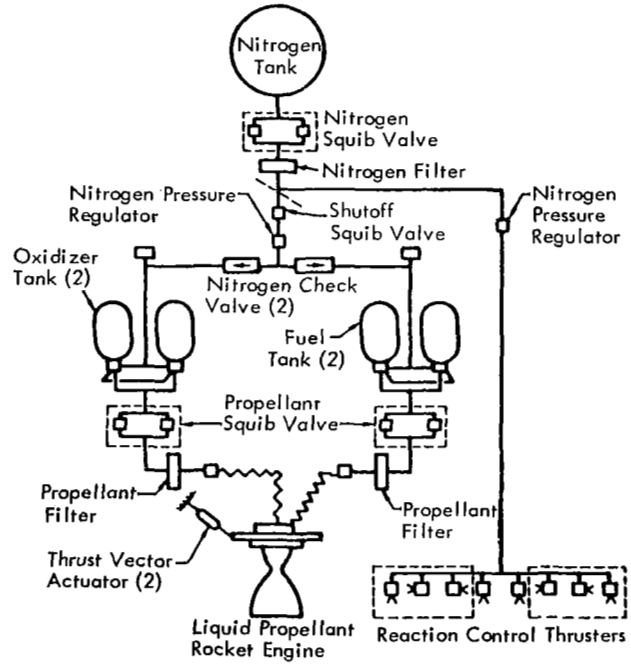

Figure 5-27: Velocity and Reaction Control Subsystems

inertial hold in all three axes during the major part of the extended mission. Maneuvers were generally limited to those required for updating of the spacecraft pitch and yaw position for thermal control and for special tests. To minimize nitrogen consumption, most maneuvers were performed with the attitude control subsystem operating in wide deadband. The time histories of nitrogen tank pressure and temperature are shown in Figures 5-28 and 5-29, respectively.

Subsystem performance was evaluated on the basis of nitrogen gas consumption for attitude control and thruster performance. It was concluded that reaction control subsystem per-

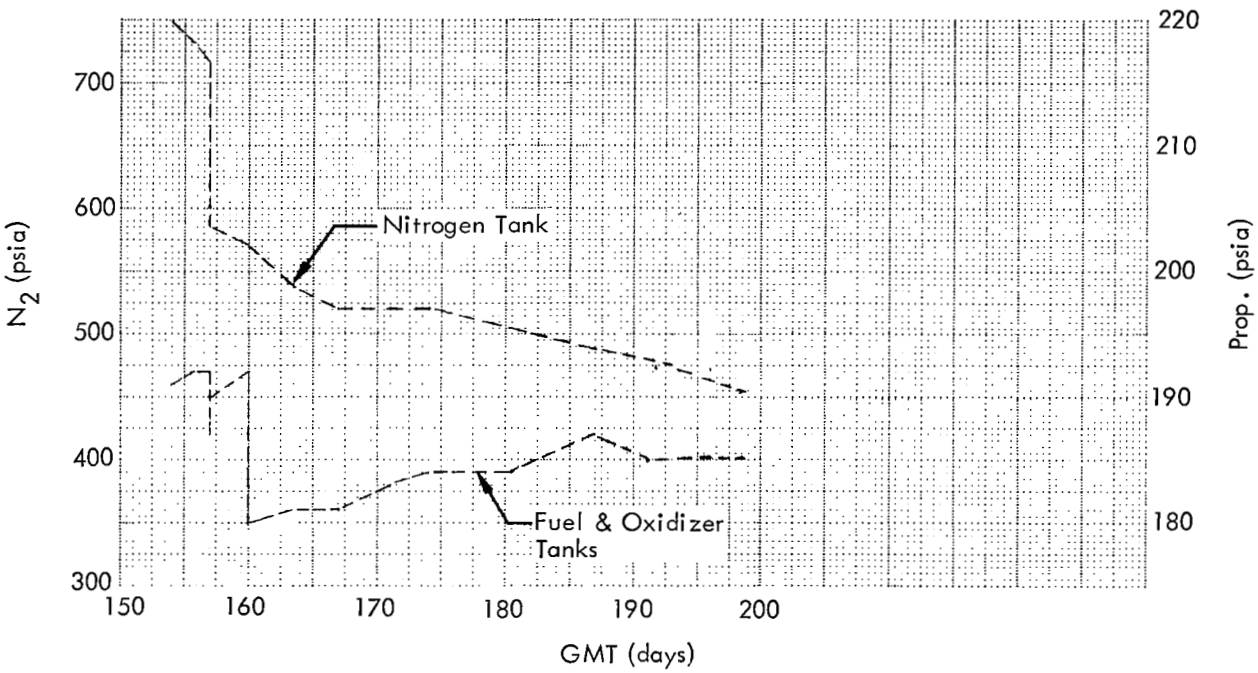

Figure 5-28: Spacecraft Tankage Pressure History

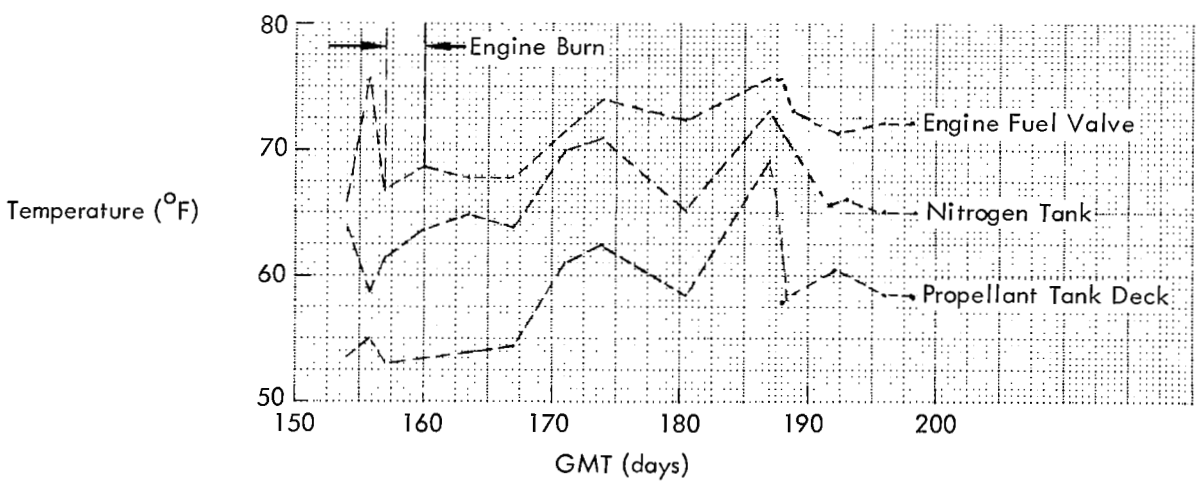

Figure 5-29: Extended Mission Profile — Temperature

formance was nominal throughout the extended mission; there was no evidence of degradation in performance from primary mission performance.

Nitrogen Usage — Nitrogen usage (see Figure 5-30) is calculated from the telemetered nitrogen storage bottle pressure and temperature, and the volume of the high-pressure system. Predicted usage rate calculations are based on the maneuvers performed, the spacecraft moment of inertia about each axis, estimated limit cycle usage rates, and estimated disturbances. Minimum predicted nitrogen usage is based on minimum 12-m/sec-duration single pulses of the thrusters during limit cycle operation. The maximum usage limit is based on pulse durations for limit cycle operation that result in 0.0025-degree-per-second angular rates in each axis. To obtain such angular rates, the equivalent pulse duration would be 35 m/sec in pitch and yaw and 65 m/sec in roll. Predicted usage rates for maneuvers (including Sun and Canopus acquisitions) and disturbances are the same for the minimum and maximum limits.

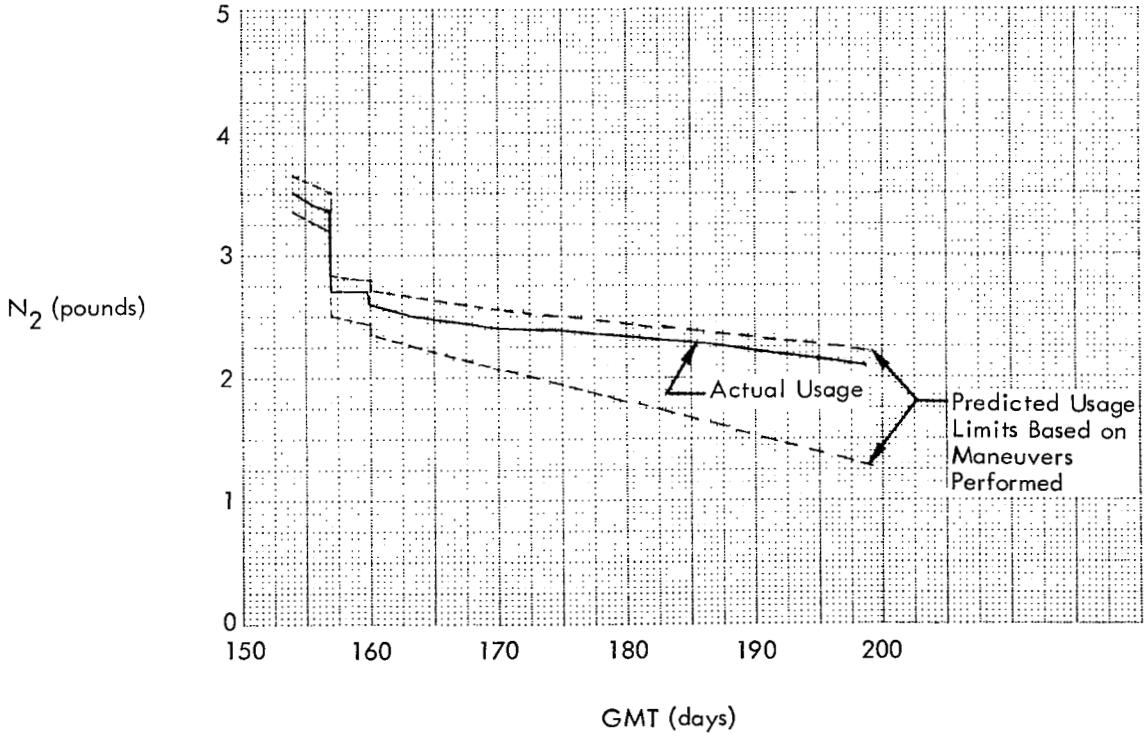

Figure 5-30:
Nitrogen Supply Utilization

The major events that caused the higher usage rates are summarized in Table 5-13. Nitrogen usage for the normal extended-mission mode of operation, which includes thermal maneuvers and ± 2.0-degree limit cycling, ranged from 0.0162 to 0.0091 pound per day with an average of 0.0103 pound per day. Maximum and minimum predicted rates are 0.018 and 0.010 pound per day, respectively. Typical variations in spacecraft attitude while operating in the sunlight are shown in Figure 5-31. The spacecraft is cycling near the negative deadband limit because of solar pressure disturbances. The excursion in roll and pitch to the positive limit is the result of cross coupling caused by pitch and yaw Sun acquisition maneuvers occurring between 32 and 65 minutes.

Although thruster performance cannot be determined directly from flight data, the compatibility between predicted and actual thruster

Table 5-13:
Major Events Using Nitrogen Gas

Time Period (Day)	Description of Events
155	Battery discharge test Gyro drift test
156	Apolune transfer maneuver
159	Perilune transfer maneuver
163 to 174	Canopus tracker tests Camera thermal door tests Mission V thermal data tests
186	Mission V canopus tracker test
187 to 198	Extended--mission mode of operation

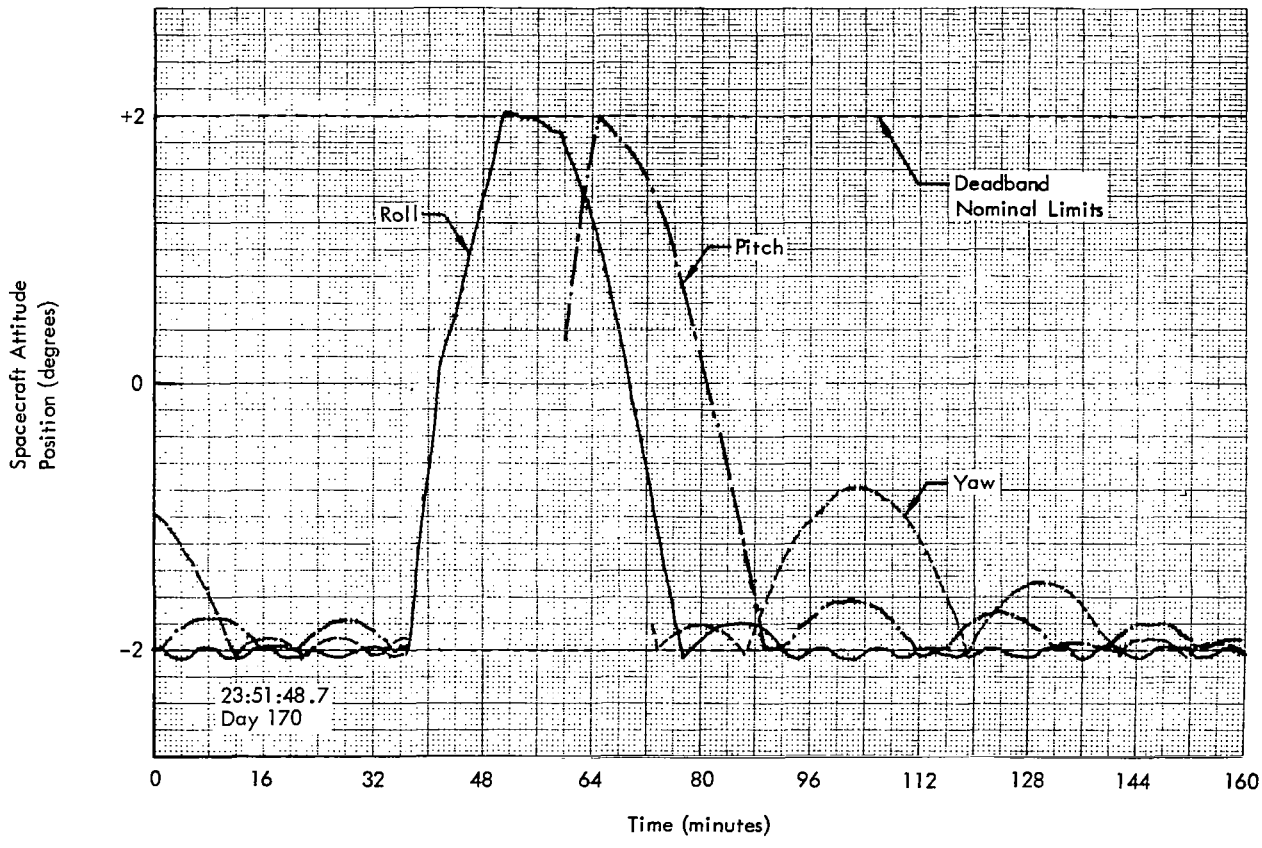

Figure 5-31: Limit Cycle Operation

operating modes and nitrogen usage verifies that the specific impulse in flight is very close to predicted values established from ground testing. The specific impulse used for predicting nitrogen usage was 68 seconds for limit cycle mode and 71 seconds for maneuvers.

5.2.6.2 Velocity Control Subsystem Performance

Velocity control subsystem performance was analyzed on the basis of telemetered propellant tank pressures, actuator position, and incremental velocity change. The velocity control subsystem was operated two times during the extended mission, each successfully, with no evidence of degradation throughout the extended mission. The propellant tank pressures and system temperatures during the extended mission are shown in Figures 5-28 and 5-29, respectively.

There were two velocity maneuvers performed to lower the orbit perilune and apolune to simulate the planned orbit parameters for Mission V. The first maneuver was performed to lower orbit perilune prior to firing the shutoff squib valve which isolates the velocity control subsystem from the nitrogen gas supply. The second maneuver, performed at perilune to lower orbit apolune, was performed after firing the shutoff squib valve. The sequence of squib valve operation was selected to avoid operation of the engine in a "blowdown" mode at inlet pressures below those experienced during test. The propellant tank pressure increase following the second maneuver, as shown by Figure 5-28, is attributed to leakage across the shutoff squib valve. The rate of pressure rise indicated the leakage rate was 80 standard cubic centimeters per hour. A leakage rate of this mangitude would not be detrimental to the mission. Details of each velocity maneuver performed during the extended mission are discussed below.

Perilune Decrease — On Day 156 at 23:16 GMT, a velocity change maneuver was performed to change the orbit perilune from 2,590 to 75 kilometers (approximate values). The maneuver provided a velocity change to the spacecraft of 186.72 meters per second, which is shown as a function of time in Figure 5-32. The perilune

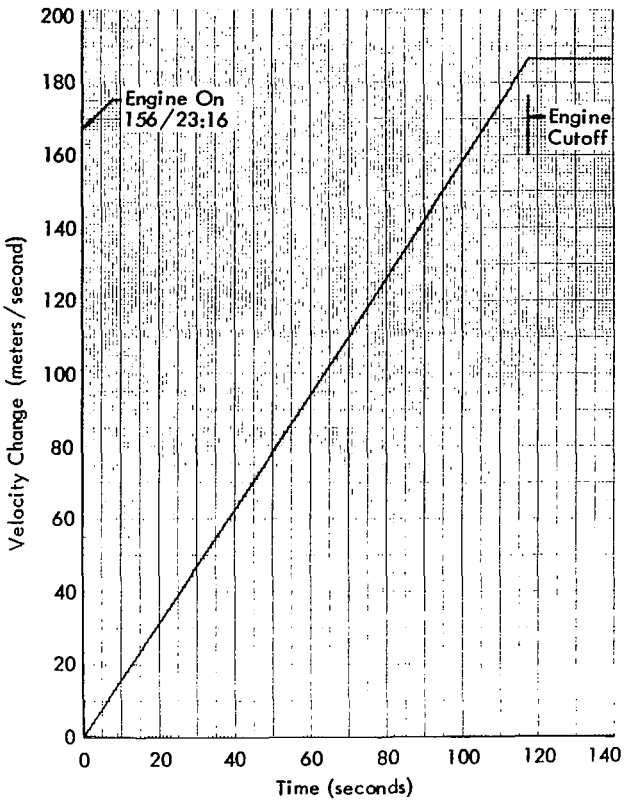

Figure 5-32: Velocity Change — Perilune Decrease Maneuver

altitude achieved was 74.96 kilometers. The average thrust during the burn was 101.4 pounds as computed from acceleration data and spacecraft weight. The engine burn time was 119.2 seconds. Nitrogen gas supply and propellant feed system pressures for the maneuver are shown as a function of time in Figure 5-33. Fuel and oxidizer tank pressures were within normal operating limits during the burn and were consistent with system performance during the primary mission.

The engine position data shown in Figure 5-34 confirms the stability of the system during the velocity maneuver. Thrust vector control system performance was satisfactory throughout the burn as shown by Figure 5-35. No excursions in spacecraft attitude beyond ± 0.1 degree were observed from telemetry data during the time period the thrust vector control system had control capability.

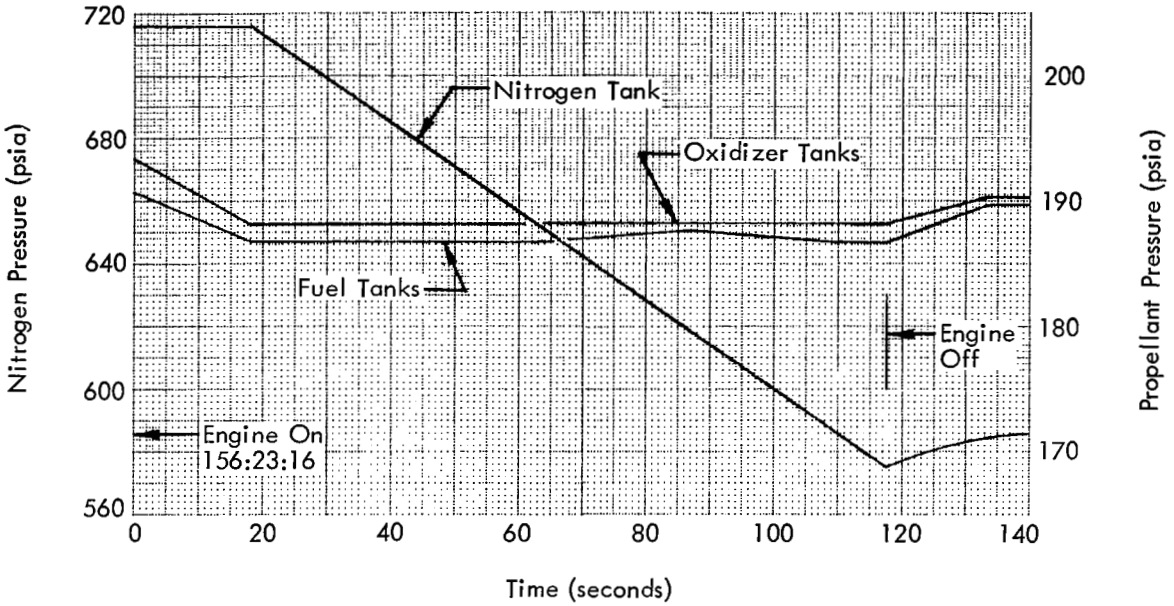

Figure 5-33: Tank Pressures – Perilune Decrease Maneuver

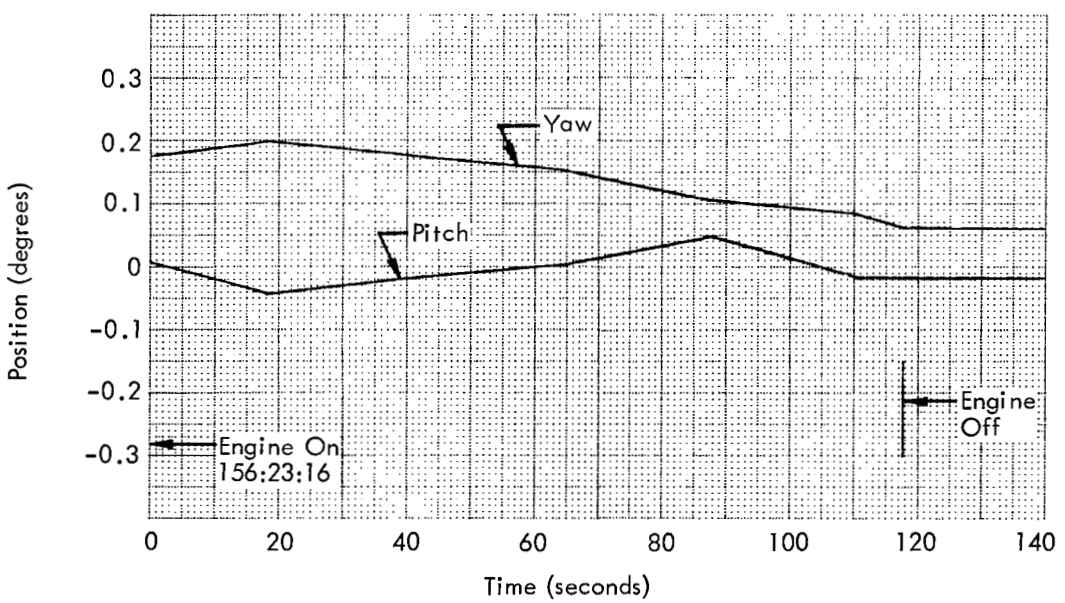

Figure 5-34: TVC Actuator Position – Perilune Decrease Maneuver

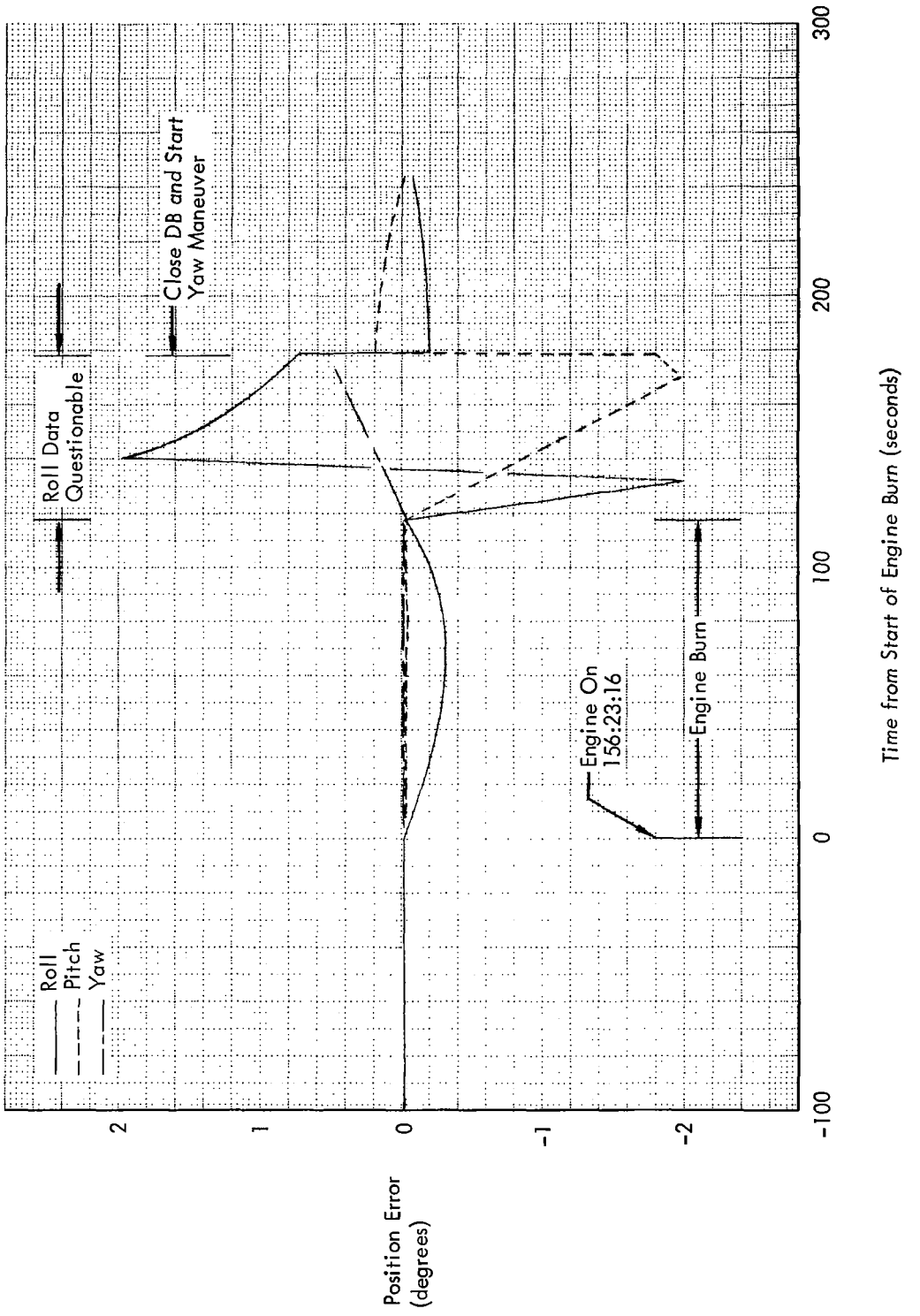

Figure 5-35: Attitude Control – Perilune Decrease Maneuver

Apolune Decrease – On Day 159 at 22:40 GMT, a velocity change maneuver was performed to change the orbit apolune from 6,090 to 3,950 kilometers (approximate values). The maneuver provided a velocity change of 70.53 meters per second, which is shown as a function of time in Figure 5-36.

The apolune altitude achieved was 3,959 kilometers. The average thrust during the burn was 100.0 pounds as computed from acceleration data and spacecraft weight. The engine burn time established from telemetry data was 42.8 seconds, whereas the predicted burn time was 43.1 seconds.

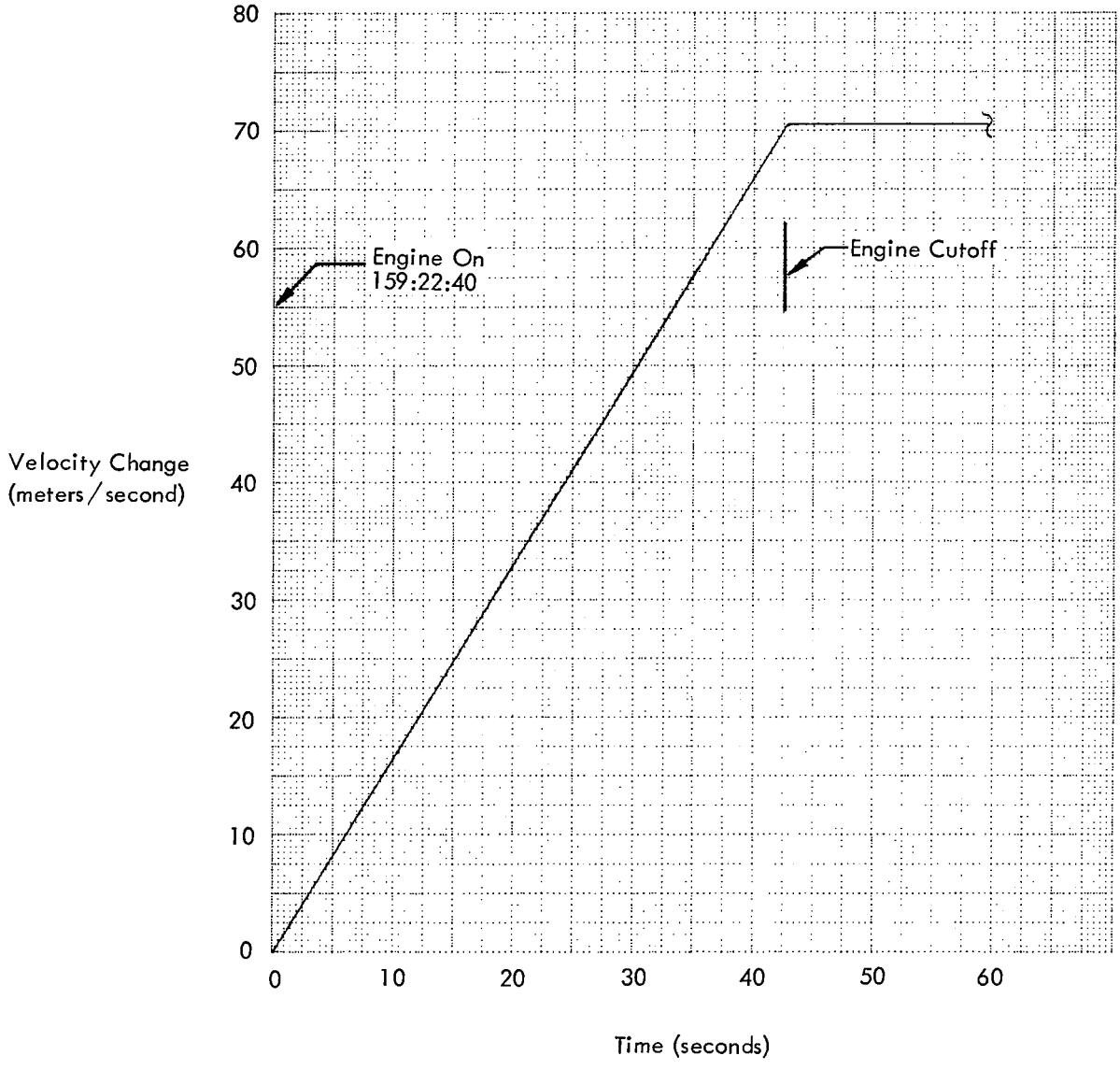

Figure 5-36:
Velocity Change – Apolune Decrease Maneuver

Nitrogen gas supply and propellant feed system pressures for the maneuver are shown as a function of time in Figure 5-37. The nitrogen gas supply pressure remained constant (as the shutoff squib valve had been actuated) and the fuel and oxidizer tank pressures decayed as expected for system operation in a blowdown mode.

Thrust vector control system performance was satisfactory throughout the burn, as shown by Figure 5-39. No excursions in spacecraft attitude beyond ± 0.05 degree was observed from telemetry data during the time period the thrust vector control system had control capability. The engine position data shown in Figure 5-38 confirms the stability of the system and that the spacecraft center of gravity location relative to the engine pointing angle remained essentially constant during the maneuver.

Overall Subsystem Performance – Four velocity control maneuvers were performed during the photographic and extended mission

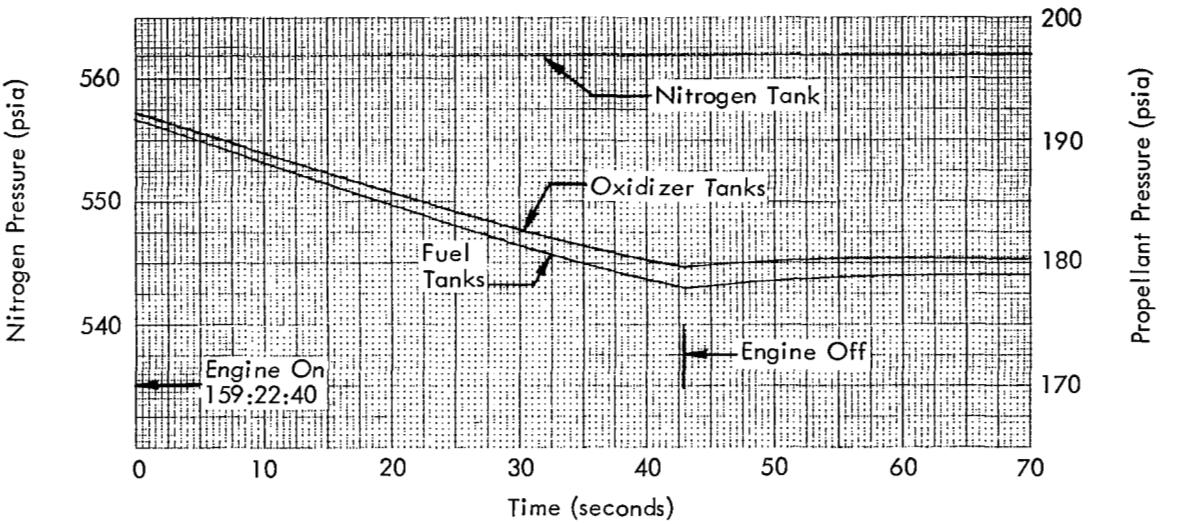

Figure 5-37: Tank Pressures – Apolune Decrease Maneuver

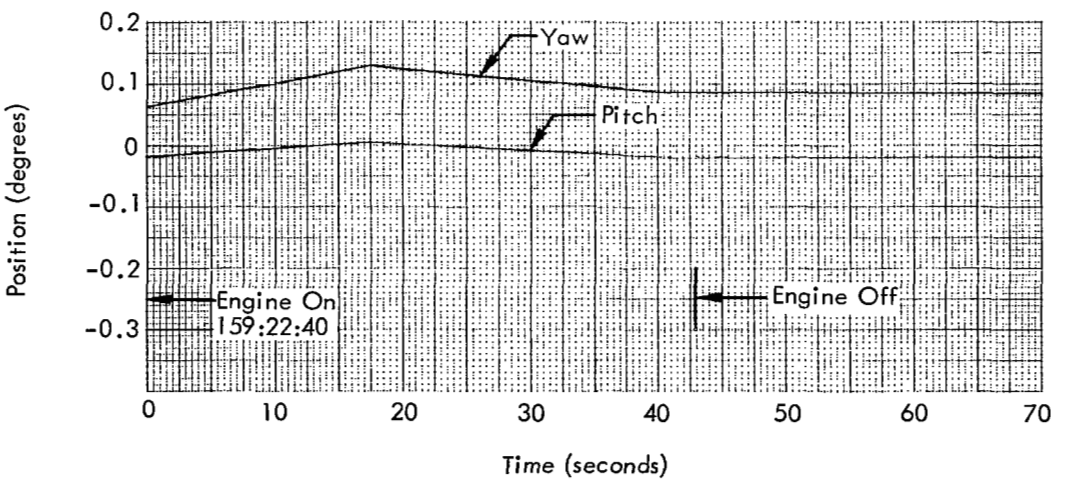

Figure 5-38: TVC Actuator Position – Apolune Decrease Maneuver

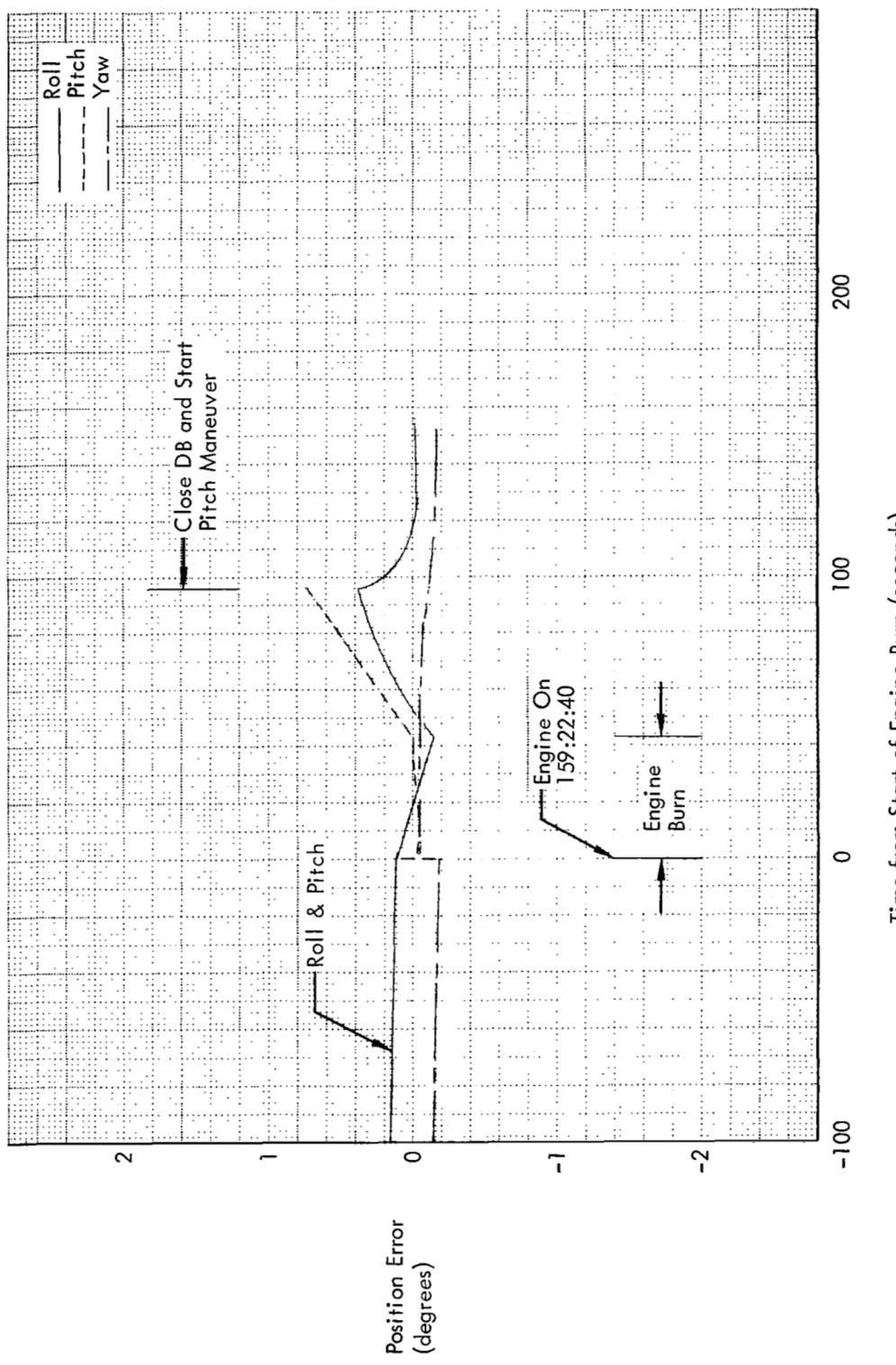

Figure 5-39: Attitude Control – Apolune Decrease Maneuver

(see Table 5-14). An analysis of subsystem performance during each burn confirmed the engine average specific impulse to be 276 ±2 seconds. The velocity control subsystem imparted a total velocity change to the spacecraft of 977.72 meters per second using 259.55 pounds of propellant based on an engine specific impulse of 276. The estimated 3-sigma minimum performance of the system based on an expulsion efficiency of 98% was 965 meters per second. Experience from ground test and Mission I has indicated the system would impart a nominal velocity change of 1,033 meters per second to the spacecraft based on the actual propellants loaded and a 99% expulsion efficiency. It is therefore concluded that 55.8 meters/second velocity change capability remained on board the spacecraft at the time contact was lost.

5.3 SPECIAL FLIGHT TESTS

Special tests performed during the extended mission fall into two categories: (1) special experiments using the Lunar Orbiter spacecraft as a tool to obtain scientific data; and (2) special exercises that are tests of the spacecraft or equipment on board.Only the latter are reported herein; special experiments are to be reported by the particular agency requesting the experiment. However, subsystem performance during a special test designed to obtain scientific data, such as the orbit transfer maneuvers that were designed to simulate the Mission V orbit, is reported in the general discussion on each subsystem.

5.3.1 Three-Axis Gyro Drift Measurement

The test, to determine if gyro drift rates had changed from those recorded at the beginning of the prime mission, was started after the spacecraft had been locked on the Sun in pitch and yaw with Canopus in the star tracker field of view. Spacecraft attitude control was placed in the narrow deadband mode and the Sun sensors were energized. At apolune the attitude control was placed in the inertial-hold mode. The

Table 5-14: Velocity Control Maneuvers

Event	GMT Time and Day	ΔV (m/sec)	Engine Burn Time (sec)	Thrust (lbs)	Propellant Used (lbs) ▷
Launch	22:25 124				
Midcourse	16:45 125	60.84	52.7	100.0	19.11
Injection	15:08 128	659.63	501.7	100.0	181.68
Perilune Decrease	23:16 156	186.72	117.9	101.4	43.20
Apolune Decrease	22:40 159	70.53	42.8	100.0	15.56
Total		977.72	715.1		259.55

▷ Estimated on the basis of an engine specific impulse of 276 seconds.
276.35 pounds of propellants were loaded at launch.

Canopus star tracker was turned on and the output monitored every half hour, then turned off.

The test was terminated after 2.5 hours due to increasing spacecraft temperatures; however, the following gyro drift rates were determined.

- Roll, -0.065 ± 0.005 degree/hour;
- Pitch, -0.092 ± 0.005 degree/hour;
- Yaw, $+0.008 \pm 0.005$ degree/hour;

Figure 5-40 shows the trend about each axis from launch to the test. There is very little change about any axis. Even though the test was short, it appears that the figure is accurate and within tolerance. When the tracker locked on glint during a roll update maneuver, it was corrected by turning the tracker off, then on. Data from tests conducted in early July (1 month later) showed no significant drift about either axis.

Gyro drift, then, was minimal and displayed little if any degradation since launch.

Figure 5-41 shows the average drift for gyros during all missions up to IV. Note that only one gyro shows an out-of-specification condition

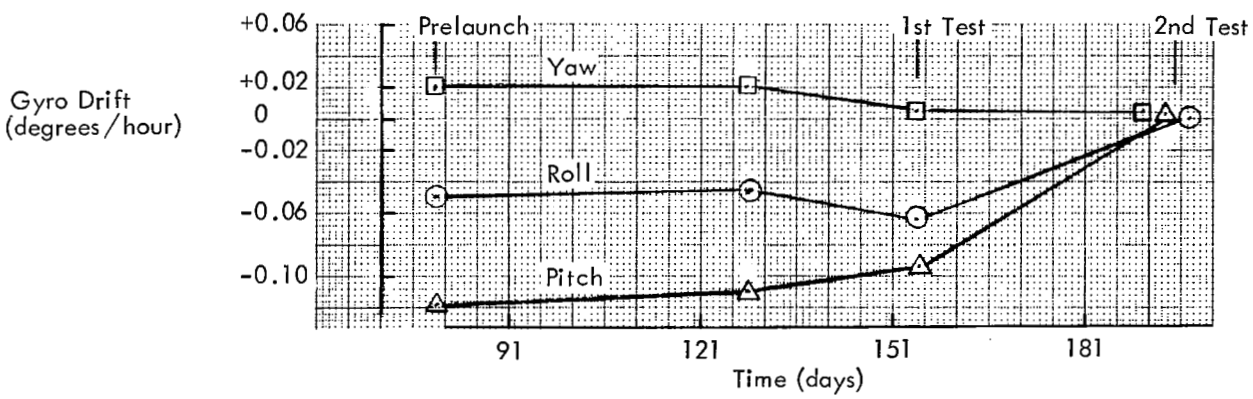

Figure 5-40: Gyro Drift Test

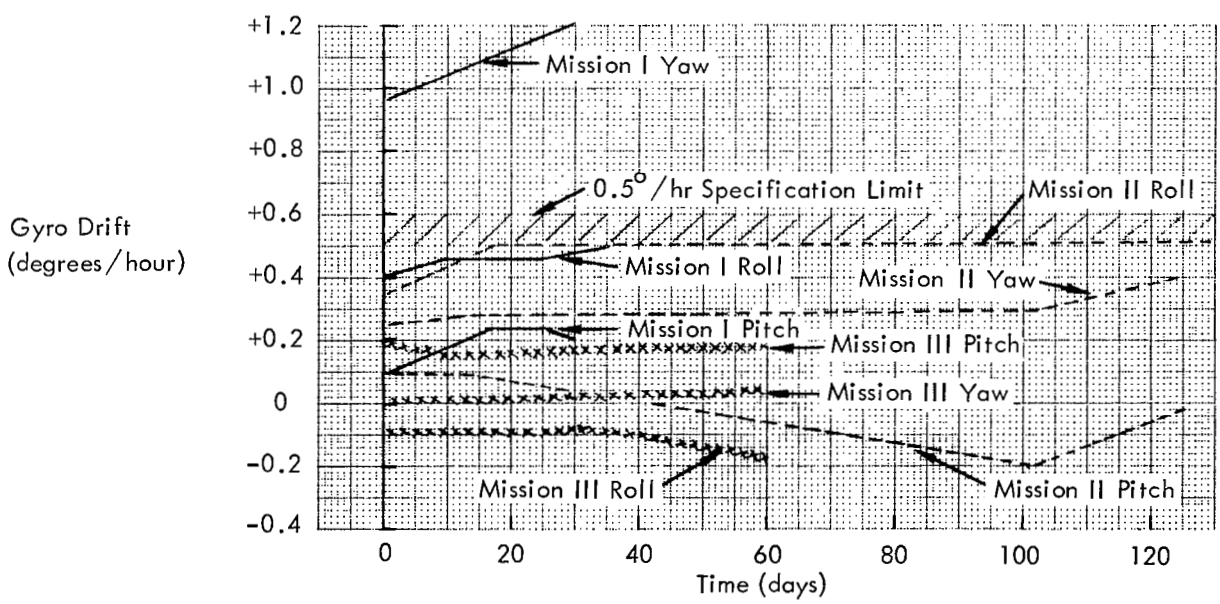

Figure 5-41: Gyro Drift Comparison

and the greatest change in drift rate, namely 0.062 degree/day, as compared to the next highest at 0.004 degree/day. Mission IV drift data, Figure 5-40, are uniformly the best of all previous missions. A comparison of average absolute drift rates for each mission follows.

- Mission I, 0.6 degree per hour;
- Mission II, 0.3 degree per hour;
- Mission III, 0.1 degree per hour;
- Mission IV, 0.05 degree per hour.

5.3.2 Canopus Star Tracker Bright-Object Shutter and Map Voltage Test

The test, to determine the yaw angle at which the bright-object sensor closes and opens the shutter and star tracker sensitivity as a function of yaw and pitch angles, was initiated near apolune with the spacecraft locked on the Sun in pitch and yaw and the roll axis oriented on Canopus. The wide (2-degree) deadband was used throughout the test. The spacecraft was then maneuvered in yaw to establish the plus and minus yaw angles at which the bright-object sensor would open and close the shutter. The spacecraft then reacquired the Sun and was maneuvered in pitch and yaw to establish glint conditions over a 20-degree Canopus cone angle. At the conclusion of these maneuvers, the Sun was reacquired and the spacecraft was pitched plus 45 degrees off Sun for thermal relief. The sequence of events is shown in Table 5-15.

Figure 5-42 gives the approximate orbit geometry throughout the test. The first part of the test was to verify correct tracker bright-object sensor operation and to map possible glint sources. Approximately 1 minute after power was applied to the Canopus tracker, GMT 15:26, it went into the search mode and locked on negative glint. Canopus could not be acquired since it was minus 5.5 degrees in roll from space reference.

Table 5-15: Test Sequence

GMT day:hr.:min.	Event
163 15 15	Two-degree deadband, pitch minus 36 degrees
15 26	Acquire Sun, tracker on
15 30	Yaw minus 15 degrees
15 38	Yaw plus 15 degrees
15 41	Acquire Sun
15 44	Yaw plus 17 degrees
15 54	Pitch minus 20 degrees
16 02	Pitch plus 40 degrees
16 12	Pitch minus 20 degrees
16 21	Yaw minus 17 degrees
16 27	Acquire Sun
16 30	Tracker off, pitch plus 45 degrees

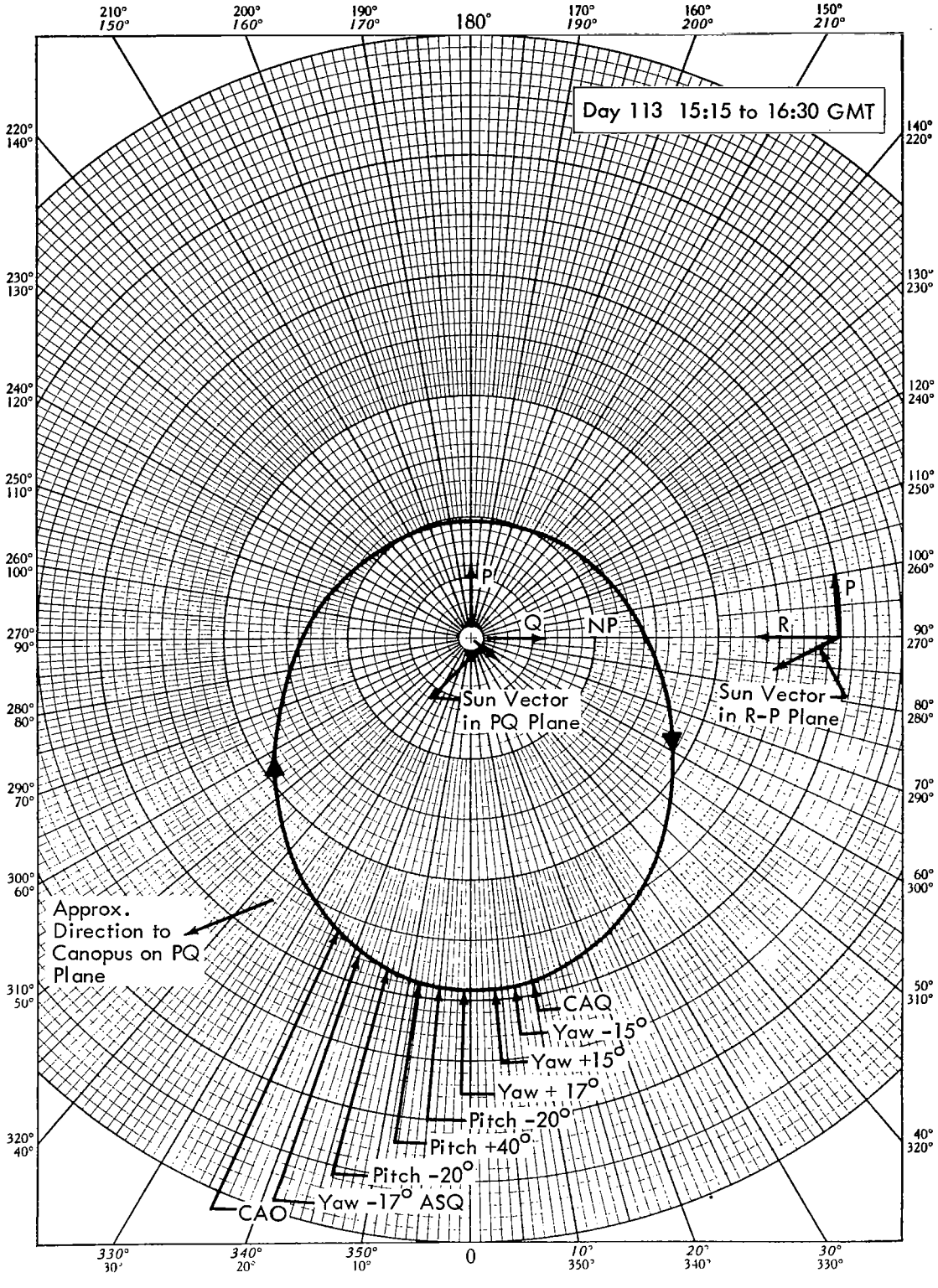

Figure 5-42: Orbit Geometry

Figure 5-43 shows the spacecraft position, and star map at tracker turnon. At GMT 15:30 a minus-15-degree yaw maneuver was started. Referring to Figure 5-44, it can be seen that the shutter closed at 15:55, which is 3.1 degrees into the yaw maneuver. Since the maneuver started at minus 1.6-degree yaw (within the 2.0-degree deadband), it has been determined that the shutter closed at minus 4.7 degrees from the zero position on Sun.

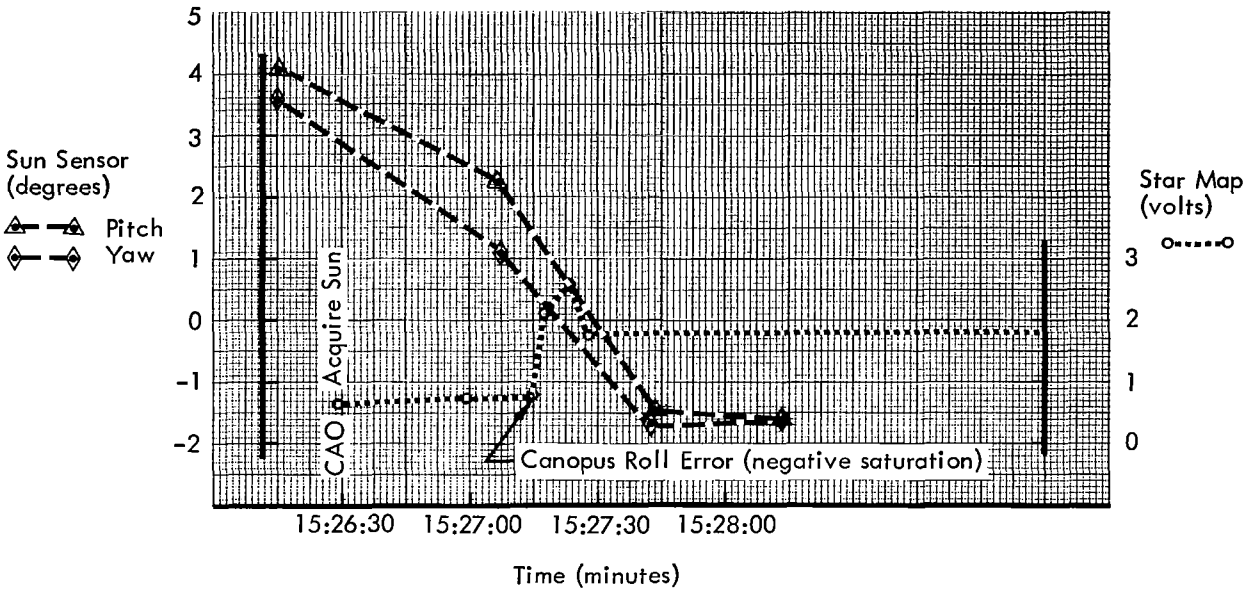

Figure 5-43: Sun Sensor Position

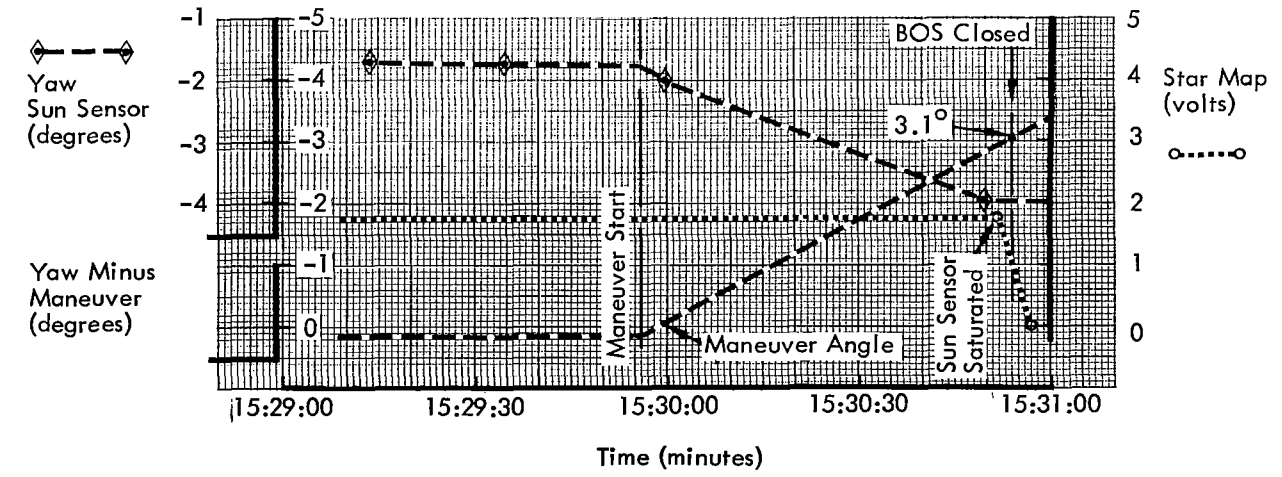

Figure 5-44: Bright Object Sensor Operation (−Yaw)

The shutter remained closed throughout the maneuver. At GMT 15:38 a plus-15-degree yaw was executed (back to Sun). Figure 5-45 shows that the BOS opened when 14.4 degrees of the 15-degree maneuver were completed. Two seconds after the shutter opened, the yaw Sun sensor showed a minus 4.0-degree error. Projecting the yaw Sun sensor position back in time, we find that the BOS opened at minus 4.2 degrees from the zero position on Sun. The 0.5 degree difference between opening and closing is well within the BOS tolerance. Since the tracker used a minus-8.5-degree insert, the cone angle from the Sun for BOS closing would be 76.8 degrees, for opening, 77.3 degrees. Maximum qualification test data was 78.0 degrees. It is concluded that BOS operation was within expected tolerances and that no glint sources were uncovered.

The second part of the test was to map glint sources at positive yaw angles. At GMT 15:44 a positive 17.0-degree yaw maneuver was started from plus 1.1 degrees in the yaw deadband. Figure 5-46 plots map voltage and yaw maneuver against time. When 4.0 degrees of the ma-

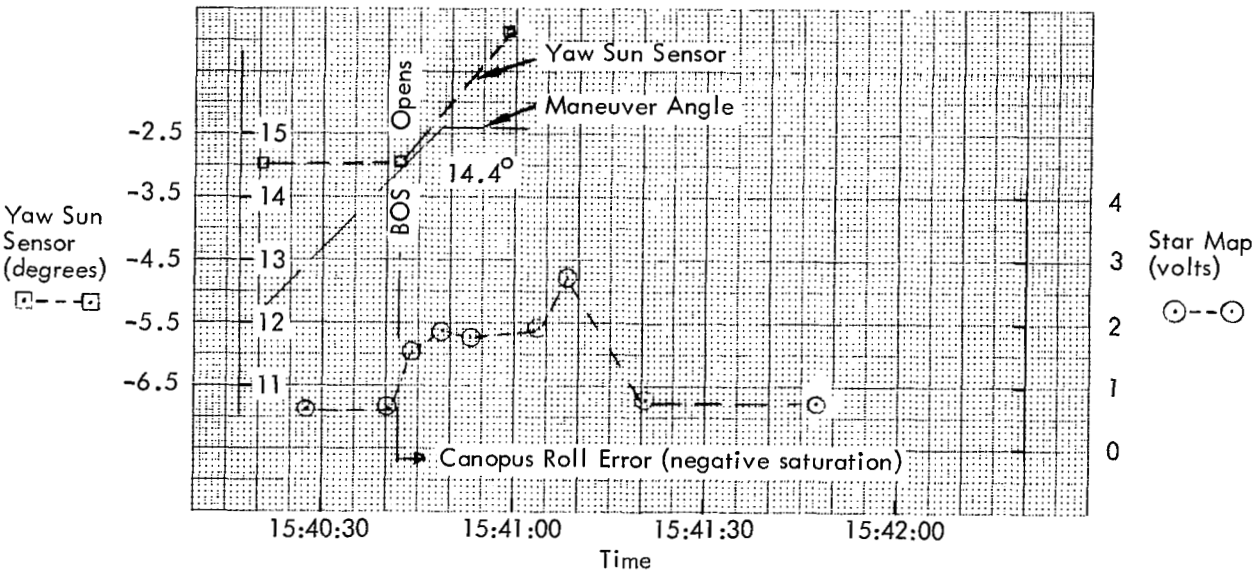

Figure 5-45: Bright Object Sensor Operation (+Yaw)

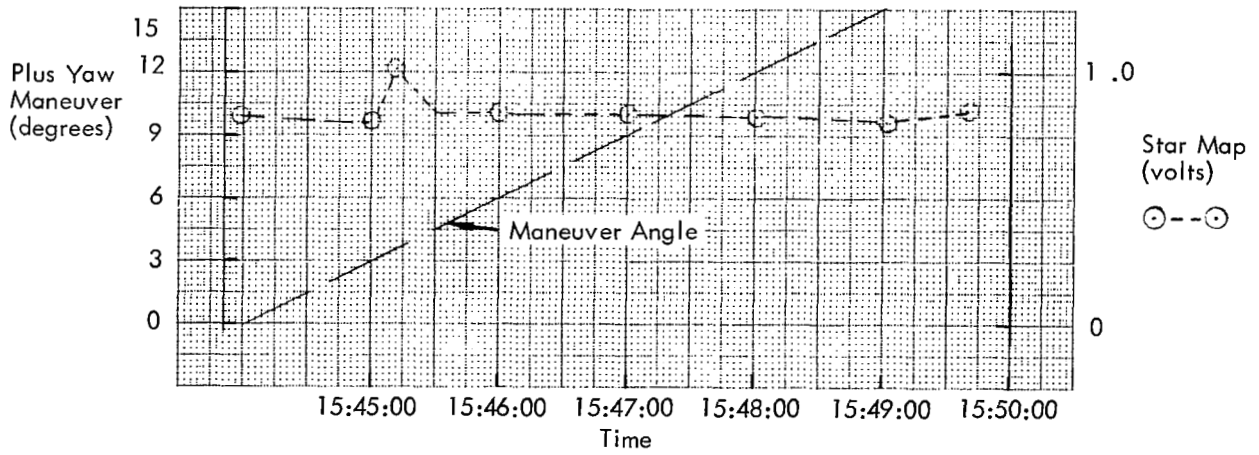

Figure 5-46: Star Map (+17 Degrees Yaw)

neuver were completed, the map voltage jumped from 0.82 volt to about 1.0 volt. The probable cause was light reflection on the low-gain antenna. One degree later the map voltage dropped back to 0.82 to 0.86 volt and remained there for the remainder of the maneuver. No significant glint sources were detected during the maneuver.

At GMT 15:54 a minus-20.0-degree pitch maneuver was initiated at minus-0.9-degree deadband. Figure 5-47 shows that the map voltage does not change significantly throughout the maneuver. The slight variation in map voltage from 0.9 to 0.8 volt and back to 0.92 volt does not correspond to any spacecraft movement in the yaw or roll axis. There were no glint sources uncovered during the maneuver.

At GMT 16:02 a plus-40.0-degree pitch maneuver was initiated at minus 1.8 degrees in the deadband. Figure 5-48 shows that map voltage does not change significantly throughout the maneuver. Map voltage is maintained between

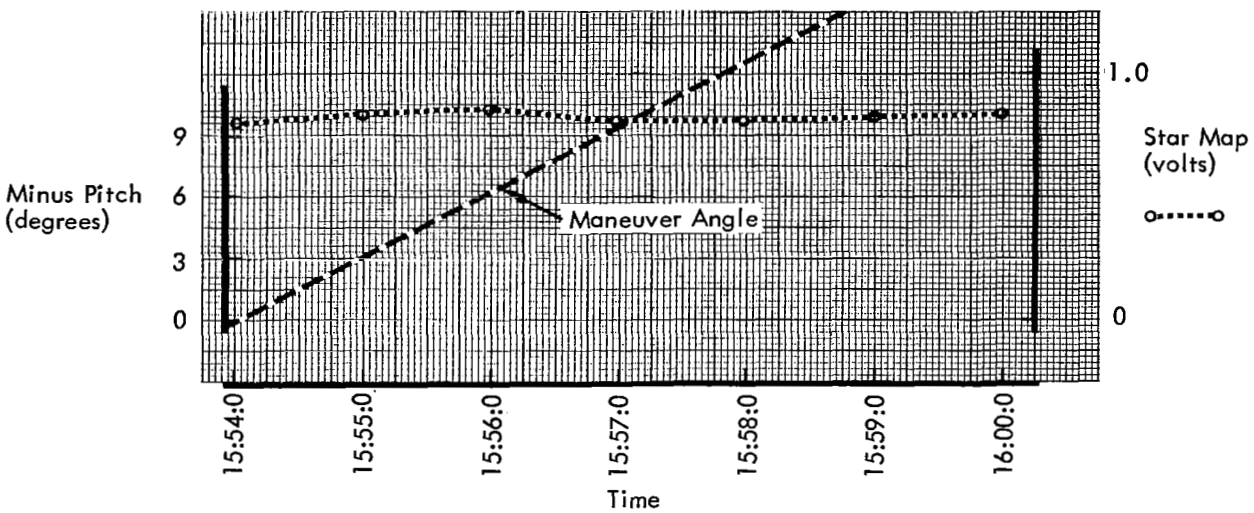

Figure 5-47: Star Map (−20 Degrees Pitch)

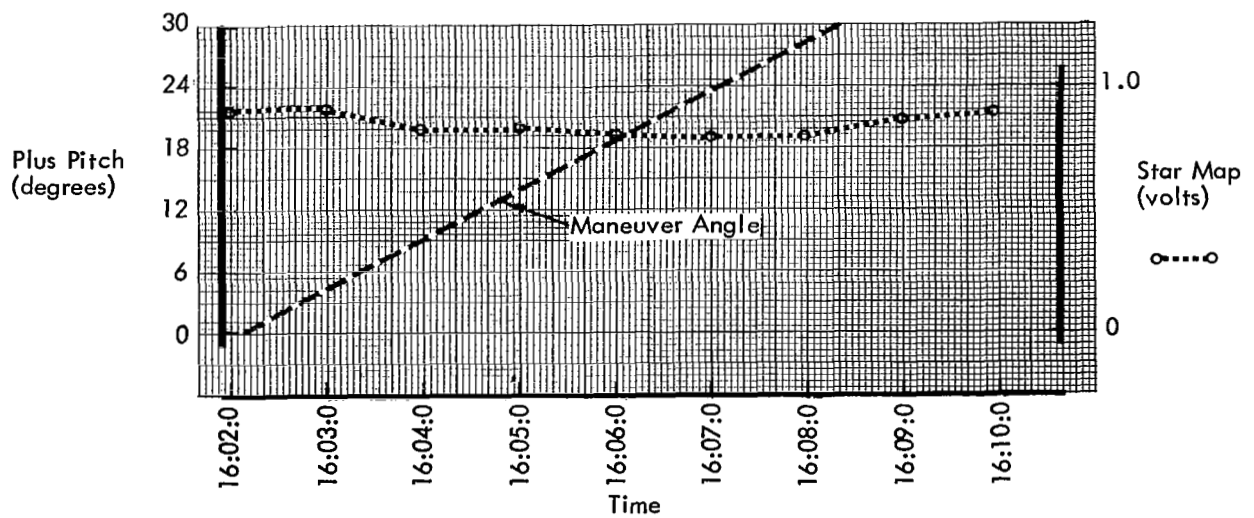

Figure 5-48: Star Map (+40 Degrees Pitch)

0.8 and 0.9 volt; the slightly cyclic variation in map voltage did not correspond to any variations in spacecraft position. At GMT 16:12, a pitch-minus-20.0-degree maneuver was executed. Figure 5-49 is a plot of this maneuver along with star map voltage. No glint sources are detectable. At GMT 16:21, a yaw-minus-17.0-degree maneuver was performed to get back on Sun (see Figure 5-50). Again no glint source was detected.

There appears to be a general level of background radiation throughout the maneuver area that corresponds to approximately 0.85

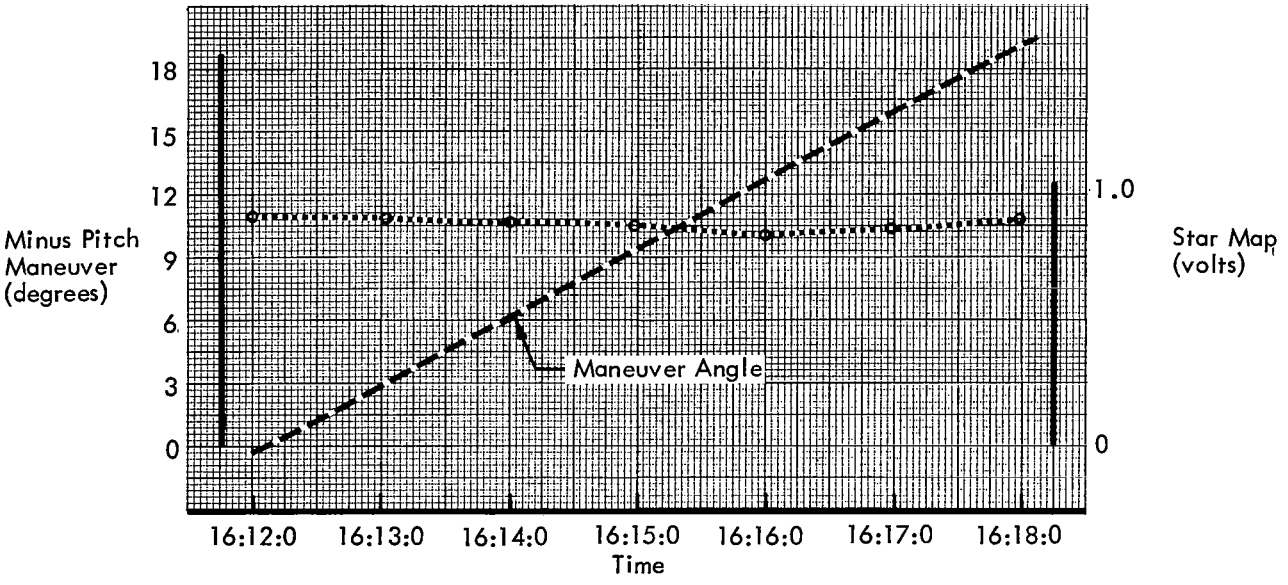

Figure 5-49: Star Map (−20 Degrees Pitch)

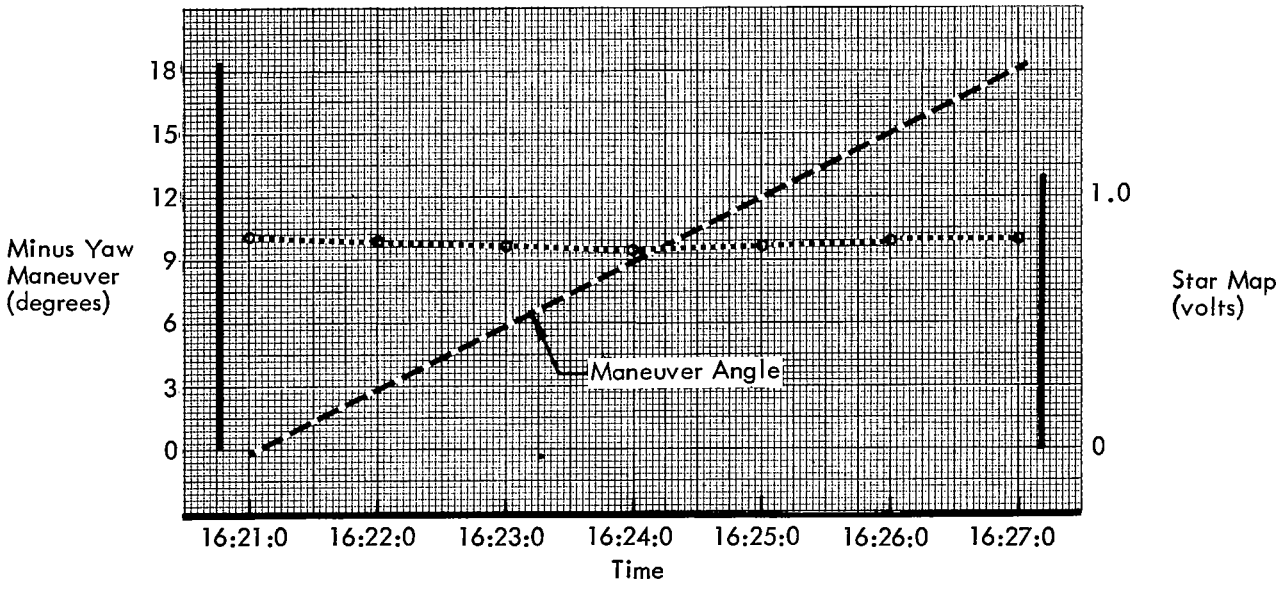

Figure 5-50: Star Map (−17 Degrees Yaw)

volt of star map. There do not appear to be any sources of high glint such as observed in Mission I. The BOS appears to operate normally at approximately the correct cone angle.

5.3.3 Special Star Tracker Test

The test, to determine problems associated with Canopus acquisition and tracking in a simulated Lunar Orbiter Mission V orbit in the presence of glint, was started after the spacecraft had been locked on Sun in pitch and yaw. The Canopus tracker was turned on every 10 degrees for several minutes, then off, starting approximately 45 degrees after apolune and continuing to 45 degrees before perilune. Tracker star map and roll error were recorded each time the tracker was turned on. The sequence of events is shown in Table 5-16.

Table 5-16: Star Tracker Test Sequence

GMT day:hr:min	Event
186:17:40	Acquire Sun
17:50	BOS closed, true anomoly = 137 degrees (tracker on)
17:57	
18:06	BOS opened, tracker on glint, true anomoly = 147 degrees
18:15	Tracker off
18:17	Tracker on glint, true anomoly = 152 degrees (tracker on)
18:29	Roll plus 7 degrees
18:37	Tracker off
18:39	Tracker on glint, true anomoly = 162 degrees
18:58	Roll minus 5 degrees
	Tracker off
	Tracker on glint (tracker on)
19:07	Yaw plus 3 degrees
19:12	Tracker in search mode (tracker on)
19:18	Roll minus 5 degrees
19:24	Tracker on glint, true anomoly = 180 degrees
19:34	Close dead zone
19:37	Tracker off

Table 5-16 (continued)

GMT day:hr:min	Event
19:38	Tracker in search (tracker on)
19:42	Canopus tracked, true anomoly = 187.5 degrees (roll plus 10 degrees)
19:48	Tracker off
20:10	Canopus tracked, true anomoly = 199.0 degrees (tracker on)
20:22	Tracker off
20:24	Tracker on glint, true anomoly = 205.0 degrees (tracker on)
186:20:31	Tracker off
20:45	Canopus tracked, true anomoly = 215.5 degrees (tracker on)
20:49	Tracker off
21:05	Canopus tracked, true anomoly = 228 degrees (tracker on)
21:09	Tracker off
21:32	Canopus tracked, true anomoly = 235.5 degrees (tracker on)
21:35	Tracker off
21:43	Canopus tracked, true anomoly = 269.5 degrees (tracker on)
21:44	Tracker off
21:52	Tracker on glint, true anomoly = 287 degrees (tracker on)
21:56	Tracker off
21:59	Canopus tracked, true anomoly = 305 degrees (tracker on)
22:05	Sunset, Canopus tracked, true anomoly = 323 degrees
22:08	Tracker off

Due to a glint problem aggravated by yaw excursions within the deadzone, it was about 2 hours and four on-off cycles before Canopus could be acquired. To alleviate this problem, the deadband was changed to 0.2 degree and Canopus was acquired the next turn-on. A summary of tracker test results is shown in Table 5-17. Three of the ten tracker on-off cycles resulted in lockup on glint. The glint occurred at scattered points and therefore does not indicate any relationship between orbit true anomoly and glint.

Conclusion – It would be possible for Lunar Orbiter V to track Canopus from 80 degrees before to 35 degrees after South Pole passage. Glint would be encountered, making monitoring and acquisition difficult. Successful tracking is a matter of chance over the range of angles tested. Yaw movement would continue to be a problem, which could be overcome by moving the mechanical angle in yaw of the tracker back from minus 9 degrees to approximately 6 degrees.

Table 5-17: Star Tracker Test Results

GMT	Time from Perilune (minutes)	Angle from Perilune (degrees)	Canopus Roll Error (degrees)	Star Map (volts)	
186:19:23	172	180	– –	– –	Apolune
186:19:42	167	172.5	-1.70	1.7	NDZ, IH all axes yaw +1.0 degree
186:20:10	125	161.0	-1.78	1.78	NDZ, IH all axes yaw +1.0 degree
186:20:16	119	158.3	-1.3	1.9	NDZ, CLC pitch and yaw, IH roll
186:20:24	111	155.0	-4.115	2.14	Glint
186:20:45	90	144.5	-1.38	1.9	
186:21:05	70	131.3	-4.115	2.08	Glint
186:21:32	43	106.5	-1.48	1.9	
186:21:43	32	90.5	-1.24	1.88	
186:21:52	23	73.5	-4.115	1.92	Glint
186:21:59	16	55.0	-1.34	1.90	
186:22:05	10	37.0	-1.45	1.82	Sunset, tracker remained on and tracking from 21:59 to 22:08
186:22:15	0	0	– –	– –	Perilune

5.3.4 TWTA On/Off Cycling Exercise

The purpose of this exercise was to provide data relative to TWTA life when subjected to on/off cycling. This data was to be used to assist in formulating Mission V TWTA operating conditions.

The above exercise was deleted in lieu of special low-voltage tests conducted on a ground test qualification unit. From the results of these tests, it was concluded that the TWTA could be safely operated at input voltages down to 20 v.d.c if required during the photographic maneuvers of Mission V.

5.3.5 Battery Discharge Test

The purpose of this test was to check battery discharge characteristics after a prolonged period of overcharge to ensure adequate power during engine burn and approaching periods of Sun occult.

The spacecraft was pitched 90 degrees off Sun so that the battery was in a discharge mode on Day 155. The discharge was continued until approximately 26% of the nominal battery capacity was discharged. Battery performance was monitored throughout the discharge period.

A total energy of 3.33 ampere-hours was removed from the battery, resulting in an end-of-discharge voltage of 24.75 volts. Battery temperature through the discharge dropped from 111.5 to 95.5°F. Figure 5-18 is a graphical representation of battery performance.

Conclusion – The battery discharge test was successful in demonstrating that a prolonged period of 31 days of constant overcharge did not affect normal battery characteristics; the battery would support the required off-Sun maneuvers and approaching periods of Sun occult.

5.3.6 High-Gain-Antenna 360-Degree Rotation

This test was conducted to obtain TWTA performance data as the high-gain antenna was rotated. This data was intended to verify earlier indications that the TWTA power output is affected by changes in the angular position of the high-gain antenna.

On Day 191/192, the high-gain antenna was rotated left (CCW) at 1 degree per data frame during the following times.

Time (GMT)	Antenna Angle
23:00:20 to 00:17:54	11 to 191 degrees
01:50:04 to 03:08:01	191 to 11 degrees

The desired temperature stability was not possible due to a Sun occultation preceding the experiment.

Figures 5-51 and 5-52 show TWTA power output and temperature during the experiment.

Transponder power output and the power subsystem were stable in terms of effects on the TWTA.

A comparison of thermal effects on TWTA power output following a Sun occultation is shown in Figure 5-53. The indicated power did not change more than one data bit between data frames.

TWTA temperature rose at an increased rate on Day 186 due to spacecraft attitude, causing erratic variations in indicated power output (see Figure 5-54).

Conclusion – There is some uncertainty about the effect of temperature on the data presented, but the variations at 200- and 290-degree positions must be attributed to rotation of the high-gain antenna. Therefore, the telemetry-indicated power output of the TWTA on Mission IV was sensitive to the rotational position of the high-gain antenna.

The variation resulting from VSWR change and/or phase-angle effects on the TWTA power is more likely caused by reflection of the high-gain antenna side lobes from Solar Panel 1.

5.3.7 TWTA Operation at Reduced Voltage

The object of this test was to determine, under space environmental conditions, whether the TWTA could be left on during Mission V off-Sun photography maneuvers.

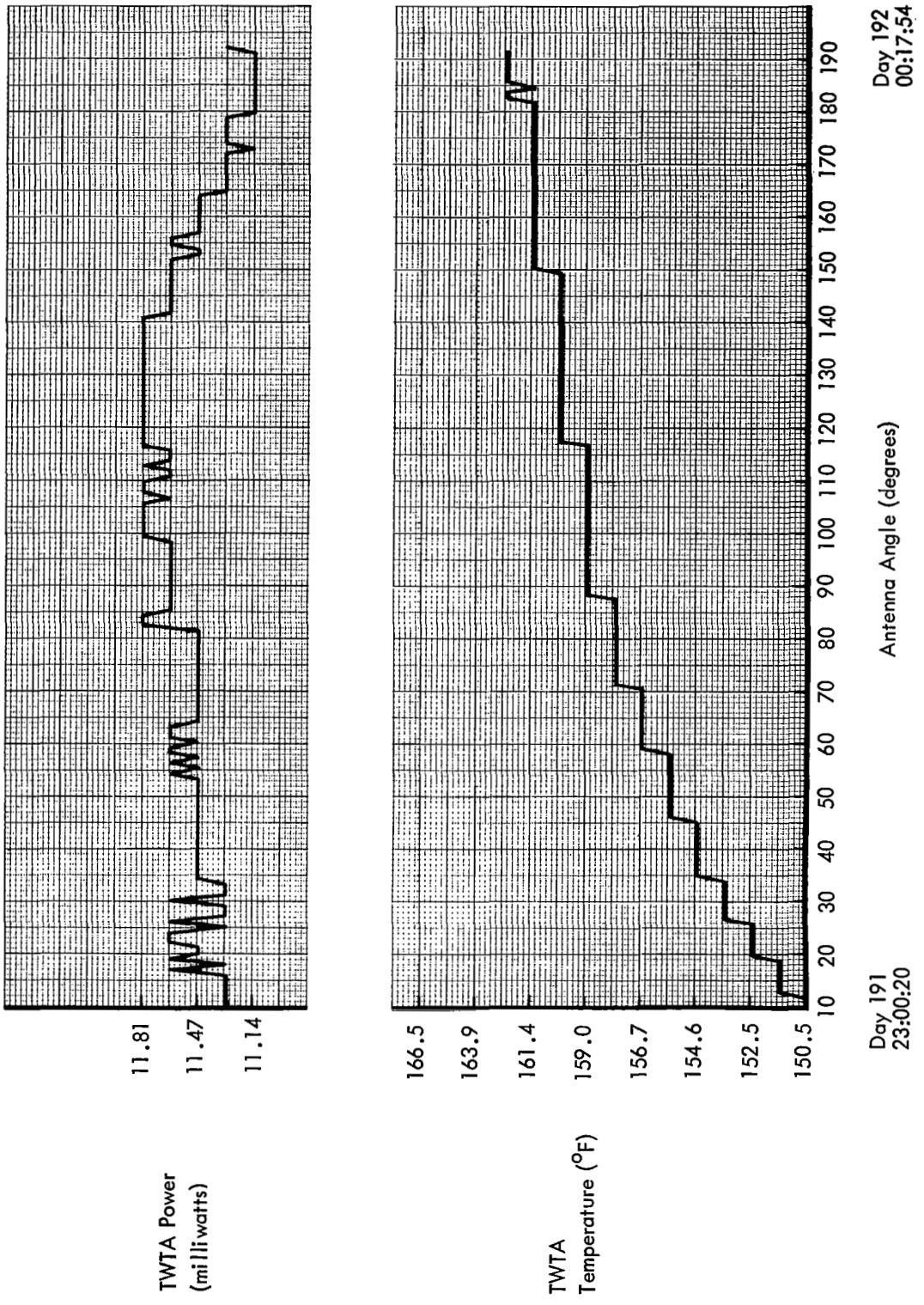

Figure 5-51: High-Gain-Antenna Rotation Test

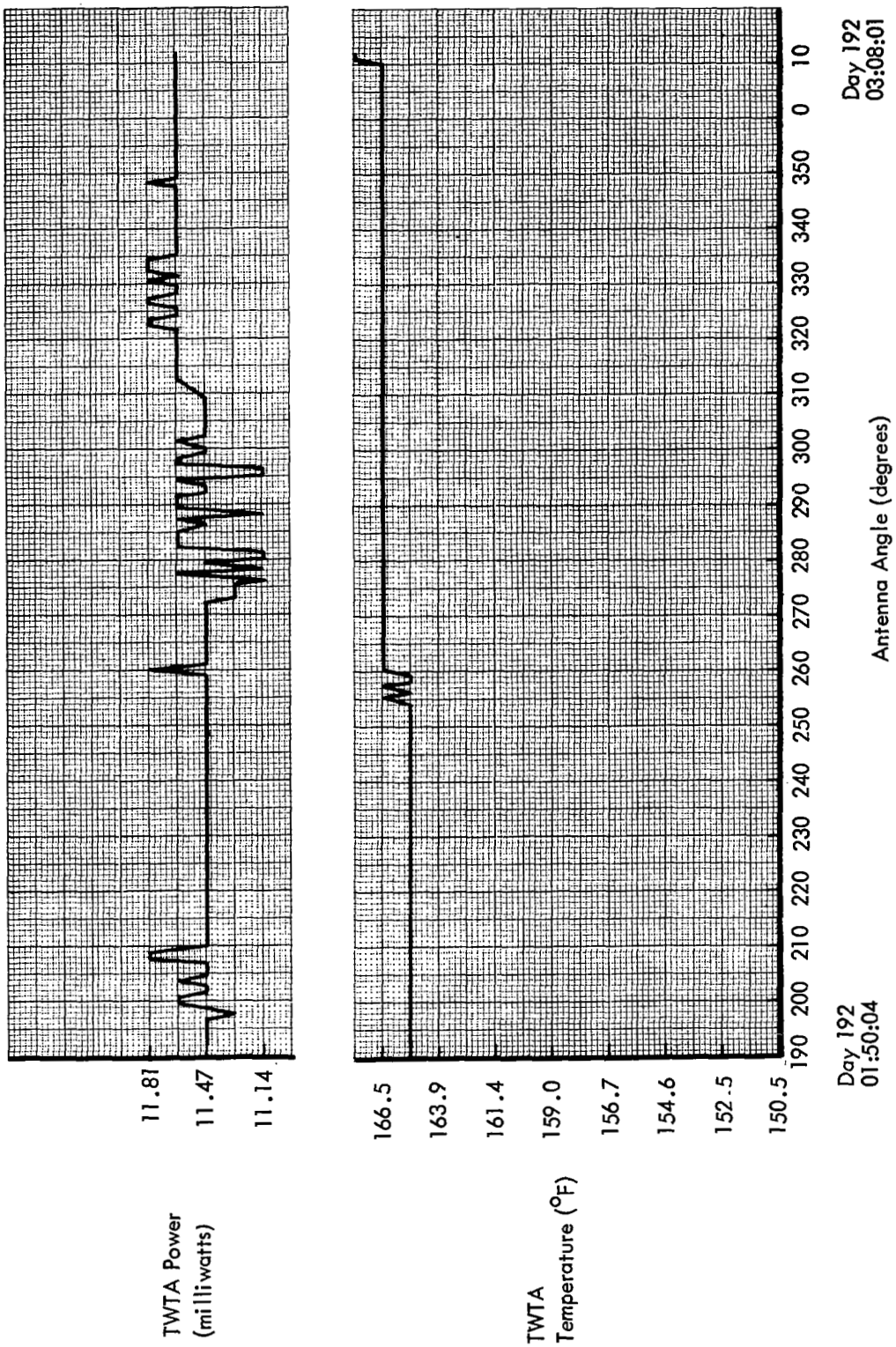

Figure 5-52: High-Gain-Antenna Rotation Test

Figure 5-53: High-Gain-Antenna Rotation Test

Figure 5-54: High-Gain-Antenna Rotation Test

The TWTA was on during seven Sun occultation periods. Two of these periods lasted approximately 14 minutes and five were approximately 18 minutes.

As of Day 192, the TWTA had been cycled on and off four times with a total operating time of 1,010 hours during the life of the spacecraft.

Figures 5-55 and 5-56 indicate typical performance of bus voltage and TWTA power output. It can be seen that the power remained relatively constant until the bus voltage dropped below 24.9 volts. TWTA temperature decreased to an indicated low value of about 130°F. From two TWTA low-voltage tests performed at Seattle, it is known that the TWTA power supply loses regulation at input voltages between 24.7 and 24.9 v.d.c. At this point all TWTA telemetry values are affected and therefore do not reflect the actual voltage, current, and temperature conditions existing at the TWT itself. As indicated by the results of this flight test and ground facility low-voltage tests, no degradation in

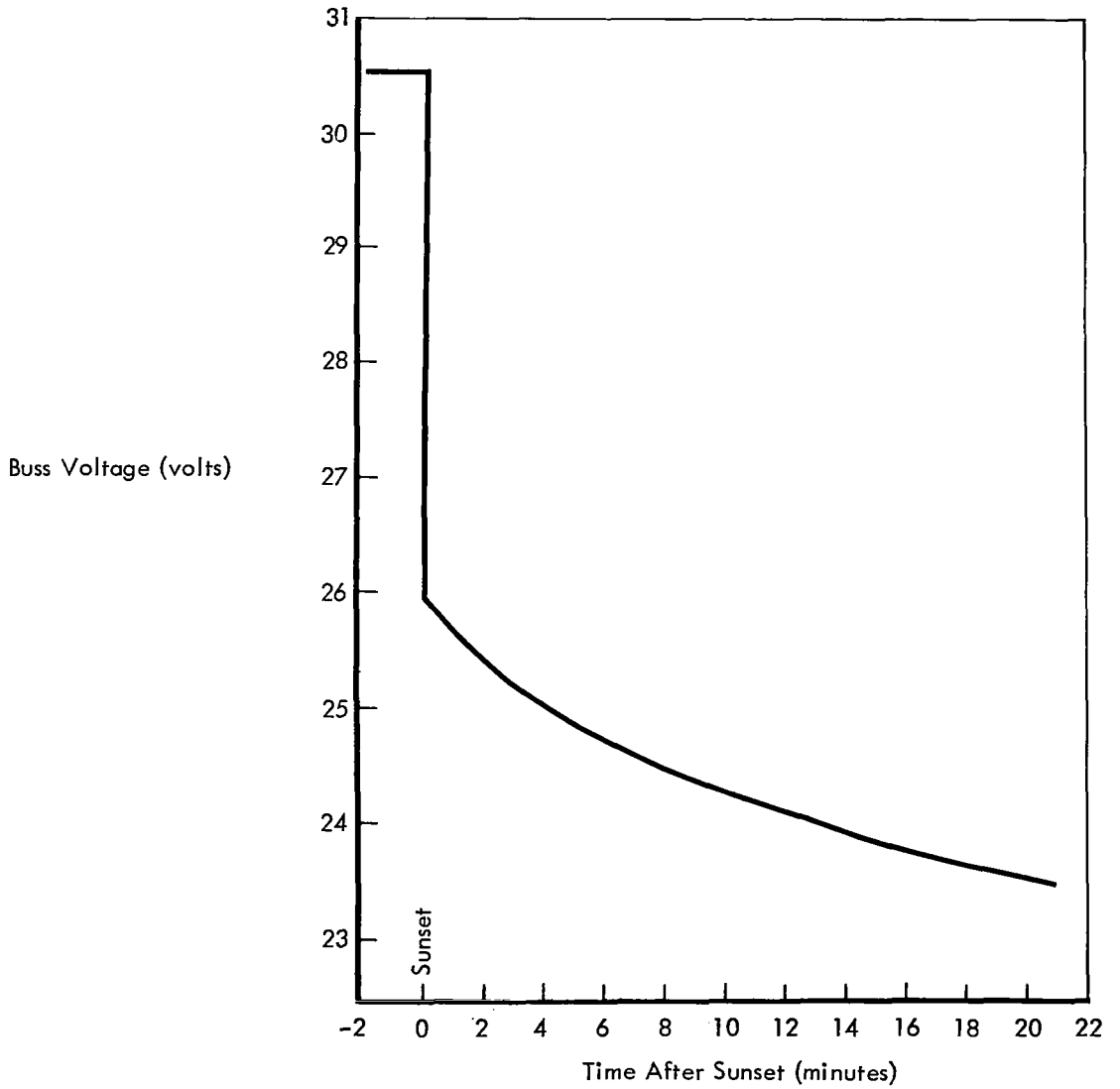

Figure 5-55: Bus Voltage Performance

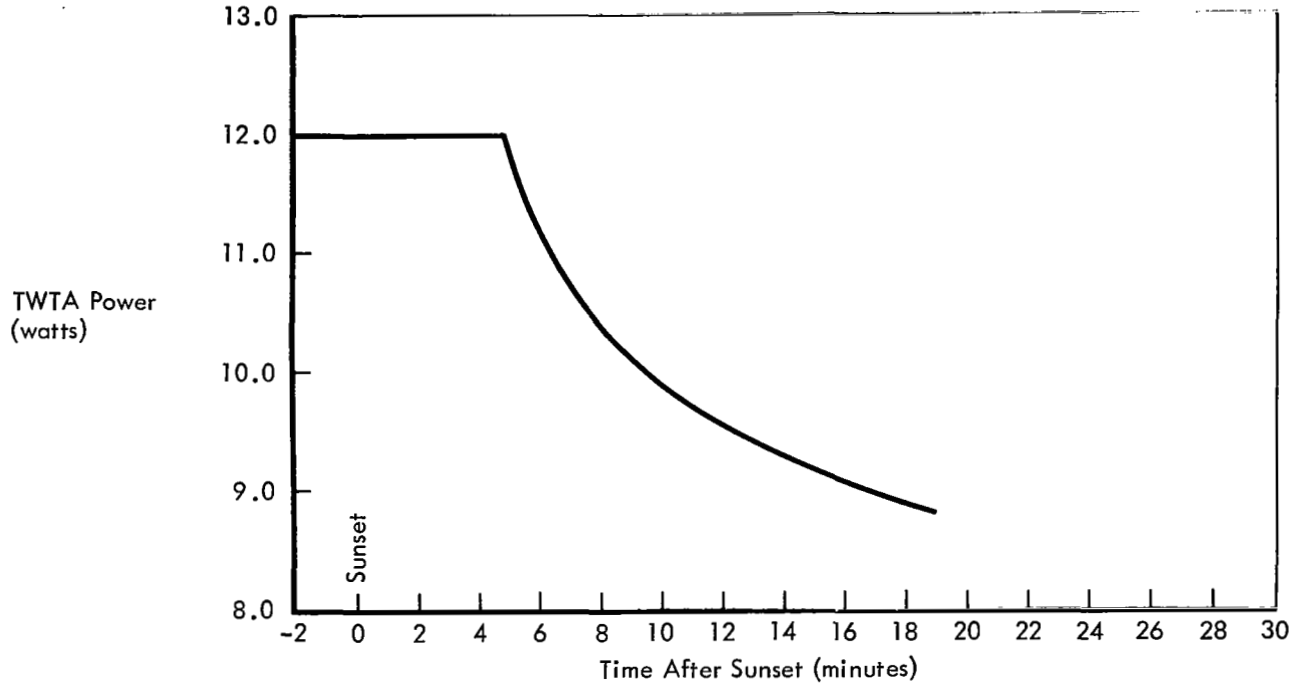

Figure 5-56: TWTA Power

TWTA operation was observed with return of the input voltage to normal values.

Conclusion – The TWTA may be safely operated at the input voltages encountered during Mission V off-Sun photography maneuvers.

5.3.8 Camera Thermal Door Test

The test objective was to obtain additional information concerning why the camera thermal door failed during the photo mission.

The test was performed in the following steps.

1) The spacecraft was oriented with the door at least 90% shaded when open and the photo system pointed toward deep space. The door was operated through an open and close cycle, allowing approximately 15 minutes between the "door open" and "door close" commands. A minimum of 30 minutes was allowed after the "door close" command for window temperature to respond. The normal continuous 65 pulse operation used for opening and closing the door. If PTO3 indicated the door was not closed, the number of additional single pulses required to close the door was recorded. This step was repeated four times (total of five cycles).
2) The spacecraft was oriented so that the door was at least 90% shaded when open with the photo system pointed toward deep space and the door closed. Twenty-five single, "door open" pulses at 23-second intervals were executed. Single, "door open" pulses at 23-second intervals were next executed until a door-open indication was observed. The total number of pulses to obtain a door-open indication was recorded. Four additional single "door open" pulses at 3-second intervals were executed next. The door was then closed with 50 single pulses at 3-second intervals and the door was verified closed by observing window temperature, allowing up to 30 minutes for the temperature to respond before executing additional closing pulses.

3) Step 2) above was repeated four times (total of five).
4) If the results of 1), 2), and 3) indicated that the door was operating normally, step 5) was performed next. If the results indicated that the door was sticking, the following steps were performed with the door shaded and the photo system pointed toward deep space.

   Single, "door close" pulses at ≥ 23-second intervals were executed until the door-open indication was removed. The number of required pulses was recorded.

   Single, "door open" pulses at ≥ 23-second intervals were recorded until a door-open indication was observed. The number of required pulses was recorded.

   Two single, "door close" pulses at ≥ 3-second intervals were executed.

   Single, "door open" pulses at ≥ 23-second intervals were executed until a door-open indication was observed. The number of required "open" pulses was recorded.

   The above sequence was continued, increasing the number of "close" pulses by one on each added closing cycle until the door-fully-closed position was reached. The 23-second delay between opening pulses could be decreased to 3 seconds until the door approached the open microswitch, at which time the delay between opening pulses could again be increased to 23 seconds to determine the exact number of pulses required to activate the switch.

5) With the spacecraft oriented so that the door was fully illuminated when open, steps 1), 2), and 3) above were repeated.

6) If the results of step 5) above indicated that the door was operating normally, the test was terminated. If the results indicated that the door was sticking, step 4) above was repeated, except with the door fully illuminated when open.

Part 1) of the test was performed only twice. The door opened normally on both occasions as indicated by the door-open switch. After a normal 65-pulse "close" command, the absence of a door-closed switch and the slow thermal response of the camera window temperature caused the number of pulses required to close the door to be indeterminant.

The plan was altered to perform part 2) before completing part 1). The door-open indication was observed after applying 47 single, "door open" pulses, which indicates that the door was operating as required. After 50 single, "door closed" pulses, a door-closed indication could not be established. After an additional normal 65-pulse "close" command, temperature data indicated the door was closed but could not be confirmed. The plan was to complete parts 2), 3), and 4) to define the number of pulses required to close the door based on the number of pulses required to open the door from each incremental closed position rather than by the window temperature response. However, contact with the spacecraft was lost before the test could be completed and the obtained data was not sufficient to completely evaluate the anomaly.

Conclusion – The tests completed prior to losing contact with the spacecraft indicated normal door operation. However, the window thermal response did not permit verification of closing characteristics.

5.3.9 Paint Degradation Test

The test was performed to obtain temperature data on paint coupons used to evaluate degradation characteristics of each paint.

The spacecraft was positioned on Sun for a sufficient period of time for temperature stabilization to occur. The timing requirement was critical to minimize the effect of lunar thermal radiation on temperature measurements. The on-Sun maneuver had to occur 1.5 hours prior to apolune and be left on Sun for a

period of not less than 2 hours. All critical temperatures had to be monitored during the time the spacecraft was on sun; the test was to be terminated if any temperature constraints were exceeded. Measurements were to be recorded at least every 5 minutes during the test.

The test was performed and data recorded as shown in Figure 5-57. The spacecraft was positioned on Sun from 17:41:14 until sunset (22:04:25 GMT). This particular area of interest is shown on an expanded scale by Figure 5-58 up to the point where the lunar thermal radiation effect became significant at approximately 21:00. This produced 3 hours of on-Sun data, showing that each of the four coupons had sufficient time to reach temperature stabilization. This test was performed only once prior to losing contact with the spacecraft.

Conclusion – The telemetry data from Figure 5-55 was corrected for all extraneous energy sources affecting coupon temperatures (see Table 5-18; the results are with ST13 showing best total performance and ST14 showing lowest degradation).

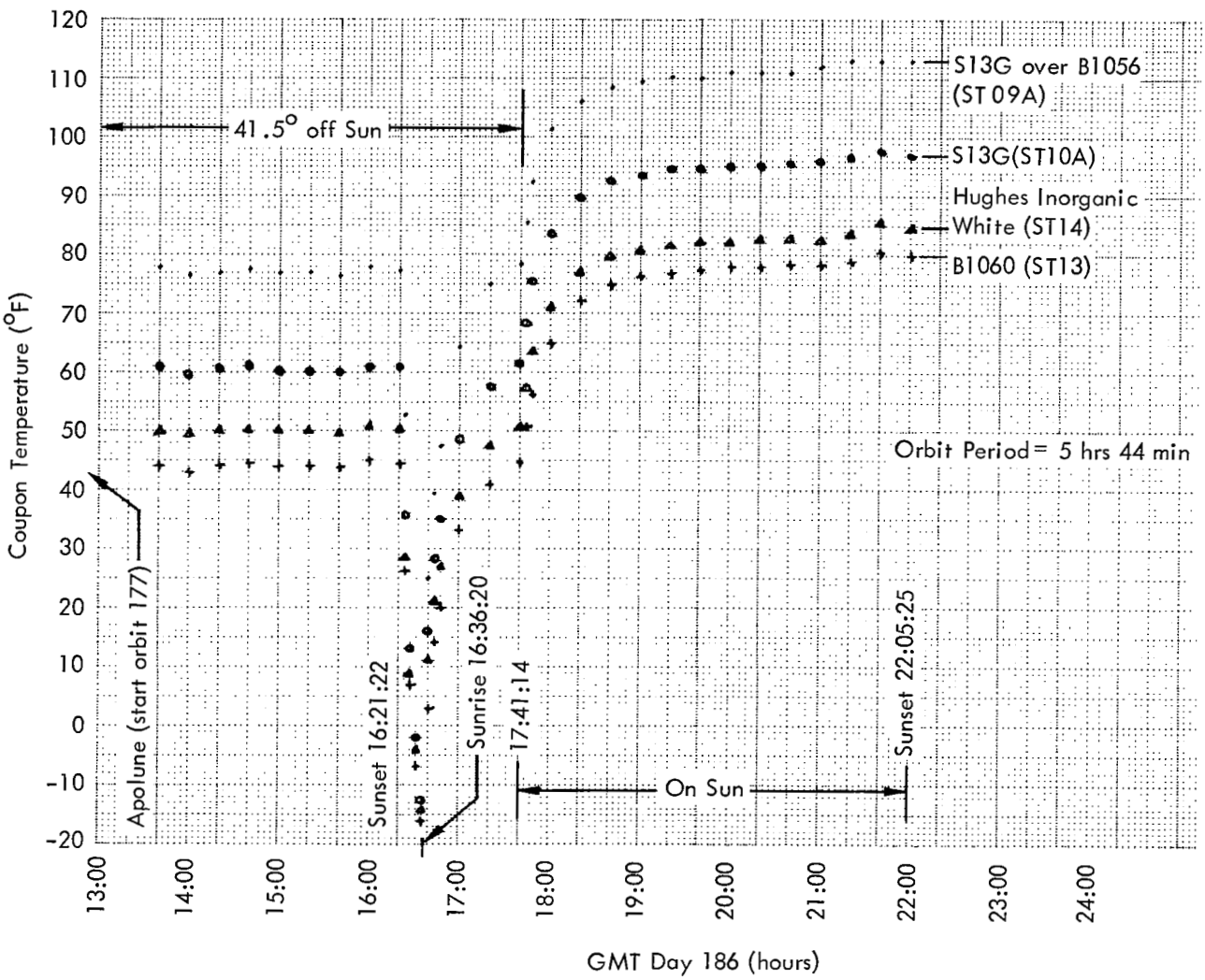

Figure 5-57: Paint Coupon Performance

Figure 5-58: Paint Coupon Performance

Table 5-18: Paint Coupon Performance

Telemetry Measurement	Corrected Temperature °F	α/ε	$\Delta\ \alpha/\varepsilon$ (since launch)
ST09A	108.3	0.408	0.224
ST10A	89.2	0.357	0.172
ST14	75.8	0.323	0.116
ST13	70.5	0.311	0.132

ST09A = S13G over B1056

ST10A = S13G

ST13 = B1060

ST14 = Hughes' Inorganic White

Appendix

PHOTO SUBSYSTEM COMMAND SEQUENCES

1. JMP 043 Camera on

   Wait 3.2 seconds

   Solar eclipse on

   Wait 51.2 seconds

   Solar eclipse off

   Infinite jump

This sequence is used to "bump" the film into a slight advance.

2. RTC 028 Jump to location 137

3. JMP 137 Solar eclipse off

   R/O electronics on

   R/O drive on

   Wait 25.6 seconds

   R/O drive on

   Infinite jump

This stored sequence initiates readout in a normal sequence, as would a series of real-time commands.

4. JMP 132 R/O drive on, solar eclipse off

   Camera on

   Wait 3.2 seconds

   V/H sensor off

   Infinite jump

This sequence resets the camera logic for readout.

5. JMP 164 R/O drive on

   Wait 25.6 seconds

   Wait 12.8 seconds

   Wait 3.2 seconds

   R/O electronics on

   Wait 3.2 seconds

   Restarts cycle

This sequence continues until it is halted by placement in infinite jump mode. It was implemented to prevent spurious signals from terminating readout. The wait times of 25.6, 12.8, and 3.2 seconds are sufficient for one scan period of approximately 44 seconds. The next "ROC BA" places the scanner in "focus stop" at a time to prevent the spurious signal from terminating read out. The next ROC BC restarts scanning.

6. JMP 173 RO/ Drive OFF

   Wait 102.4 seconds

   R/O Drive ON, Solar Eclipse ON

   Infinite Jump

This stored sequence is identical to the standard stored sequence to set the R/O memory to an "off" state and contains a backup "R/O drive on" command to restart scanning, if the scanner should fail to come to rest in the spot stop position, thereby turning the R/O electronics off.

FILM REWIND SEQUENCE OF EVENTS

Time (GMT)	Commands	Event
152:08:12	R/O drive off	PBO3 = 28.71; End of R/O of LO IV photo mission
08:21	RTC 028*	R/O initiated; rewind started
09:35	R/O drive off	R/O terminated normally
09:51	RTC 028*	R/O initiated
12:07	R/O drive off	R/O terminated to discontinue film rewind; Looper dumped normally
13:00	RTC 028*	R/O initiated
13:10	R/O drive off	R/O terminated normally
153:21:33	RTC 028*	R/O initiated
23:15	R/O drive off	R/O terminated; PB03 required approximately 9 min to dump
23:26	JMP 137*	R/O initiated
23:41	R/O drive off	R/O terminated normally
155:16:40	JMP 137*	R/O initiated
19:02	R/O drive off	R/O terminated; PB03 required 3 min. to dump
19:29	JMP 137*	R/O initiated
20:10	R/O drive off	R/O terminated; looper PB03 remained at 14.23
156:15:22	JPM 137*	R/O initiated at PB03 = 14.23
17:00	R/O drive off	R/O terminated; PB03 remained at :40
17:13	JMP 043*	PBO3 = 37.44
17:18	JMP 043*	PBO3 decreased to 27.22
17:22	JMP 043*	PBO3 decreased to 36.31
17:25	JMP 043*	PBO3 decreased to 3.30
156:17:30	R/O electronics on	R/O initiated
17:31	R/O drive on	R/O initiated

Time (GMT)	Command	Event
17:33	R/O drive on	R/O initiated
19:45	R/O drive off	R/O terminated; PBO3 decreased from 38.81 to 18.55
19:54	JMP 043*	PBO3 decreased to 16.73
19:59	JMP 043*	PBO3 decreased to 16.50
20:02	JMP 043*	PBO3 decreased to 15.59
20:05	JMP 043*	
20:10	JMP 043*	PBO3 decreased to 14.91
20:16	JMP 137*	R/O initiated at PBO3 = 14.91
20:31	R/O drive off	R/O terminated; PBO3 remained at 18.55
20:44	JMP 137*	R/O initiated; PBO3 = 18.55
20:54	r/o drive off	R/O terminated; PBO3 remained at 19.46
21:02	JMP 137*	R/O initiated; PBO3 = 19.46
21:12	R/O drive off	R/O terminated; PBO3 decreased from 21.96 to 19.91
21:17	JMP 043*	No change
21:19	JMP 043*	PBO3 decreased to 18.77
21:23	JMP 043*	No change
21:27	JMP 043*	No change
21:29	JMP 043*	No change
158:16:10	JMP 137*	R/O initiated at PBO3 = 18.55
16:25	R/O drive off	R/O terminated; PBO3 remained at 22.19
16:32	JMP 043*	PBO3 decreased to 21.74
16:35	JMP 043*	PBO3 decreased to 20.37
158:16:39	JMP 043*	PBO3 decreased to 18.55
16:44	JMP 043*	PBO3 decreased to 16.73

Time (GMT)	Command	Event
16:48	JMP 043*	PBO3 decreased to 14.45
16:57	JMP 137*	R/O initiated at PBO3 = 14.45, 15.59 at 17:04
17:06	S. E. on	PBO3 remained at 15.59
18:35	S. E. off	
18:37	JMP 043*	PBO3 decreased at 12.86
18:40	JMP 043*	PBO3 decreased at 10.81
18:44	JMP 043*	PBO3 decreased to 8.54
18:48	JMP 043*	PBO3 decreased to 6.49
18:54	JMP 043*	PBO3 decreased to 4.21
19:03	JMP 137*	R/O initiated at PBO3 = 4.21, 5.34 at 19:07
19:12	S. E. on	
22:45	JMP 132*	PBO3 decreased to 3.07
22:45	Cut Bimat	PBO3 = 3.30
22:35	JMP 137*	R/O initiated
159:00:35	R/O drive off	R/O terminated; PBO3 remained at 31.07
00:47	JMP 043*	PBO3 = 20.84
00:51	JMP 043*	No change
00:55	JMP 043*	PBO3 = 30.61
00:59	JMP 043*	PBO3 = 28.33
01:03	JMP 043*	BPO3 = 28.56
01:07	JMP 043*	PBO3 decreased gradually from 28.56 to 22.87
01:17	S. E. on	
159:20:39	R/O electronics on	
20:40	R/O drive on	

Time (GMT)	Command	Event
20:42	R/O drive on	Scanning started at PBO3 = 22.87; hangup at 23.10
20:48	R/O drive off	Load did not decrease immediately, EEO7 = 5.04, 4.98, 4.80, 4.80, 4.80, 4.80, 4.80, 4.30, 4.18, 3.55, 3.55
20:53	S. E. on	Load EEO7 decreased to steady value of 3.42
23:47	S. E. off	
23:50	JMP 043*	PBO3 decreased from 23.10 to 21.05
23:54	JMP 043*	PBO3 decreased from 21.06 to 19.01
160:00:06	JMP 043*	PBO3 decreased from 19.01 to 16.95
161:18:30	JMP 137*	R/O Sequence initiated but PBO3 did not increase from 16.95
18:35	R/O drive off	R/O terminated but PBO3 did not dump as it should
18:44	JMP 132*	PBO3 did not dump. PBO4 decreased from 22 to 21 counts (Command sequence must be preceded with "But Bimat")
18:47	Cut Bimat	Cut Bimat - To reset logic
18:50	S. E. on	All PS action inhibited
19:00	JMP 132*	Resets Camera logic - PBO4 decreased from 21 to 20 counts. PBO3 completely dumped to 4.43 inches
19:06	JMP 137*	R/O sequence initiated; PBO3 increased to 8.54 at 19:22
19:29	R/O drive off	PBO3 did not dump
165:03:10	JMP 043*	PBO3 decreased from 8.54 to 6.25
03:13	JMP 043*	PBO3 decreased from 6.25 to 4.21
03:26	R/O electronics on	
165:03:28	R/O drive on	

Time (GMT)	Command	Event
03:30	JMP 164*	Scanning initiated; PBO3 increased from 4.21 to 4.87 at 03:30
00:43	JMP 173*	R/O terminated
166:21:20	JMP 132*	Reset camera logic
21:23	Cut Bimat	
21:28	JMP 137*	R/O initiated, PBO3 increased from 4.44 to 5.39 at 21:33
21:42	R/O drive off	R/O electronics remain on
21:47	S. E. on	R/O electronics remain on
21:53	S. E. off	R/O electronics remain on
21:55	R/O drive on	R/O electronics remain on
12:57	R/O drive off	R/O electronics remain on
21:57 to 22:10	R/O drive on (7 times)	R/O electronics remain on
22:25	JMP 137*	Normal scanning, but PB03 not increasing beyond 5.12
22:34	JMP 173*	Commands verified; voltages momentarily decreased
23:00 to 23:04	R/O drive on (6 times)	R/O electronics remain on
167:01:24 to 01:28	R/O drive on (10 times)	Electronics off at 01:24

* See Description of Command Sequences

NASA-Langley, 1968 — 31 CR-1092